

RIGA TECHNICAL UNIVERSITY
Civil Engineering Faculty
Institute of Heat, Gas and Water Technology

Romāns NEILANDS

Student of doctorate program of Heat, Gas and Water Technology

The theoretical analysis of the method of scour development in time for engineering structures

PROMOTIONAL WORK

Scientific supervisor

Prof., Dr. Sc. Eng.

B.GJUNSBURGS

Riga 2010

UDK 624.159.2.04 (03)

Ne 231 t

Neilands Romans. Metodes teorētiskā analīze izskalojuma lieluma attīstībai laikā inženierbūvēs. Promocijas darbs./ The theoretical analysis of the method of scour development in time for engineering structures. Ph.D.thesis. – R. RTU, 2010. – 99 lpp.

Printed according to the Promotion Council „RTU P-12” decision November 15th, 2010. Protocol No.3.



© Rīgas Tehniskā universitāte 2010

© Romāns NEILANDS 2010

ISBN

ABSTRACT

Because of scour, bridge failure lead to considerable damages and financial losses. Since 1998, till now Europe have suffered over 100 damaging floods and over €25 billion in insured economic losses. The coming decades are likely to see a higher flood risk in Europe and greater economic damage.

The prediction of depth of scouring development in time during the flood is very important for bridge and engineering constructions to ensure their stability and safety.

To study the particle scouring mechanism there large amount of literature has been published on the local scour depth determination and bed sediment movement at bridge abutments or piers, but local scour development in time for engineering structures such as abutments or wastewater process tanks has not been studied yet, while other subjects were under research. Equations describing the conditions of local scour at bridge sites are complex and hence the initial research into the problem was empirical. More recently, attempts have been made at analytical solutions, but these too have had to rely heavily on the results of experiments. Thus, there is no rigorous theoretical solution to the problem.

To control the activated sludge particle escaping from secondary clarifier the practical application of new development method on scouring development in time was implemented.

The sediment blanket level in clarifiers and grit tanks is subject to continuous change. The incoming flow rates and gravity settling tanks operation traditions may settle or resuspend particles from deposit influencing the treated wastewater quality. The sediment resuspension is governed by the scouring process load, which develops, stays at equilibrium or stops. The grit tanks or sedimentation clarifiers are designed on simple criteria, such as detention time and hydraulic load on surface area assume that the fluid distribution and particle settling in the clarifier is uniform and removal efficiency of particles with a known settling velocity in a settling tank can be simply calculated by ideal horizontal flow reactor theory. The analysis from field studies show that effluent quality about 60% of clarifiers is unstable during the operation and the knowledge of the particle hydraulic can therefore used to improve their performance. In wastewater treatment (WWT) plant field studies found that settler (etc. grit, primary and secondary clarifier tank) wall and effluent launder weir shape certain similarity to bridge abutments, and influence of flow performances, such as local velocities and overflow, tank water level and level in weir variation rate accord to bridge

scouring characteristics, and it was accepted that river hydraulic scouring process calculation method can be used as a base in this study.

A large number research has been undertaken on sand and activated sludge particle sedimentation, but very little research has been done on resuspension the sediment particles in tanks. The local scour development mechanism in WWT plant process tanks has not been studied and to improve understandings of this process development there was the aim of this study. Literature analysis shows that there is no one opinion which velocity is forming scour hole and no methods for computing local scour development during the time at the abutments. In formulas or methods for calculation depth of scour at abutments are used mean velocities of approach flow or Froude number with that velocity, like the same for sedimentation tanks.

Promotional work consists of: introduction, 4 chapters, conclusions, 3 appendixes, 84 references, 55 figures, 7 tables, and together 99 pages.

ANOTĀCIJA

Izskalojumi tiltu konstrukcijām izraisa ievērojamus bojājumus un rada finansiālus zaudējumus. Kopš 1998. gada līdz mūsdienām Eiropā ir notikuši vairāk ne kā 100 nozīmīgu plūdu un ir radīti zaudējumi, kuri pārsniedz 25 miljonus eiro. Nākamajās dekādēs paredzams vēl lielāks plūdu risks, kas var radīt vēl lielākus zaudējumus ekonomikai.

Tiltu un citām inženierbūvēm ir svarīgi paredzēt izskalojuma dziļumu attīstību plūdos tādējādi nodrošinot to konstrukcijām stabilitāti un drošumu.

Veicot izpēti par daļiņu izskalojuma mehānismu, vairums pētījumu tiek publicēti par izskalojuma bedres dziļuma noteikšanu un sanešu kustību pie tilta vai krasta balsta, bet vietējā izskalojuma bedres attīstība laikā tādām inženierbūvēm kā krasta balsti vai attīrīšanas iekārtu procesa tvertnes nav tikušas pētītas, tikmēr pārējas tēmas ir skatītas.

Esošie aprēķinu vienādojumi, kuri nosaka vietējā izskalojuma dziļumu ir sarežģīti, jo kopš problēmas izpētes paša sākuma tās bija empīriskas. Vairums pēdējā laikā veiktie pētījumi, bija mēģinājumi atrast analītisku risinājumu, bet arī tie pamatojas uz eksperimentu rezultātiem. Tātad, nav precīzs problēmas teorētiskais risinājums.

Diferenciāl vienādojums nogulšņu kustībai tīra ūdens pieteces apstākļos tika pielietots un izstrādāta jauna metode izskalojuma lieluma attīstības aprēķinam laikā plūdos krasta balstam.

Lai pārbaudītu izstrādāto metodi eksperimentu un aprēķinu lielumi tika salīdzināti un eksperimentos iegūtie rezultāti apstiprina doto metodi. Izmantojot jauno metodi katram hidrogrāfa punktam var noteikt izskalojuma dziļumu pēc viena, diviem vai vairākiem plūdiem.

Lai kontrolētu aktīvo dūņu daļiņu iznesumu no otrējā nostādinātāja lauka izpētes tests tika veikts, kur jaunā metode izskalojuma lieluma attīstības laikā noteikšanai tika pielietota.

Nogulšņu slānis nostādinātāju un smilšu uztvērēju baseinos pakļauts nepārtrauktai izmaiņai. Ienākošo ūdens plūsma un nostādināšanas baseinu ekspluatācijas paņēmieni var daļiņas izgulsnēt vai atkārtoti tās suspendēt no nogulsnēm, tādējādi ietekmējot attīrītā notekūdens kvalitāti. Nogulšņu slāņa uzduļķošanās pakļaujas izskalojuma mehānismam, kurš to paātrina, paliek līdzsvarā vai aptur. Smilšu uztvērēji vai nostādinātāji tiek projektēti pēc vienkāršotiem to darbības kritērijiem tādiem kā uzturēšanās laiks un hidrauliskā slodze uz virsmu, pieņemot kā plūsmas sadale un daļiņu izgulsnēšanās baseinā ir viendabīga un daļiņu

izdalīšanas efektivitāti, kurai zināms tās izgulsnēšanās ātrums var aprēķināt izmantojot ideālas plūsmas horizontālā reaktora teoriju.

Lauka pētījumu analīzes liecina, ka notekūdeņu kvalitāte, apmēram 60% no nostādinātāju ir nestabila, un daļiņu hidrauliskās plūsmas kustības pārzināšanu var izmantot, lai uzlabotu to veiktspēju. Notekūdeņu attīrīšanas iekārtu lauku pētījumos konstatēts, ka nostādinātāju (t.i., smilšu uztvērēji, pirmējie un otrējie nostādinātāji) siena un izteces pārplūdes teknes formai ir zināma līdzība ar tilta krasta balstiem, un plūsmas ietekme, piemēram, tā ātrums un pārtece pār sliekšni, rezervuāra ūdens līmeņa un ātruma izmaiņas pakļaujas izskalojuma likumsakarībām un tika pieņemts, ka upju gultnes izskalojuma aprēķinu metodiku var izmantot kā pamatu šajā pētījumā. Ir veikti daudzi pētījumi par smilšu un aktīvo dūņu daļiņu izgulsnēšanos, bet ļoti maz pētījumu attiecībā uz nogulšņu daļiņu izskalojumu no rezervuāra. Izskalojuma procesa attīstības mehānisms notekūdeņu attīrīšanas iekārtās līdz šim nav pētīts, un, lai sekmētu izpratni par doto procesu, tad tas arī bija viens no dotā pētījuma mērķiem. Literatūras analīze liecina, ka nepastāv vienots viedoklis, kurš no ātrumiem veido izskalojuma bedri un nav nevienas metodes, ar kuru varētu aprēķināt izskalojuma bedres attīstību laikā pie krasta balsta. Izskalojuma dziļuma aprēķina formulās un metodēs pie krasta balstiem izmanto vidējos plūsmas ātrumus vai Frūda skaitli tam pašam ātrumam, līdzīgi kā nostādināšanas baseinam.

Promocijas darbs sastāv no: ievada, 4 nodaļām, secinājumiem, 3 pielikumiem, 84 literatūras norādēm, 55 zīmējumiem, 7 tabulām un kopā 99 lapas.

TABLE OF CONTENT

INTRODUCTION	9
1 RESEARCH OBJECTIVE AND TASKS	12
2 BACKGROUND AND LITERATURE REVIEW	13
2.1 Scour prediction methods	14
2.1.1 Regime approach.....	14
2.1.2 Dimensional analyses	16
2.2 Summary of scour calculation methods.....	29
3 METHOD OF ESTIMATION SCOUR DEPTH DEVELOPMENT IN TIME.....	31
3.1 Laboratory set-up	31
3.2 Scour depth development in time.....	33
3.3 Calculation of local flow velocity	41
3.4 Comparison of calculated and experimental scour depth values	45
3.5 Analysis of the scour depth calculation method	48
3.6 Conclusions.....	53
4 PRACTICAL APPLICATION SLOKA WWTP	54
4.1 Clarifier standard parameter evaluation	55
4.1.1 Flow velocity measurements.....	55
4.1.2 Clarifier performance control.....	56
4.1.3 Sludge particle size and settling velocity.....	57
4.1.4 Relation between effluent suspended solids concentration and SVI.....	59
4.1.5 Secondary clarifier working zones	60
4.1.6 Flow loading rates	61
4.1.7 Detention time t.....	61
4.1.8 Overflow rate OFR.....	62
4.1.9 Effluent hydraulic	62
4.1.10 Weir loading rate	65
4.1.11 Sludge blanket height H_{sb} and concentration X_{sb}	67
4.1.12 Dilution zone concentration X_f	69
4.1.13 The scouring velocity determination	70
4.1.14 CFD	71
4.2 Application results.....	73

4.2.1 Sedimentation velocities V_s and V_0	73
4.2.2 Scouring development variation for different flow rates.....	74
4.2.3 Effluent suspended solids variation.....	76
CONCLUSIONS	78
REFERENCES	80
APPENDIXES.....	89
APPENDIX 1. ROBO. Calculation example	90
APPENDIX 2. Results of computer modelling, experimental and calculated SLOKA WWTP data.....	91
APPENDIX 3. Aqua model. Summary of calculated and experimental SLOKA WWTP performance data.....	93

INTRODUCTION

Because of scour, bridge failure lead to considerable damages and financial losses. Since 1998, till now Europe have suffered over 100 damaging floods and over €25 billion in insured economic losses. The coming decades are likely to see a higher flood risk in Europe and greater economic damage.

In present study, a differential equation of equilibrium of the sediment movement for clear water is used and a new method for calculating the scour development with time at the abutment wall during the rapid flow increase or flood is elaborated. Depth of scour by this method can be determined at any steps of hydrograph or after one, two or several floods. After one flood, because of the shortage of the time, depth of scour go on at the next flood of the same intensity, but development starts closer to the peak of the flood. Equilibrium depth of scour sometimes can't be reached during one, two or even several equal floods because the time of the flood is restricted. To verify developed method, calculated and experimental equilibrium scour depth values will be compared. The method was confirmed by experimental data. The full-scale test in Sloka WWTP activated sludge plant for secondary clarifier was done and new method on scouring development in time for clarifier process control was used.

A survey of 27 activated sludge plants in the Latvia is of interest and is notable that only 60 percent of the plants studied produced permanent SS values of 35 mg/l or less. The reasons is permanently increase the irregularity of the flow rate, especially after intensive rainfalls, as a result the increase of pollutants from water treatment units due to suspended solids scouring.

A detailed statistical analysis of Neilands et al. ^[43] of river basins in Latvia and Lithuania showed that sediment accumulation in rivers take place on regularly basis and local wastewater treatment plant performance can significant influence water quality.

The aim of practical application was to examine the individual effect of the scouring on sludge particle escaping from clarifier due to local velocities increase. The new developed method on scouring development in time for clarifier as a controlled measure was used.

The problem of scouring resulting the sludge particle escaping from clarifier working zones exist, thus increasing the effluent TSS concentration due to development the excessive flow hydraulic pattern inside the tanks, especially as a result of storm runoff often occurs at many wastewater treatment plants. The local scour development mechanism in WWT plant process tanks has not been studied and to improve understandings of this process development

there was the aim of this study. In wastewater treatment (WWT) plant field studies found that settler (etc. grit, primary and secondary clarifier tank) wall and effluent launder weir shape certain similarity to bridge abutments, and influence of flow performances, such as local velocities and overflow, tank water level and level in weir variation rate accord to bridge scouring characteristics, and it was accepted that river hydraulic scouring process calculation method can be used as a base in this study.

The sand from grit tanks or activated sludge particles escaping from secondary clarifier in biological processes is affected by the performance of the gravity type sedimentation tanks. In turn, escaping solids carry a significant portion of other regulated constituents, e.g., suspended solids, BOD, COD, nitrogen and phosphorus. Thus, the capacity and stability of the settling tanks is critical to the overall performance of the wastewater treatment process. Low effluent suspended solids (SS) are not always obtained from the activated sludge process. A survey of 27 activated sludge plants in the Latvia is of interest and is notable that only 60 percent of the plants studied produced permanent SS values of 35 mg/l or less. A detailed statistical analysis of river basins in Latvia and Lithuania showed that sediment accumulation in rivers take place on regularly basis and local wastewater treatment plant performance can significant influence water quality. The grit tanks or sedimentation clarifiers are designed on simple criteria, such as detention time and hydraulic load on surface area assume that the fluid distribution and particle settling in the clarifier is uniform and removal efficiency of particles with a known settling velocity in a settling tank can be simply calculated by ideal horizontal flow reactor theory.

The first theory about the efficiency of settling tanks has developed by Hazen^[21] for individual particle settling in a uniform flow. Anderson^[4] discovered that the flow is far from uniform because of density stratification. The solids-loaded influent has a higher density than the ambient water and, hence, plunges as a density jet to the bottom. Density currents, circulation, and short-circuiting are hydraulic phenomena, which occur in sedimentation tanks due to the density differences, stratification of liquid-solids, and tank geometry as concluded by Clark^[11]. To define the different settling characteristics of aqueous suspension, particulates have been categorized into three general classes: discrete, flocculent and hindered particles as supposed by Katz and Geinopolos^[24], Weber and Rowe^[67], and Tchobanoglous and Burton^[62]. Tekippe^[63] showed that minor temperature differences would affect the design variables in inlet and outlet. Hudson, after Ahmed et al.^[3], concluded that the addition

of warm influent water to a sedimentation basin containing coolers water could lead to short circuiting phenomena.

1 RESEARCH OBJECTIVE AND TASKS

The objective of this research is to develop the new method of clear-water scour development in time near the engineering structures, taking into account the widely used and new hydraulic and river bed scour-control parameters, thus predicting the scour depth development during floods in advance and ensuring safety of hydraulic structures.

Developed method could be used in preventing the similar scour process development in other engineering structures, such as wastewater treatment process tanks, avoiding escaping sludge particles from clarifiers and thus preventing the river basin pollution from untreated wastewater effluent.

The contraction of the flow by engineering structures leads to considerable changes in flow pattern, a local increase in velocities, increase turbulence, and the origin of eddy and vortex structures. All these changes in the system are the reasons for a local scour development at the engineering structures. The local scour development during the time at engineering constructions has not been studied yet.

To achieve research objective following tasks are defined:

- Research existing abutment scour development calculation methods to find out the parameters which are already used for scour depth development calculation at engineering structures;
- Perform the abutment scour laboratory tests (Gjunsburgs and Neilands ^[17]), and basis on the tests develop the calculation method of scour depth development in time, during floods at abutments.
- Compare experimental and calculated scour development in time values to validate method.
- Perform the theoretical analysis of the calculation method of scour depth development in time and define the evaluation parameters.
- Determine the sedimentation tank cross-sectional velocities profiles and study the effect of local velocities on sludge particle escaping from clarifier dilution and clarifier zones.

2 BACKGROUND AND LITERATURE REVIEW

Prediction of depth of scour during the flood is very important for bridge constructions to ensure stability and safety. Bridge failure during a flood as a result of local scour at piers, abutments, or guide banks, or contraction scour can lead to considerable environmental damages and losses. To study the particle scouring mechanism there large amount of literature has been published on the local scour depth determination and bed sediment movement at bridge abutments or piers, but local scour development in time for engineering structures such as abutments or wastewater process tanks has not been studied yet, while other subjects were under research.

A large number research has been undertaken on sand and activated sludge particle sedimentation, but very little research has been done on resuspension the sediment particles from the wastewater treatment tanks. The local scour development mechanism in WWT plant process tanks has not been studied.

The first theory about the efficiency of settling tanks has developed by Hazen^[21] for individual particle settling in a uniform flow. Anderson^[4] discovered that the flow is far from uniform because of density stratification. The solids-loaded influent has a higher density than the ambient water and, hence, plunges as a density jet to the bottom. Density currents, circulation, and short-circuiting are hydraulic phenomena, which occur in sedimentation tanks due to the density differences, stratification of liquid-solids, and tank geometry as concluded by Clark^[11]. To define the different settling characteristics of aqueous suspension, particulates have been categorized into three general classes: discrete, flocculent and hindered particles as supposed by Katz and Geinopolos^[24], Weber and Rowe^[67] and Tchobanoglous and Burton^[63]. Tekippe^[64] showed that minor temperature differences would affect the design variables in inlet and outlet. Hudson, after Ahmed et al.^[3], concluded that the addition of warm influent water to a sedimentation basin containing coolers water could lead to short circuiting phenomena.

Data by Tekippe^[64] have shown that changes in the velocity gradient path can affect the clarifier operation criteria. Larsen^[31] stated the difficulties of flow fields in final settling tanks. Bretscher et al.^[7] have measured the horizontal velocity components by observing a drifting body located at selected positions above the tank bottom. As a result, a secondary counter-current is induced at the surface; even a three- or four-layered structure in the flow field can be experimentally observed^{[31]; [7]; [65]}. Kinnear^[25] stated that the density current is

characterized by high velocities and appears in the vicinity of the solids blanket. Therefore, settled solids may resuspend with increasing flow rates and can be transported to the effluent weirs; consequently, the effluent quality deteriorates. It is clear from the results of studies that the flow field in the settling tank determines the breakup of flocculated particles. Obviously, it will affect the settling and resuspension of solids in the tank as well, Takamatsu et al. ^[62]. In this respect, Baud and Hager ^[6] observed tornado vortices in the corners of rectangular settling tanks. They were capable of scouring the top of the solids blanket and significantly reduce the solids removal efficiency. The hydraulics of secondary settling tanks therefore has a large influence on the efficiency of the WWTP. The existing grit tanks or sedimentation clarifiers are designed on simple criteria, such as detention time and hydraulic load on surface area assume that the fluid distribution and particle settling in the clarifier is uniform and removal efficiency of particles with a known settling velocity in a settling tank can be simply calculated by ideal horizontal flow reactor theory.

A large amount of literature has been published on the local scour development at bridge abutments and piers. This chapter attempts to summarize the present state of understanding of local scour developments during the floods at the abutments of the bridge constructions and presented a critical review of relevant literature and concepts that are controversial are highlighted.

2.1 Scour prediction methods

Equations describing the conditions of local scour at bridge sites are complex and hence the initial research into the problem was empirical. More recently, attempts have been made at analytical solutions, but these too have had to rely heavily on the results of experiments. Thus, there is no rigorous theoretical solution to the problem.

To estimate the scour depth the formulas are grouped into two categories ^[5]:

- 1) Regime approach relating scours depth to the increased discharge intensity;
- 2) Dimensional analysis approach based on experimental or field data.

2.1.1 Regime approach

In the regime approach Lacey ^[29], after Rahman and Haque ^[47], introduced the formula for the prediction of the maximum scour depth around the piers and abutment like structures. The scour depth is a function of the flow discharge at the contracted section. There were used

field data from irrigation canals and introduced the formula for prediction of the maximum scour depth around piers and spur dikes.

$$\frac{h_s}{h_l} = 0.47k_l \left(\frac{Q}{f \cdot h_l^3} \right)^{1/3} - I, \quad (2.1)$$

where h_s = scour depth measured from the initial bed level; h_l = approach flow depth; Q = regime discharge; f = silt factor; k_l = amplification factor for local scour depth depending on the type of obstruction; and d_{50} = mean diameter of bed sediment.

Equation (2.1) is developed within the following ranges of hydraulic condition: $0.70 \leq Q \leq 1.73$, $0.5 \leq h_l \leq 3.0$, $0.14 \leq Fr \leq 0.21$, $0.00013 \leq I \leq 0.0005$, where, Fr and I are the Froude number and longitudinal energy gradient, respectively. The silt factor is $f = 1.76\sqrt{d_{50}}$.

Based on Lacey regime formula Sir Claude Inglis, after Chiew^[10], proposed a scour prediction equation (Inglis-Lacey):

$$h_s = 0.946 \cdot \left(\frac{Q}{f} \right)^{1/3}, \quad (2.2)$$

where h_s = scour depth; Q = flow discharge; f = silt factor (Lacey silt factor $f = 1.59\sqrt{d_{50}}$); and d_{50} = mean diameter of bed material.

The equation resulted from collection of scour data at various bridge sites in India. He reasoned that the effect of bridge piers is to deflect the current like bend and therefore proposed that the maximum scour depth h_s is proportional to Lacey^[29] regime depth.

Inglis-Poona equation, after Melville^[37]:

$$\frac{h_s}{h_l} = 2.32 \cdot \left(\frac{Q^{2/3}}{h_l} \right)^{0.78}, \quad (2.3)$$

where h_s = scour depth; h_l = approach flow depth; Q = regime discharge.

The results were based on the model tests carried out by Inglis, after Melville^[37]. It was assumed that the maximum scour depth at an obstruction could be estimated by multiplying this flood regime depth by a factor dependent on the geometry of this obstruction.

In the practice, no distinction is made between clear-water scour and scour with continuous sediment motion, although researchers stated explicitly that the Poona experiments were run without sediment load.

Based on laboratory experiments Ahmad ^[1] used regime approach and proposed a maximum scour-depth relationship for spur dikes that used the “flow intensity” or flow rate per unit width in the contracted section, as the independent variable:

$$h_s + h_I = k_2 \cdot q^{2/3}, \quad (2.4)$$

where h_s = scour depth at spur dikes; h_I = approach flow depth; q = flow rate per unit width; k_2 = constant depending on flow intensity and angle of inclination of spur dike (k_2 = multiplying factor dependent on the shape of the pier or abutment - and ranging from 1.9 to 3.4). In practice, the equation is very dependent on choice of k_2 , which was inadequately defined.

The regime concept was originated from the analysis of general scour in live-bed conditions and was extended to local scour prediction at spur dikes and abutments on the basis of observations. However, the sediment characteristics, rate of scour and mode of sediment transport was not considered, after Barbhuiya and Dey ^[5], as well as hydraulic and geometric regularity because of obstruction.

2.1.2 Dimensional analyses

Using the Buckingham p-theorem and employing physical reasoning, various investigators combined the appropriate parameters affecting the scour depth at an abutment in different non-dimensional forms, which are as follows.

Garde et al. ^[14] correlated the scour depth with dimensionless parameters as:

$$\frac{(h_s + h_I)}{h_I} = f(a, q, Fr, C_D) \quad \text{or} \quad \frac{(h_s + h_I)}{h_I} = \left(\frac{K_I}{a} \right) Fr^n \quad (2.5)$$

where $a = (L - L_a)/L$ = the opening ration in which L = the width of the channel and L_a = abutment width; θ = angle of inclination of spur dyke with the direction of approaching flow; $Fr = V_I / \sqrt{gh_I}$ = Froude number, in which V_I = the approaching flow velocity, and $C_D = [4(S - 1)gd] / (3rw_s^2)$ = drag coefficient of sediment; $S = \rho_s / \rho$; and w_s = settling velocity of sediment.

Liu et al. ^[36] considered the scour around bridge constrictions caused by abutment models in 1.2 m wide and 2.4 m wide flumes. Their experimental results for live-bed scour indicated that the ratio of the abutment length to the normal depth, L_a/h_0 , and the uniform-flow Froude number were the most important influences on the dimensionless scour depth. The normal depth was determined with sediment in equilibrium transport before the abutment was placed in the flume. They proposed an equation for equilibrium live-bed scour depth h_s at spill-through abutments:

$$\frac{h_s}{h_0} = 1.1 \left(\frac{L_a}{h_0} \right)^{0.4} Fr_0^{1/3} \quad (2.6)$$

For clear-water scour at wing wall or vertical wall abutments Liu et al. ^[36] presented:

$$\frac{h_s}{h_0} = 2.15 \left(\frac{L_a}{h_0} \right)^{0.4} Fr_0^{1/3} \quad , \quad (2.7)$$

where L_a = abutment length (vertical wall); h_0 = normal depth of flow; and Fr_0 = Froude number of uniform flow. The experimental values of L_a/h_0 varied from approx. 1 to 10, and the Froude numbers varied from 0.3 to 1.2. In a separate series of experiments, clear-water scour was studied by pre-forming the scour hole and determining the flow conditions necessary to just initiate sediment motion in the bottom of the scour hole. In this case, the dimensionless clear-water scour depth was found to be directly proportional to Fr/M , where M = geometric contraction ratio defined by the ratio of the constricted channel width to the approach channel width. The coefficient of proportionality was approximately 12.5.

Laursen ^[32] developed scour-depth relationships for bridge abutments that were based on treating the abutment as a limiting case of scour through a long flow constriction and applies to the live-bed scour at an abutment encroaching into the main channel as follows:

$$\frac{L_a}{h_I} = 2.75 \frac{h_s}{h_I} \left[\left(\frac{h_s}{11.5h_I} + 1 \right)^{1.7} - 1 \right], \quad (2.8)$$

The equation applies to live-bed scour at an abutment encroaching into the main channel, when $L_a/h_I > 25$ and where conditions are similar to the field conditions from which the equation was derived; h_I = approach flow depth.

Live-bed scour was considered to be a function only of the ratio of the abutment length to the approach flow depth, L_a/h_1 , and the ratio of the discharge per unit width in the over-bank flow region to the discharge per unit width in the scour region. The scour region was assumed to have a constant width of 2.75 times the scour depth. In a subsequent analysis of relief-bridge scour, which was considered to be a case of clear-water scour, the same approach was taken in relating the abutment scour to that which would take place in a long constriction. The contracted width was assumed to be equal to a scour-hole width of 2.75 times the scour-hole depth.

Gill ^[15] argued from his experimental results on the scour of sand beds around spur dikes that the distinction between clear-water and live-bed scour is unimportant for the design determination of maximum scour depth. He proposed that the maximum scour depth be based on the geometric contraction ratio M , and on the ratio of the sediment size to the flow depth based on both clear-water and live-bed scour experiments having a duration of 6 hours. His proposed equation is:

$$\frac{h_s}{h_0} + 1 = 8.38 \left(\frac{d_{50}}{h_0} \right)^{1/4} \left(\frac{1}{M} \right)^{6/7}, \quad (2.9)$$

where h_0 = initial uniform flow depth; d_{50} = median sediment grain size; and $M = L/(L-L_a)$ = geometric contraction ratio given by the ratio of the full channel width to the contracted width of channel.

He had been tested 252 data of clear-water scour case in rectangular channels and employs general properties of sediment and flow. These points provide generality of the formula to be improved towards the case of abutment terminating in a floodplain:

$$\frac{h_{equil}}{h_1} = K_s \left\{ 2 \left(\frac{u_*}{u_{*c}} \right)^{0.75} \left[0.9 \left(\frac{L_a}{h_1} \right)^{0.5} + 1 \right] - 2 \right\}, \quad (2.10)$$

where h_{equil} = equilibrium scour depth; K_s = abutment shape coefficient; u_{*1} = shear velocity at approach section; u_{*c} = critical shear velocity; h_1 = approach flow depth.

The u_* = shear velocity can be expressed as a function of mean velocity V , Manning's n roughness coefficient, gravitational acceleration g and hydraulic radius R , as follows:

$u_* = \sqrt{t/r} = \sqrt{gRS_f} = Vn\sqrt{g/R^{1/3}}$. As the shear velocity is proportional to the mean velocity and assuming that the rest of the parameters have same value, the ratio of the

approach and critical value of shear velocity can be substituted by their corresponding mean velocity as in (2.10). Equation (2.11) is preferred as it uses bulk parameters of the flow and abutment, which are more practical to use:

$$\frac{h_{equil}}{h_1} = K_s \left\{ 2 \left(\frac{V_1}{V_c} \right)^{0.75} \left[0.9 \left(\frac{L_a}{h_1} \right)^{0.5} + 1 \right] - 2 \right\} \quad (2.11)$$

The equation (2.11) is valid only for: $(V_1/V_c)^{0.75} [0.9(L_a/h_1)^{0.5} + 1] \geq 1$ so that $h_{equil}/h_1 = 0$ when $(V_1/V_c)^{0.75} [0.9(L_a/h_1)^{0.5} + 1] = 1$.

Laursen, after Richardson et al. ^[52], developed the formula that applies to clear-water scour at an abutment encroaching into the main channel as follows:

$$\frac{L_a}{h_1} = 2.75 \frac{h_s}{h_1} \left[\frac{\left(\frac{1}{11.5} \frac{h_s}{h_1} + 1 \right)^{7/6}}{\sqrt{\frac{\tau_0}{\tau_c}}} - 1 \right], \quad (2.12)$$

where τ_0 = bed shear stress of approach flow; and τ_c = critical shear stress for initiation of sediment motion for sediment size d_{50} . Maximum scour depth that should be accepted from Laursen's equation is $h_s = 4h_1$, because the field observations of scour around spur dikes on the Mississippi River from which the equation was derived never exceeded $4h_1$.

Froehlich ^[13] completed a regression analysis of 164 laboratory experiments from 11 separate sources on clear-water scour around abutments or spur dikes. His proposed regression equation is:

$$\frac{h_s}{h_1} = 0.78 K_1 K_2 \left(\frac{L'_a}{h_1} \right)^{0.63} Fr_1^{1.16} \left(\frac{h_1}{d_{50}} \right)^{0.43} S_g^{-1.87} + 1 \quad \text{for clear-water scour} \quad (2.13)$$

$$\frac{h_s}{h_1} = 2.27 K_1 K_2 \left(\frac{L'_a}{h_1} \right)^{0.43} Fr_1^{0.61} + 1 \quad \text{for live-bed scour} \quad (2.14)$$

where h_s = scour depth; h_1 = approach flow depth, K_1 = geometric shape factor for abutment and embankment, K_2 = embankment alignment factor, L'_a = abutment length projected normal to flow, Fr_1 = approach flow Froude number, d_{50} = median sediment grain size, and

$S_g = (d_{84}/d_{16})^{0.5}$ = geometric standard deviation of the sediment size distribution, where d_{84} and d_{16} = median sediment grain size (particle size for which 84% and 16% are finer by weight, respectively). Froehlich calculated the approach Froude number based on an average velocity and depth in the obstructed area of the approach-flow cross section. While this worked well for the experimental results that he used, which were for rectangular channels, it is not clear what the representative approach velocity and depth should be in natural channels subject to over bank flow. Froehlich further proposed that a factor of safety FS of 1 should be added to the value of h_s/h_l obtained from the regression analysis, and it has been included on the right-hand side of equations (2.13) and (2.14). Safety factor makes the equation predict a scour depth larger than any of measured scour depth in the data.

HIRE (“Highways In The River Environment”) by Richardson et al. ^[53] and U.S. Department of Transportation recommended using the live-bed and clear-water abutment scour calculation equations obtained by Liu et al. ^[36], Laursen ^[32] and Froehlich ^[13] for bridge foundation design in the United States.

For predicting scour around long abutments (with $L_a/h > 25$) terminating in the main channel, original equation was presented in HIRE ^[52], while later HEC-18 (Hydraulic Engineering Circular No. 18 issued by Federal Highway Administration for bridge engineers in U.S.) by Richardson and Davis ^{[50]; [51]} recommended using modified HIRE equation for calculation of clear-water and live-bed scour:

$$\frac{h_s}{h_c} = \frac{4}{0.55} Fr^{0.33} K_1 K_2, \quad (2.15)$$

where h_s = scour depth, h_c = depth of flow at the abutment on the over-bank or in the main channel, Fr = Froude number based on the velocity and depth adjacent to and upstream of the abutment; K_1 = coefficient for abutment shape, and K_2 = coefficient for angle of embankment to flow calculated as for Froehlich’s Eqs. (2.13) and (2.14). Equation (2.15) was developed from the U.S. Army Corps of Engineers’ field data for scour at the end of spur dikes on the Mississippi River, and it should be accented that scour depth was recommended to calculate at bridge abutments if conditions are similar to the field conditions from which the equation was derived.

In HEC-18, by Richardson and Davis ^[51], was published modified Froehlich’s ^[13] equation (2.13), where L_a' was replaced with L' = length of active flow obstructed by embankment, and were used $Fr = V_e/(gh)^{0.5}$ = Froude number of approach flow upstream of

the abutment, $V_e = Q_e / A_e$; Q_e = flow obstructed by the abutment and approach embankment; A_e = flow area of the approach cross section obstructed by embankment; h = average depth of flow on the floodplain.

Melville^{[37]; [38]; [39]} summarized a large number of experimental results on clear-water abutment scour from rectangular channels and proposed a design method for maximum scour depth that depends on empirical correction factors for flow intensity, abutment shape, alignment, and length. He classified abutments as short ($L_a/h_1 < 1$) or long ($L_a/h_1 > 25$), and suggested that the maximum clear-water scour depth was $2L_a$ for the former case and $10h_1$ for the latter case. For intermediate abutment lengths, the equilibrium clear-water scour depth was given as:

$$h_s = 2K_I K_S^* K_q^* (h_1 L_a)^{0.5}, \quad (2.16)$$

where K_I = flow-intensity factor (V_1/V_c), V_1 = approach flow velocity, V_c = critical flow velocity for initiation of sediment motion, K_S^* = adjusted abutment shape factor, K_q^* = adjusted abutment alignment factor, h_1 = approach flow depth, and L_a = abutment length.

Subsequently, Melville suggested that the same methodology could be applied to both bridge piers and abutments, albeit with slightly different equations. He further showed that sediment size effects appear only in the flow-intensity factor for clear-water scour as long as $L_a/d_{50} > 25$. Abutment shape effects were reported to be important only for shorter abutments (i.e., $K_S = 1.0$ for vertical-wall abutments; 0.75 for wing-wall abutments; and from 0.45 to 0.60 for spill-through abutments), depending on the side-slope, but only if $L_a/h_1 = 10$. For long abutments ($L_a/h_1 \geq 25$), $K_S \leq 1.0$ with a linear relationship between K_S and L_a/h_1 for the intermediate range of $L_a/h_1 = 10$ to 25. It must be emphasized that all of Melville's integrated abutment/pier results^[39] are considered to be for abutments that are significantly shorter than the floodplain width itself so that flow contraction effects are not important.

Live-bed abutment scour results were also summarized by Melville^[39], for short abutments using Dongol's^[12] data under clear-water conditions ($V_1 < V_c$), the scour depth increased to a maximum at $V_1/V_c = 1$. For live-bed conditions ($V_1 > V_c$), the scour depth decreased slightly as V_1 increased, but then increased again to a value equal to the maximum clear-water scour. Piers showed the same behavior under live-bed conditions.

Melville formulated temporal maximum scour depth as equilibrium scour depth under certain conditions for following conditions:

$$\text{for short abutments} \quad \frac{h_s}{L_a} = 2K_I K_d K_\sigma K_s K_\theta K_G, \quad (2.17)$$

$$\text{for long abutments} \quad \frac{h_s}{h_l} = 10K_I K_d K_s K_q K_G, \quad (2.18)$$

$$\text{for intermediate abutments} \quad \frac{h_s}{\sqrt{L_a h_l}} = 2K_I K_d K_s K_s^* K_q^* K_G, \quad (2.19)$$

where h_s = scour depth, L_a = abutment length, h_l = approach flow depth, K_I = flow intensity factor, K_d = sediment size factor, K_σ = sediment gradation factor, K_s = abutment shape factor, K_s^* = adjusted shape factor for intermediate abutments, K_θ = abutment alignment factor, K_θ^* = adjusted alignment factor for intermediate abutments, and K_G = channel geometry factor. Melville used experimental data to define K_I , K_s , and K_θ , but admitted that insufficient or no data were then available to define other K factors.

Melville and Ettema^[41], and Melville^[38] reported research results on abutment scour in a compound channel, but for the case of an abutment terminating in the main channel rather than on the floodplain. It was proposed that the scour depth in this instance could be calculated as the scour in an equivalent rectangular channel of the same width and with a depth equal to the main-channel depth by a geometric factor given as:

$$K_G = \sqrt{1 - \frac{B_{fl}}{L_a} \left[1 - \left(\frac{h_{fl}}{h_m} \right)^{5/3} \frac{n_m}{n_{fl}} \right]}, \quad (2.20)$$

where L_a = abutment length extending into main channel; B_{fl} = width of floodplain; h_{fl} = depth of flow in floodplain; h_m = depth of flow in main channel; n_m = Manning's roughness coefficient n in main channel; and n_{fl} = Manning's n in floodplain.

Melville and Coleman^[40] improved Eqs. (1.17), (1.18), and (1.19) since with flow depth - foundation size factor K_{hL} , explained sediment size factor K_d , proposed time factor K_t , and finally scour prediction equation for all length of abutments was as follows:

$$h_s = K_{hL} K_I K_d K_s K_q K_G K_t, \quad (2.21)$$

where K_{hL} = flow depth – foundation size factor; K_d = sediment size factor; and K_t = time factor. Sediment size factor is: $K_d = 0.57 \log(2.24L_a/d_{50})$. A sediment size effects appears only in the flow-intensity factor for clear-water scour as long as $L_a/d_{50} \leq 25$. Melville and Coleman^[40] underlined that Melville's scour prediction equation (Eq. 2.21) is based on laboratory data

derived from idealized models of bridge crossings and equations have limitations due to that, as follows: rigid, idealized abutment models; straight and rectangular laboratory flumes; steady and uniform approach flow; non-cohesive, homogeneous, and often uniform size bed materials.

Sturm and Janjua ^[60] conducted the experiments in a flume with a fixed-bed main channel and a movable bed in floodplain. They emphasized that the scour depth does not directly depend on abutment length but depends on the effect of the abutment on the flow redistribution at the contracted section. Hence a contraction parameter M_I was proposed, where $M_I = (Q - Q_{obst}) / Q$; Q = total discharge in compound channel, and Q_{obst} = obstructed discharge in the approach section. The result of a last square regression analysis, based on the important variables obtained using dimensional analysis, was:

$$\frac{h_{equil}}{h_{fl}} = 7.70 \left(\frac{Fr_{fl}}{M_I Fr_c} - 0.35 \right), \quad (2.22)$$

where h_{equil} = equilibrium scour depth; h_{fl} = approach floodplain flow depth, Fr_{fl} = Froude number of the floodplain flow; Fr_c = Froude number of flow in the floodplain at critical condition of sediment motion. The parameter M_I may represent the flow condition in a two-stage channel, but its relationship as function of the geometry of two-stage channel as well as approach flow characteristics would be much more applicable in field applications.

Experimental works were done in a horizontal flume. The scouring experiments lasted only 10 to 12 hours and visual observations were used to determine the state of scouring process. According to the authors' experiences, the rate of scour depth development at near equilibrium phase is usually very slow; hence it is possible that the increase of scour depth at this phase was not easily noticeable over a short testing period.

Young et al. ^[70] developed a regression equation for clear-water as well as live-bed abutment scour using the calculated contraction scour as a non-dimensional parameter for the abutment scour depth.

More recently, Young et al. ^[69] suggested an abutment scour equation:

$$(h_I + h_s) = 1.37 \left[\frac{n^2}{t_{*c} (S-1) d_{50}} \right]^{3/7} (h_I V_R)^{6/7}, \quad (2.23)$$

where h_1 = approach flow depth; n = Manning's roughness coefficient; t_{*c} = critical value of Shields' parameter; S = specific gravity of sediment; d_{50} = median particle size; and V_R = resultant velocity adjacent to the tip of the abutment. The resultant velocity is calculated from $V_x/\cos q$, where V_x = mean contraction velocity from continuity and $q = 69.85 (a/A^*)^{0.2425}$ (with a coefficient of determination of $r_2 = 0.54$), where a = blocked flow area by the abutment and A^* = total unobstructed flow area including the main channel to the median flow bisector. Equation (2.23) is not dimensionally homogeneous and is meant for the International System of Units (SI), known as the metric system. It was tested on an experiment by Lim ^[34] with a very short abutment ($L_a/h_1 = 1$) and showed good agreement for this case.

Chang, after Sturm ^[59], has applied Laursen's long contraction theory to both clear-water and live-bed scour. He suggested a velocity adjustment factor k_v to account for the non-uniform velocity distribution in the contracted section, and a spiral-flow adjustment factor k_f at the abutment toe that depends on the approach flow Froude number. The value of k_v was based on potential flow theory, and k_f was determined from a collection of abutment scour experiments in rectangular laboratory flumes. The resulting scour equation ^[58] was:

$$\frac{h_2}{h_1} = k_f \left(\frac{k_v q_2}{q_1} \right)^q, \quad (2.24)$$

where h_2 = flow depth in contracted section after scour; h_1 = approach flow depth; q_1 = flow rate per unit width in approach section; q_2 = flow rate per unit width in contracted section, and $q = 0.857$ for clear-water scour. The value of $k_v = 0.8 (q_1/q_2)1.5 + 1$ and $k_f = 0.1 + 4.5Fr_1$ for clear-water scour, while $k_f = 0.35 + 3.2Fr_1$ for live-bed scour. The approach flow Froude number $Fr_1 = V_1/(gh_1)^{0.5}$. Equation (2.24) does not include the effect of sediment size on clear-water abutment scour. It has since been modified ^[9] to the form:

$$h_2 = k_f (k_v)^{0.857} h_{sc}, \quad (2.25)$$

where h_2 = total depth of flow at the abutment including scour depth; h_{sc} = total depth of flow including the contraction scour depth only; and k_f and k_v are unchanged from the previous formulation. The value of h_{sc} is calculated from q_2/V_c , where q_2 = unit discharge at the contraction and V_c = critical velocity obtained from the expressions given by Neill ^[44]. The

evaluation of q_2 is unclear for the case of the contracted section having a compound section with a variable q_2 across the cross section.

Chang and Davis ^[9] proposed the following equation based on work by Neill ^[44], to estimate the depth of clear-water contraction scour:

$$h = \frac{q}{V_c}, \quad (2.26)$$

where h = total flow depth in the contraction, including the clear-water scour depth; V_c = critical flow velocity for the median grain size of the bed material; and q = unit-width flow in the contraction, and is defined as: $q = Vh_{fc}$, where V = average flow velocity in the contraction prior to scour; and h_{fc} = average flow depth in the contraction prior to scour. The clear-water contraction-scour depth is determined: $h_{contr} = h - h_{fc}$, where h_{contr} = contraction scour depth; and h and h_{fc} were defined earlier.

The U.S. Maryland State Highway Administration (MSHA) ^[42] developed methods for abutment scour prediction by using coefficients applied to contraction scour. These methods were based on research of Chang and Davis ^[9], who applied Laursen's long contraction theory. The abutment scour depth including contraction scour under clear-water conditions, when shear stress of approach section is less than critical shear stress $\tau_0 < \tau_c$, can be found:

$$h_s = \left(k_f \cdot k_v^{0.857} \frac{q_2}{V_c} - h_{sc} \right) \cdot K_1 \cdot K_2, \quad (2.27)$$

where h_s = total scour depth; h_{sc} = average flow depth in contraction prior to scour; $k_f = 0.1 + 4.5Fr_1$ = spiral-flow adjustment factor; $Fr_1 = V_e/(gh_1)^{0.5}$ = approach flow Froude number upstream abutment; V_{ob} = approach flow velocity in obstructed area by embankment; g = gravitational acceleration; $k_v = 0.8(q_1/q_2)^{1.5} + 1$ = dimensionless velocity adjustment factor; q_1 = flow rate per unit width in the approach section; q_2 = flow rate per unit width in contracted section; V_c = critical velocity; K_1 = abutment shape factor; K_2 = coefficient for angle of embankment to flow as for Froehlich's equation. The values of k_v were limited to the range from 1.0 to 1.8, and k_f within range from 1.0 to 3.3. Factor of safety of 20-40% of computed scour value was proposed to use for engineers.

Lim ^[34] has derived an equation for predicting clear-water abutment scour:

$$\frac{h_s}{h_I} = K_S^* (0.9X - 2), \quad (2.28)$$

where h_s = scour depth; h_I = approach flow depth; K_S^* = abutment shape factor; and X is expressed as: $X = \left[Fr_d (d_{50} / h_I)^{0.25} / t_{*c}^{0.375} \right] \cdot [0.9(L_a / h_I) + 1]$, where Fr_d = approach flow value of the dens metric grain Froude number; t_{*c} = critical value of Shields' parameter; d_{50} = median grain size; and L_a = abutment length. Equation was derived on the basis of satisfying continuity before and after scour, evaluating the velocity before and after scour in the contracted section from a power law with an exponent of 1/3, and using an expression for the shear velocity in the contracted expression proposed by Rajaratnam and Nwachuku [48]. The latter expression is limited to values of $L_a/h_I \leq 1$. Lim tested equation on his own abutment scour data as well as on data from Dongol [12], Rajaratnam and Nwachuku [48] and Liu et al. [36] that was, for the most part, limited to very short abutments with $L_a/h_I \leq 1$.

Lim and Cheng [35] have also proposed an abutment scour-prediction equation for live-bed scour. He assumed that the sediment transport in a strip of the approach section, with a width equal to the abutment length plus the scour-hole width, is carried completely through the scour-hole width in the contracted section. The scour-hole width is estimated as $h_s / \tan j_i$, where j_i = angle of repose of the bed material.

Meyer-Peter and Muller, after Julien [23], using a sediment transport relationship similar to that of given by Lim [34] for live-bed scour, and by making the same assumptions as for his clear-water scour equation, the resulting equation is:

$$\left(1 + \frac{h_s}{2h_I} \right)^{4/3} = \frac{1 + 1.2 \sqrt{\frac{L_a}{h_I}}}{\sqrt{\frac{u_{*c}^2}{u_{*I}^2} + \left(\frac{L_a \tan j_i}{h_s} + 1 \right)^{2/3} \left(1 - \frac{u_{*c}^2}{u_{*I}^2} \right)}}, \quad (2.29)$$

where u_{*I} = approach value of shear velocity and u_{*c} = critical value of shear velocity. When $u_{*c}/u_{*I} > 1$, the term $[1 - (u_{*c}/u_{*I})^2]$ is taken as equal to zero and equation (2.29) reduces to the clear-water scour case according to Lim. This equation still suffers from the dependence on abutment length and the limitation on the expression for shear stress for very short abutments as pointed out for the clear-water scour case by Richardson [49].

Kouchakzadeh and Townsend [26] shows that the ratio of flow obstructed by abutment Q_e to the flow at a specific width near the tip of the abutment Q_w , was a significant parameter

in estimating the equilibrium scour depth. The formulation of the functional relationship is based on:

$$\frac{h_{equil}}{h_I} = f\left(Fr_c, Fr_I, \frac{Q_e}{Q_w}, K_I\right), \quad (2.30)$$

where Q_w = specific discharge for a certain width “w” near the abutment tip; h_I = approach flow depth; K_I = shape factor, Q_e = discharge for width “w” at the approach section; Fr_I = Froude number of at approach section; and Fr_c = Froude number when the sediment is at incipient motion condition.

Cardoso and Bettés ^[81] based on several short and long period of scouring experiments which indicated that the scour depth at 5 hours was approximately 60% and 65% of equilibrium scour depth for d_{50} of 0.5 and 0.7 mm, respectively. The flow depth ratios in their experiments were in the range of 0.22 to 0.29. The final formulation was obtained from regression-analysis by using their experimental data:

$$\frac{h_{equil}}{h_{fl}} = 13.5 \left(\frac{Q_w}{Q_e}\right)^{3.9} Fr_I^{1.17} Fr_c^{-0.25} \quad (2.31)$$

where h_{equil} = equilibrium scour depth; h_{fl} = floodplain flow depth; Q_w = specific discharge for a certain width “w” near the abutment tip; Q_e = discharge for width “w” at the approach section; Fr_I = Froude number of at approach section; and Fr_c = Froude number when the sediment is at incipient motion condition. The Q_w quantity is related to the abutment length as well as the geometry of the two-stage channel. The value of Q_w/Q_e in eq. (2.31) ranges from 0.78 to 0.85.

Kothyari and Ranga Raju ^[28] admitted that scour processes at bridge piers, abutments and spur dikes have been found to be similar, except boundary layer effect induced by the channel wall upstream of the abutment or spur dike causes less scour around these compared to the case of piers, and used Kothyari et al. ^[27] equilibrium depth of scour at bridge piers calculation method to calculate equilibrium depth of scour at abutments or spur dikes under clear-water and live-bed conditions. Author used concept of analogous pier, which would have the same equilibrium depth of scour as the given abutment or spur dike under similar hydraulic conditions. Equilibrium depth of scour at abutment under clear-water conditions can be found:

$$\frac{h_{equil}}{b_s} = 0.66 \left(\frac{b_s}{d} \right)^{-0.25} \left(\frac{h}{d} \right)^{0.16} \left(\frac{V^2 - V_c^2}{\frac{Dg_s}{r_f} d} \right)^{0.4} a_1^{-0.3}, \quad (2.32)$$

where h_{equil} = equilibrium scour depth; b_s = size of analogous pier; d = sediment size; h = flow depth; $a_1 = (L - b_s) / L$ = opening ratio; L = flume width; V = average flow velocity; $V_c = [1.2(\Delta\gamma_s d / \rho_f)(b_s/d)^{-0.11}(h/d)^{0.16}]^{0.5}$ = critical flow velocity, $\Delta\gamma_s = \gamma_s - \gamma_f$, where γ_s = specific weight of sediment; γ_f = specific weight of water; and ρ_f = mass density of water.

Sturm ^[59] performed a large number of experiments on the abutment scour in compound channel flume. The scour depth was measured as a function of discharge, sediment size, abutment shape and length, as well as water-surface profiles, velocities and scour hole contours were measured. Sturm observed that discharge distribution factor is the appropriate variable to use rather than abutment length to measure the effects of flow contraction and flow redistribution in the contracted section on local scour depths. He suggested scour prediction equation for either setback (shorter abutments terminating in floodplain) and bank-line abutments (located at the edge of the main channel) under clear-water conditions:

$$\frac{h_{equil}}{h_{fl}} = K_{ST} \cdot C_r \cdot \left(\frac{q_1}{M_1 \cdot V_{xc} \cdot h_{fl}} - C_0 \right) + FS \quad (2.33)$$

where h_{equil} = equilibrium scour depth; h_{fl} = normal flow depth in floodplain for un-constricted conditions; K_{ST} = spill-through abutment shape factor; $C_r = 8.14$ = best-fit coefficient in proposed equation; $C_0 = 0.40$ = best-fit constant in proposed equation; $M_1 = [Q_c + (Q_{fl} - Q_a)] / Q$ = discharge distribution factor in approach section; Q = total discharge; Q_c = discharge in main channel for uniform flow in compound channel; Q_{fl} = discharge in approach floodplain; Q_a = discharge in obstructed area over a length equal to abutment length; $q_1 = V_e h_{fl}$ = flow rate per unit width in the approach obstructed portion of floodplain; V_e = average approach flow velocity in the obstructed portion of floodplain; h_{fl} = average approach flow depth in the obstructed portion of floodplain; $V_{xc} = V_{flc}$ for abutments located on the floodplain and $V_{xc} = V_{cc}$ for abutments located near the bank of the main channel, where V_{flc} = critical velocity for the un-constricted approach flow in the floodplain evaluated for h_{fl} , V_{cc} = critical velocity for the un-constricted approach flow in the main channel evaluated for normal flow depth h_c in the main channel. Sturm recommended to add a value

of $FS = 1$, because FS is greater than the standard error of 0.75 for h_s/h_{fl} for the best fit of the experimental data. Spill-through abutment shape factor is: $K_{ST} = 1.52(\zeta-0.67)/(\zeta-0.40)$ for $0.67 \leq \zeta \leq 1.2$; $K_{ST} = 1$ for $\zeta \geq 1.2$; and $K_{ST} = 0$ for $\zeta \leq 0.67$, where $\zeta = q_l/(M_1 V_{xc} h_{fl})$.

Pirestani et al. ^[46] from their experiments under different h_l/L , φ and Fr values, optimized the following relationship: $h_s/L = f(Fr, Fr^*, Re^*, \frac{h_l}{L}, j, q)$, where $Fr^* = u_*^2/[g(S-1)d_{50}]$; u_* = shear velocity. Fr^* and Re^* are negligible by considering a constant value for d_{50} and also intake location is constant, therefore equation is simplified as:

$$\frac{h_s}{L} = 0.7314 Fr^{0.691} j^{0.231} \left(\frac{h_l}{L} \right)^{0.293}, \quad (2.34)$$

where h_s = scour depth; h_l = approach flow depth; L = width of the main channel; φ = main channel radius of curvature R . Dimensionless parameter for maximum scour hole depth h_s was obtained by applying the dimensional analysis and π theory.

The time to equilibrium of the scour process is important in establishing the necessary duration of the experiments. One consequence of developing scour equations from laboratory data for the equilibrium condition is that in the field case for small watersheds, the duration of the design discharge may be considerably shorter than the time to reach equilibrium. The result is an overestimate of field scour for a given design event. The time development of scour better describe the effect of event duration on the scour depth. It should be considered that scour can be cumulative over many events, like multiple floods.

2.2 Summary of scour calculation methods

Most of scour calculation methods were derived by empirical approach from idealized laboratory flume experiments with steady flow conditions, and results were correlated through dimensional analysis. Analyze of scour calculation methods showed that there is no unified approach which hydraulic and riverbed parameters should be used as scour control parameters.

In discussed scour calculation equations either average upstream approach flow velocity or approach flow velocity in obstructed area by embankment and abutment were used while many researches ^{[30]; [2]; [59]; [69]} were done underlining importance of local flow velocity at protruding obstacles. It will be showed further in the text that local flow velocity is

important scour control parameter, and that local flow velocity together with vortex structures is forming scour hole at abutments.

Bulk of scour calculation methods are using abutment length or geometric contraction rate as scour control parameter, otherwise it is in nature, in plain rivers, where interaction of the flow discharge between channel and floodplain exists that should be considered. Same abutment length may result in different scour depths depending on the approach flow distribution in the compound channel and its redistribution as it flows through bridge opening [59]. Therefore flow discharge contraction rate instead of abutment length should be used as appropriate variable to measure the effects of flow contraction and flow redistribution in the bridge opening on local scour depth.

In nature, the action of flow loads on river engineering structures has the form of hydrograph with unsteady flow conditions, and multiple floods forms scour holes at structures. Analyze of scour calculation methods revealed that existing scour calculation methods can not take into account flow load as flood hydrograph, local flow, and flow contraction effects at protruding structures. Because of the difference between laboratory tests and physical process of scour in nature, the existing equations overestimates the scour depth values [51], leading to over-expensive construction costs.

3 METHOD OF ESTIMATION SCOUR DEPTH DEVELOPMENT IN TIME

3.1 Laboratory set-up

Tests were carried out in the two flumes: first flume was 3.5 m wide and 21 m long (see Figure 3.1), and second flume was 1.35 m wide and 9 m long. Experimental data in flumes for open flow conditions are presented in Table 3.1.

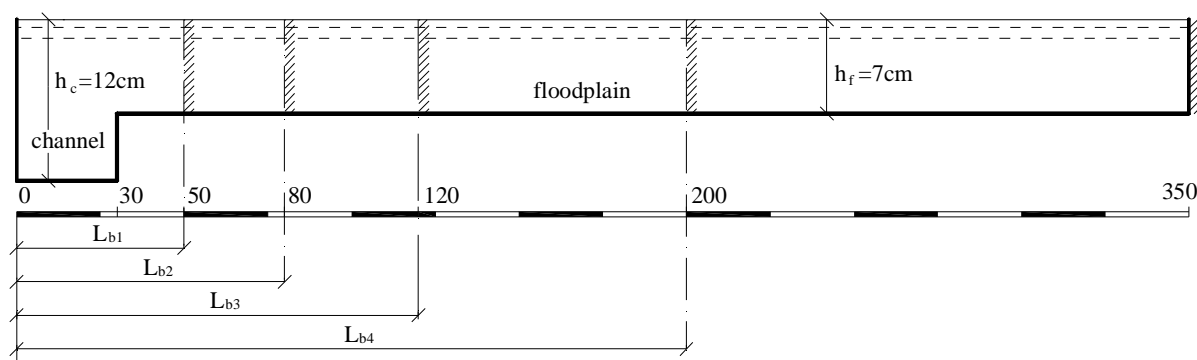


Figure 3.1. Laboratory flume cross section with model bridge openings 50-200 cm

The tests were carried out under open-flow conditions studying the flow distribution between the channel and the floodplain. Tests were performed with rigid (fixed) and sand beds.

The tests with a rigid bed were made for different flow contractions, in order to investigate the velocity and the water level changes in approach to the embankment, along it, and near a model of abutment.

The aim of the tests with a sand bed was to study the scour processes, the changes in the velocity with time, the influence of hydraulic parameters - contraction rate of the flow, grain size of the bed material, and time of scour.

In tests the openings of the bridge model L_b were 50; 80; 120; and 200 cm in the first flume and 44.5; 57.5; 77.5; and 97.5 cm in the second one. The contraction rate of the flow Q/Q_b (Q = total discharge of the flow, and Q_b = discharge of the flow in the bridge opening area in open-flow conditions) varied from 1.25 to 5.69 at a depth of floodplain h_f of 5, 7, and 13 cm. The Froude number Fr varied from 0.0103 to 0.151. The slope in the first and second flumes i_0 was 0.0012 and 0.0015 m/m, respectively. The experimental data for open-flow

conditions are presented in Table 3.1, where Re_R and Re_f are Reynold's numbers for river and flume, respectively.

Table 3.1

Experimental data for open-flow conditions in flumes

Test	L (cm)	h_f (cm)	V (cm/s)	Q (l/s)	Fr	Re_R	Re_f
L1	350	7	6.47	16.60	0.0780	7500	4390
L2	350	7	8.58	22.70	0.0103	10010	6060
L3	350	7	10.30	23.60	0.1243	12280	7190
L4	350	7	8.16	20.81	0.0984	10270	5590/5660
L5	350	7	9.07	23.48	0.1094	11280	6140/6410
L6	350	7	11.10	28.13	0.1339	13800	7550/7840
L7	350	13	7.51	35.48	0.0665	13700	9740
L8	350	13	8.74	41.38	0.0756	16010	11395
L9	350	13	9.90	47.10	0.0876	14300	14300
S1	134.5	5	6.30	4.24	0.0890	7110	3000
S2	134.5	5	9.52	6.50	0.1360	10400	4450
S3	134.5	5	10.58	7.30	0.1510	12090	5000

The tests with sand bed were carried out under clear-water conditions. The sand was placed 1 m up and down the contraction of the flumes. The mean size of grains was 0.24 and 0.67 mm in the first flume and 0.5 and 1.0 mm in the second one with a standard deviation. The scour development in time for the bed materials with different grain size was studied to estimate the identity of the processes. The condition that $Fr_R = Fr_f$ was fulfilled, where Fr_R and Fr_f are the Froude numbers for the plain river and for the flume, respectively. A photo from typical laboratory experiment can be seen in Figure 3.2.



Figure 3.2. Typical scour experiment in flume

The tests in the flumes lasted for 7 hours, the vertical scale was 50, and the time scale was 7. With respect to the real conditions, the test time was equal to 2 days. That was the mean duration of time steps into which the flood hydrograph was divided in presented method.

The tests were made to study scour development in time intervals within one step for 7 hours and for two steps of hydrograph for 7 hours each, with different flow parameters.

3.2 Scour depth development in time

Contraction of the river by bridge crossing causes flow changes and because of that more bed material is transported from contracted section and vicinity of abutments and piers [33]. Increased flow velocities in contracted section, local flow velocities near abutments and piers as well other hydraulic changes of the river causes general and local scours.

Differential equation of equilibrium of the bed sediment movement for local scour near abutments located on the floodplain with no sediment transport from upstream (clear-water conditions) is:

$$\frac{dw}{dt} = Q_s, \quad (3.1)$$

where w = volume of scour hole; t = time; Q_s = sediment discharge out of scour hole through cross section I-I (see Fig.3.3).

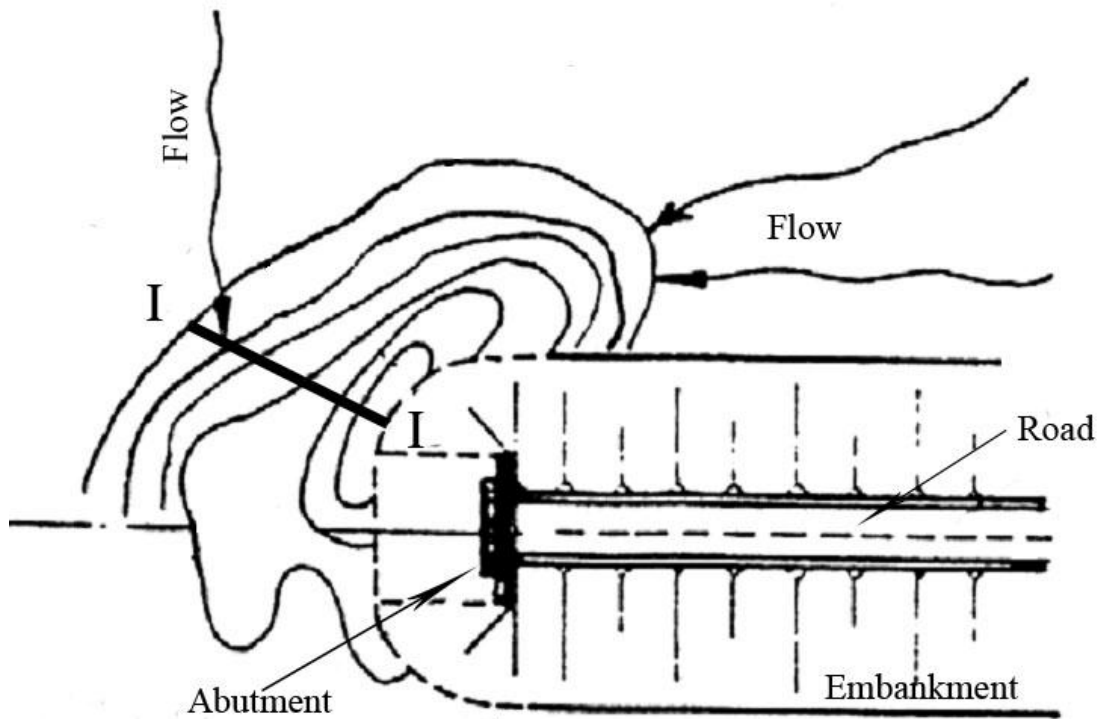


Figure 3.3. Scour near abutment of the bridge

It is necessary to know shape, volume of scour hole, and sediment discharge out of the vicinity area of the abutment, for solving equation (3.1) and to determine scour development in time during the flood.

According to the laboratory tests, the scour hole near abutment is cone – shaped and this shape was the same during the tests and can be determined as:

$$w = \frac{l}{6} p \cdot m^2 h_s^3 \quad (3.2)$$

where l/m = steepness of scour hole; h_s = depth of scour hole.

Shape of scour hole was not depending from hydraulic characteristics of the flow and from the size of the bed material during laboratory tests. The comparison of the same laboratory test results and calculations according to formula (3.2) are given in Table 3.2.

Table 3.2

Comparison of scour hole volume in tests and calculated

Test	Time of test t (min)	Depth of scour hole h_s (cm)	W_{test} (cm ³)	W_{calc} (cm ³)	$W_{\text{test}} / W_{\text{calc}}$
21	220	14.60	4912.0	4760.0	1.032
22	40	13.10	3519.7	3498.0	1.010
22	70	15.20	5660.9	5800.0	0.976
22	90	16.00	6901.0	7520.0	0.920
22	300	19.30	11722.4	11950.0	0.980
27	80	10.10	3072.0	3045.0	1.010
30	120	7.40	1240.9	1255.0	0.987
30	240	7.90	2003.5	1820.0	1.110
31	270	11.50	3165.6	3465.0	0.913

Left part of the equation (3.1) can be written as:

$$\frac{dw}{dt} = \frac{d}{dt} \frac{1}{6} p m^2 h_s^3 = \frac{1}{2} p m^2 h_s^2 \frac{dh_s}{dt} = a h_s^2 \frac{dh_s}{dt}, \quad (3.3)$$

where $a = \frac{1}{2} p m^2$.

Sediment discharge Q_{sc} out of area near abutment through cross section I-I (see Fig.3.3) is determined by Levi^[33] formula:

$$Q_s = A \cdot B \cdot V_l^4 = A \cdot m h_s \cdot V_l^4, \quad (3.4)$$

where $B = m h_s$ = width of scour hole in cross section I-I; V_l = local flow velocity at the abutment; A = parameter in Levi^[33] formula.

Parameter A at the stage of the plain bed is equal to:

$$A_l = \frac{5.62}{g} \left(1 - \frac{b V_0}{V_l} \right) \frac{1}{d^{0.25} h_f^{0.25}}, \quad (3.5)$$

where γ = specific weight of sediments; b = coefficient of velocity V_0 reduction because of vortex system (according to Rozovskij^[54]); V_0 = flow velocity required to start sediment movement; d = medium grain size of the bed material; h_f = depth of water on the floodplain.

According to investigation by Rozovskij^[54] on circulation of curved river flow, it was found that curved flow streamlines induces flow turbulence and vortex structures near

protruding obstacle, and flow velocity, which is necessary for sediment motion, reduces because of turbulence (coefficient β depends on the Reynolds number). Coefficient $\beta = 1.0$ for laboratory flume, and $\beta = 0.8$ for natural river conditions ^[54].

Critical flow velocity at which incoherent sediment movement starts can be found with the help of medium flow depth of floodplain h_{mid} in scour:

$$V_0 = b \cdot d^x \cdot h_{mid}^y, \quad (3.6)$$

where $b, x, y =$ coefficients.

Medium flow depth of cross section I-I with area of scour hole near abutment is found dividing cross section area by the width of scour hole:

$$h_{mid} = \frac{S}{B} = \frac{\left(mh_s h_f + mh_s \frac{h_s}{2} \right)}{mh_s} = h_f \left(1 + \frac{h_s}{2h_f} \right). \quad (3.7)$$

Critical flow velocity according to Studenitnikov ^[58] formula with $b = 3.6, x = 0.25,$ and $y = 0.25$ was used. Development of critical flow velocity changes during flood can be expressed as follows:

$$V_{0t} = 3.6 \cdot b \cdot d^{0.25} h_f^{0.25} \left(1 + \frac{h_s}{2h_f} \right)^{0.25}, \quad (3.8)$$

where $V_{0t} =$ critical flow velocity on every time interval of hydrograph, when depth of scour is equal to h_s ; $V_0 = 3.6 d^{0.5} h_f^{0.25} =$ critical flow velocity at the stage of plane bed.

Hydraulic characteristics - flow contraction rate, value of velocities V_0 and V_l , grain size in different bed layers, sediment discharge, depth and width of the scour were changing during the flood. Critical flow velocity V_{0t} is increasing during scours development, because of scour depth developed in previous time intervals.

According to changes of parameter A, V_0, V_l, h_s during flood, with scour development parameter A is equal:

$$A_2 = \frac{5.62}{g} \cdot \left[1 - \frac{bV_0}{V_l} \left(1 + \frac{h_s}{2h_f} \right)^{1.25} \right] \cdot \frac{1}{d^{0.25} \cdot h_f^{0.25} \left(1 + \frac{h_s}{2h_f} \right)^{0.25}} \quad (3.9)$$

Sediment discharge out of scour hole with development of scour is as follows:

$$Q_s = Amh_s \cdot V_{lt}^4 = b \frac{h_s}{k \left(1 + \frac{h_s}{2h_f} \right)^4} \quad (3.10)$$

where $V_{lt} = V_l / k (1 + (h_s/2h_f))$ = local flow velocity when scour depth is h_s ; $b = AmV_l^4$; k = coefficient of discharge changes because of scour.

Differential equation (3.1) according to formulas (3.3) and (3.10) can be presented as:

$$ah_s^2 \frac{dh_s}{dt} = b \frac{h_s}{k \left(1 + \frac{h_s}{2h_f} \right)^4} \quad (3.11)$$

After separation of variables, formula (3.11) is as follows:

$$D_i \cdot h_s \left(1 + \frac{h_s}{2h_f} \right)^4 dh_s = dt. \quad (3.12)$$

$$D_i = \frac{a}{b} = \frac{pm^2}{2A_i m V_l^4}. \quad (3.13)$$

According to the method hydrograph was divided in time steps and each step in turn was divided into small time intervals (Fig. 3.4). In each time interval sediment discharge is constant. Approximation was made that inside time interval D_i is constant. For one time interval after integration:

$$t = D_i \int_{x_1}^{x_2} h_s \left(1 + \frac{h_s}{2h_f} \right)^4 dh_s \quad (3.14)$$

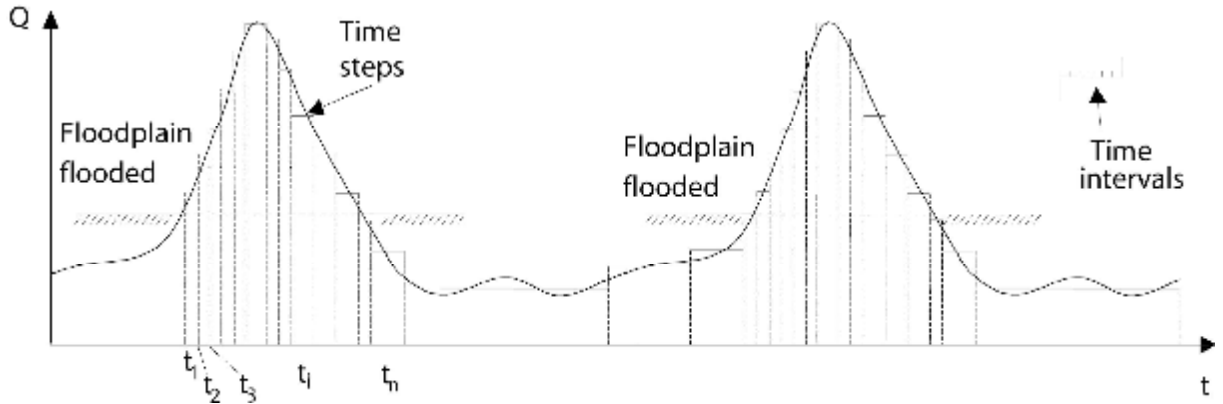


Figure 3.4. Hydrograph divided into time steps and time intervals

Using new variables: $x = 1 + (h_s / 2h_f)$; $h_s = 2h_f (x - 1)$; $dh_s = 2h_f dx$, and definite integral from x_1 to x_2 , formula (3.14) can be written as follows:

$$\int_{x_1}^{x_2} h_s \left(1 + \frac{h_s}{2h_f} \right)^4 dh_s = 4h_f (x^5 - x^4) \Big|_{x_{i-1}}^{x_i} = 4h_f^2 \left[\left(\frac{1}{6} x_i^6 - \frac{1}{5} x_i^5 \right) - \left(\frac{1}{6} x_{i-1}^6 - \frac{1}{5} x_{i-1}^5 \right) \right] \quad (3.15)$$

$$N_i = \frac{1}{6} x_i^6 - \frac{1}{5} x_i^5 \quad (3.16)$$

$$t = 4D_i h_f (N_i - N_{i-1}) \quad (3.17)$$

From formula (3.17) we determine N_i :

$$N_i = \frac{t_i}{4D_i h_f^2} + N_{i-1}, \quad (3.18)$$

where t_i = time interval inside time step of hydrograph.

With graph $N = f(x)$ or Table 3.3 for calculated N_i we determine x_i and depth of scour at the end of time interval:

$$h_s = 2h_f (x - 1) \quad (3.19)$$

Table 3.3

N_i dependence from x_i

x_i	1	1.2	1.4	1.6	1.8	2.0	2.2	2.4	2.6	2.8
N_i	-0.033	0.0002	0.18	0.70	1.90	4.29	8.62	15.98	27.20	46.07

We find parameter N_i from formula (3.18), value x_i from Table 3.3, and scour depth for the first time interval of hydrograph inside first time step of hydrograph from formula (3.19).

Further we find depth of scour for the next time interval inside the first time step of hydrograph. Parameter A_2 can be found by formula (3.9), and D_2 by formula (3.13), after calculation of N_i and reading of x_i from Table 3.3. Afterwards we find scour depth at the end of second time interval according to formula (3.19).

There can be several time intervals inside the one time step of hydrograph. After finding depth of scour at the end of the first time step of flood hydrograph, we go for the second time step with new hydraulic and riverbed characteristics and calculate A_1'' and D_1'' , according to the value of scour depth calculated for the end of the first time step of hydrograph. We determine value of $x'' = 1 + h_s / 2h_f''$ with a new floodplain depth h_f'' . According to x'' , we find the parameter N_{i-1} from Table 3.3. After N_i calculation from formula (3.18), we find x_i'' from Table 3.3, and finally determine scour depth by formula (3.19) at the end of that time interval inside second time step of hydrograph.

In such way, we take several time intervals inside one time step of hydrograph, and determine scour depth development with new steady hydraulic parameters. After calculating depth of scour at the end of the time step, we go to the next time step of hydrograph with a new hydraulic and riverbed characteristics. By this methodology we can calculate scour depth for all time intervals and time steps in which flood hydrograph was divided.

To determine scour depth during the flood hydrograph was divided in time steps with duration of 1 or 2 day and each time step was in turn divided into time intervals equal up to several hours or less. In laboratory tests time steps were divided for 20 time intervals. For each time step it is necessary to know: h_f – depth of water on floodplain, Q/Q_b – flow contraction rate, Δh – maximum backwater level, d – medium grain size, H – thickness of the bed layer with d , γ_s – specific weight of bed material. As result we have V_i , V_0 , A , D_i , N_i , N_{i-1} and h_s at the end of time intervals and finally at the end of time step. For next time step flow parameters were changed because of the flood and because of scour in previous time step.

According to researches done by Yaroslavcev ^[68], Richardson and Davis ^[50], Richardson et al. ^[52], Ahmad ^[1], and others, it was found that scour depth depends also on the slope of the side-wall and the shape of the abutment, and the angle of flow crossing. Accounting these factors, scour depth can be calculated:

$$h_s = 2h_f(x-1) \cdot k_m \cdot k_s \cdot k_a, \quad (3.20)$$

where k_m = coefficient depending on the sidewall slope of the abutment (Table 3.4 according to Yaroslavcev^[68]), k_s = coefficient depending on the abutment shape (Table 3.5 according to Richardson and Davis^[50]), and k_a = coefficient depending on the angle of flow crossing (Figure 3.5 according to Richardson et al.^[52]).

Table 3.4

Coefficient k_m versus the side-wall slope of the abutment
(after Yaroslavcev^[79])

Side-wall slope of the abutment	0	1.0	1.5	2.0	2.5	3.0
k_m	1	0.71	0.55	0.44	0.37	0.32

Table 3.5

Coefficient k_s versus the abutment shape
(after Richardson and Davis^[58])

Abutment shape	k_s
Vertical-wall	1.0
Vertical wall abutment with wing-walls	0.82
Spill-through	0.55

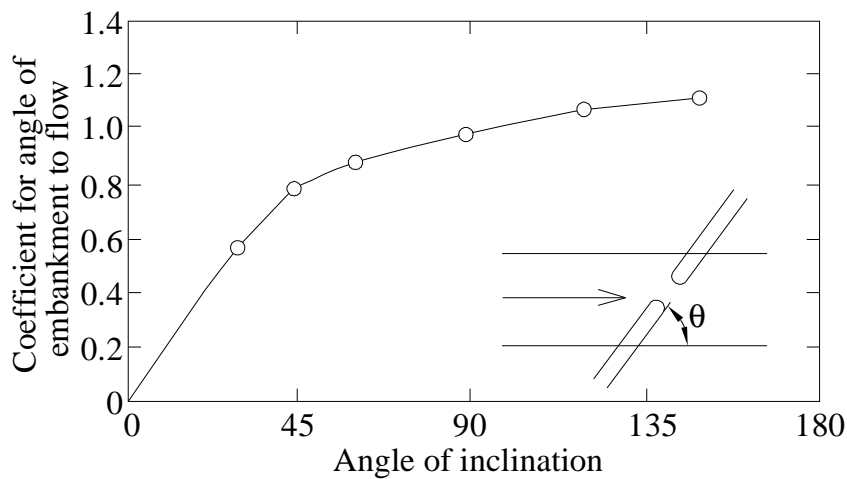


Figure 3.5. Coefficient k_a depending on angle of flow crossing
(after Richardson et al.^[52], patterned after Ahmad^[1])

3.3 Calculation of local flow velocity

In approach to contraction of the bridge, flow streamlines are bended by embankment, and then flow direction is parallel to it. Flow velocities along extreme streamline were falling to about minimum and then gradually increasing (Fig. 3.6), spiral vortex system was developing. Local flow velocity reaches maximum at the upstream corner of abutment. Flow streamline concentration, sharp water level drop and rapid increase of the velocity (Fig. 3.7) were observed at the upstream corner of the abutment near the bridge crossings on plain rivers. Horizontal vortex was developing, reducing opening of the bridge. In tests local flow velocities near abutment were observed at any contraction of the flow. As found from the tests, the local flow velocity with vortex structures forms scour hole. In general, local flow velocity occurs at the upstream corner of abutment, because of flow contraction.

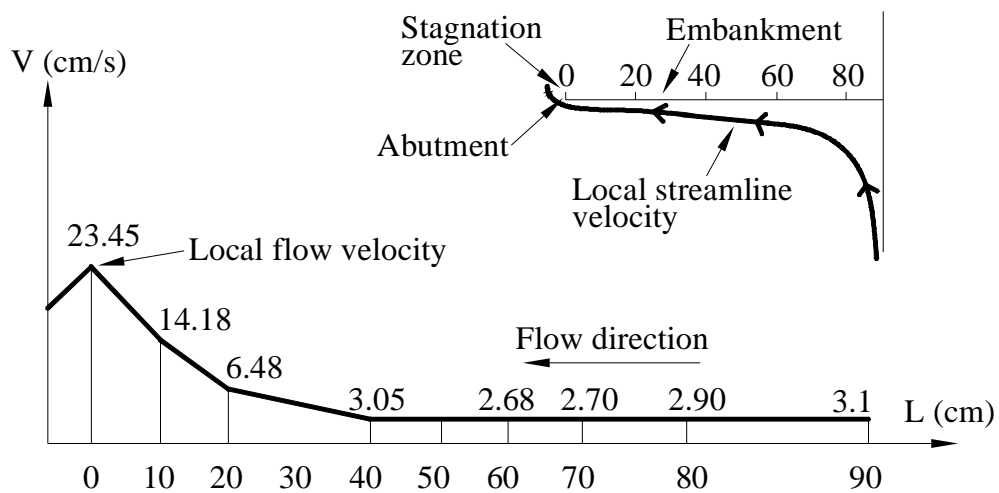


Fig.3.6. Velocity distribution in approach to abutment. Test SS1

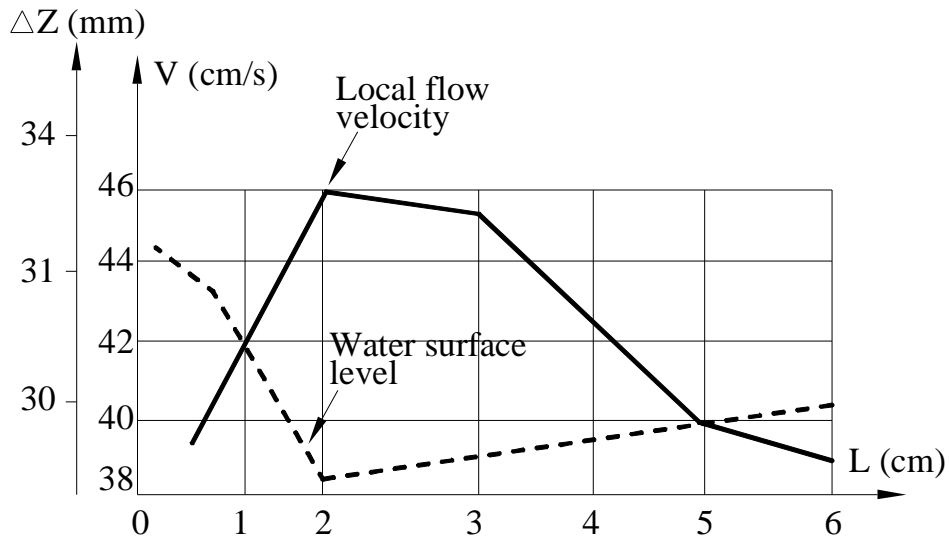


Fig.3.7. Velocity and water level changes near abutment. Test FL6.

To find local flow velocity Bernulli equation for two cross sections for unit streamline was used. Then formula for local flow velocity near abutment is:

$$V_2 = V_1 = j \sqrt{2g\Delta Z}, \quad (3.21)$$

where j = velocity coefficient (according to Figure 3.8); g = gravitational acceleration; ΔZ = water level difference at the corner of the abutment.

According to the laboratory tests, velocity coefficient ϕ is depending on flow contraction. With increase of flow contraction, coefficient ϕ is reducing, and with flow contraction reduction velocity coefficient is increasing. For known V_1 and Δh values, velocity coefficient ϕ was found for each contraction rate of the flow Q/Q_b . The coefficient ϕ as a function of the flow contraction rate is shown in Figure 3.8.

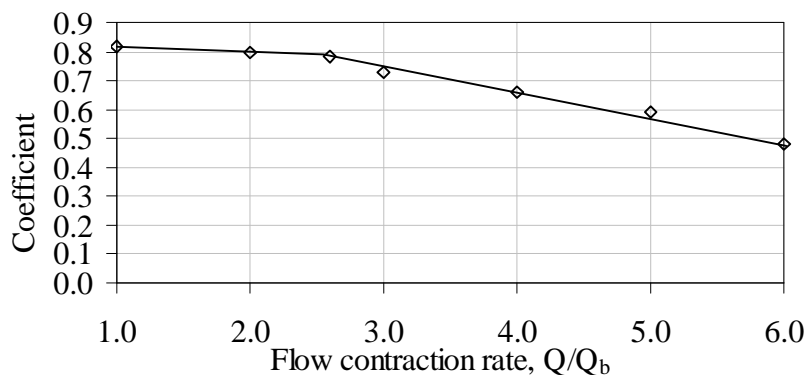


Figure 3.8. Coefficient ϕ vs. the flow contraction rate

(after Gjunsburgs and Neilands ^[17])

In tests water level difference DZ was equal to maximum backwater Dh . We checked that in tests with different width of the opening, discharge, depth of the flow and Froude numbers. Maximum backwater Dh can be determined by Rotenburg and Volnov ^[53] equation.

Rotenburg and Volnov ^[53] presented following equation for maximum backwater:

$$Dh = \frac{V_K^2}{2g} \left[\left(\frac{Q}{Q_b} \right)^2 - 1 \right] + \frac{Li_0}{2} \sqrt{\frac{Fr}{i_0}} \left[\left(\frac{Q}{Q_b} \right)^2 + 1 \right] + \frac{V^2}{g}, \quad (3.22)$$

where V_K = average flow velocity in bridge opening in open-flow conditions; Q = total discharge of the flow; Q_b = discharge of the flow in bridge opening in open-flow conditions; L = river width; i_0 = river slope; Fr = Froude number; V = average flow velocity in open-flow conditions.

Comparison of experimental data with calculated for local flow velocities at the abutments were given in Table 3.6. Results show close agreement.

Table 3.6

Comparison of experimental data with calculated local flow velocity

Test	L_b (cm)	Δh (cm)	ΔZ (cm)	$\Delta h / \Delta Z$	Q / Q_b	$V_{1\text{calc.}}$ (cm/s)	$V_{1\text{exp.}}$ (cm/s)	$V_{1\text{calc.}} / V_{1\text{exp.}}$
FL1	50	2.10	2.40	0.87	5.27	36.81	39.30	0.94
FL2	50	3.70	3.90	0.95	5.69	43.20	43.40	0.99
FL3	50	4.07	4.40	0.92	5.55	46.61	50.30	0.92
FL4	80	1.25	1.36	0.92	3.66	33.04	36.00	0.92
FL5	80	1.75	1.70	1.03	3.87	39.76	39.00	1.02
FL6	80	2.50	2.40	1.04	3.78	45.85	45.20	1.05
FL7	120	0.50	0.58	0.90	2.60	26.76	25.10	1.07
FL8	120	1.05	1.01	1.08	2.69	33.87	33.80	1.00
FL9	120	1.38	1.45	0.95	2.65	38.77	39.40	0.98
FL10	120	0.35	0.32	1.09	1.56	22.08	21.60	1.02
FL11	200	0.40	0.43	0.93	1.66	23.97	23.10	1.04
FL12	200	0.51	0.55	0.93	1.67	26.01	27.30	0.95

Based on the flow-continuity relation, the discharge across the width of a scour hole before and after the scour can be defined as:

$$Q_f = k \cdot Q_{sc}, \quad (3.23)$$

where Q_f = discharge across the width of the scour hole with a plain bed; Q_{sc} = discharge of the scour hole with a scour depth h_s ; and k = coefficient depending on flow contraction rate.

According to the experimental data, the coefficient k depends on the contraction of the flow (Figure 3.9).

The discharge across the width of the scour hole with a plain bed can be expressed:

$$Q_f = B \cdot h_f \cdot V_l = mh_s \cdot h_f \cdot V_l, \quad (3.24)$$

where B = width of scour hole; h_f = flow depth in floodplain; V_l = local flow velocity; and l/m = slope of the scour hole wall.

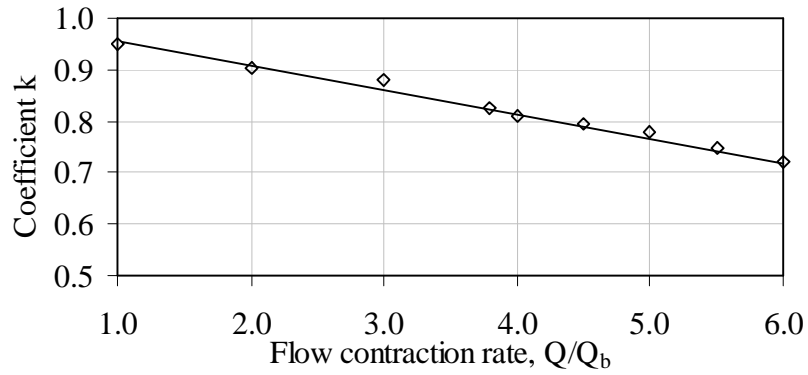


Figure 3.9. Coefficient k vs. the flow contraction rate
(after Gjunsburgs and Neilands^[22])

The discharge across the width of the scour hole with scour depth h_s can be found:

$$k \cdot Q_{sc} = k \left(B \cdot h_f + \frac{B}{2} \cdot h_s \right) \cdot V_{lt} = k \left(mh_s \cdot h_f + \frac{mh_s}{2} \cdot h_s \right) \cdot V_{lt}, \quad (3.25)$$

where h_s = depth of scour hole, and V_{lt} = local velocity after time t at a scour depth h_s .

Using equations (3.23), (3.24) and (3.25), following relation can be written:

$$mh_s \cdot h_f V_l = k \left(mh_s h_f + \frac{mh_s}{2} \cdot h_s \right) \cdot V_{lt}. \quad (3.26)$$

Local flow velocity at any depth of the scour hole can be determined from Eq. (3.26), as follows:

$$V_{lt} = \frac{V_l}{k \left(1 + \frac{h_s}{2h_f} \right)} = \frac{j \sqrt{2gDh}}{k \left(1 + \frac{h_s}{2h_f} \right)}. \quad (3.27)$$

Using formulas (3.21), (3.27) we can find local flow velocities V_l and V_{lt} at any stage of scour development at the abutment and at any time step of hydrograph.

With a scour hole development, total flow cross section increases because of increasing cross section of a scour hole, resulting in decreasing local flow velocity V_{lt} . As well as, changes in flow discharge, and consequently changes in flow contraction rate during the floods, leads to changes in local flow velocity.

3.4 Comparison of calculated and experimental scour depth values

To verify suggested depth of scour calculation method, calculated scour depth values were compared to experimentally obtained scour depth values, as showed in Table 3.7. Results show close agreement. Scour development in time for steady flow were in tests SS, SL and for unsteady flow conditions in tests TL, where 2 following time steps were used with steady flow conditions in each step.

Table 3.7

Comparisons of experimental and calculated scour depth at the abutments

Test	Q (l/s)	Q / Q _b	h (cm)	L _b (cm)	Δh (cm)	d (mm)	V _l (cm/s)	t (hours)	h _{s exp.} (cm)	h _{s calc.} (cm)	h _{s exp.} / h _{s calc.}
SS1	4.24	2.5	5	44.5	0.457	0.50	23.45	7	2.37	2.26	1.05
SS2	7.30	2.5	5	44.5	0.953	0.50	33.87	7	6.34	6.21	1.02
SS3	6.50	2.5	5	44.5	0.816	0.50	31.34	7	5.07	5.32	0.95
SS4	6.50	2.0	5	57.0	0.569	0.50	26.73	7	3.58	3.45	1.04
SS5	4.24	2.0	5	57.0	0.323	0.50	20.14	7	0.70	0.73	0.96
SS6	7.30	2.0	5	57.0	0.665	0.50	28.89	7	4.10	4.27	0.96
SS7	7.30	1.5	5	77.5	0.444	0.50	23.90	7	2.03	2.07	0.98
SS11	7.30	1.25	5	97.5	0.33	0.50	20.73	7	0.71	0.67	1.06
SL1	16.6	5.27	7	50.0	2.20	0.24	36.81	7	13.30	12.91	1.03
SL2	22.7	5.69	7	50.0	3.60	0.24	43.20	7	16.70	16.40	1.02
SL3	23.6	5.55	7	50.0	3.95	0.24	46.61	7	17.30	17.67	0.98
SL4	16.6	3.66	7	80.0	1.19	0.24	33.04	7	10.1	9.79	1.03
SL5	22.7	3.87	7	80.0	1.79	0.24	39.76	7	12.80	13.03	0.98
SL6	23.6	3.78	7	80	2.35	0.24	45.85	7	16.22	15.45	1.05
SL7	16.6	2.60	7	120	0.60	0.24	26.76	7	6.40	5.94	1.08
SL8	22.7	2.69	7	120	0.99	0.24	33.87	7	9.81	9.22	1.06

SL9	23.6	2.65	7	120	1.28	0.24	38.77	7	11.62	11.28	1.03
SL10	16.6	1.56	7	200	0.38	0.24	22.08	7	2.97	3.08	0.96
SL11	22.7	1.66	7	200	0.45	0.24	23.97	7	4.11	4.16	0.99
SL12	23.6	1.67	7	200	0.53	0.24	26.01	7	5.09	5.16	0.98
SL13	35.48	4.05	13	80	1.42	0.67	34.65	7	9.44	9.68	0.97
SL14	41.38	3.99	13	80	1.80	0.67	39.26	7	12.30	12.62	0.97
SL15	47.10	4.05	13	80	2.70	0.67	49.15	7	18.30	17.82	1.03
SL16	16.6	3.66	7	80.0	1.19	0.67	33.04	7	7.30	6.78	1.08
SL17	22.7	3.87	7	80.0	1.79	0.67	39.76	7	9.6	10.00	0.96
SL18	23.6	3.78	7	80.0	2.35	0.67	45.85	7	12.53	12.32	1.02
TL1	16.66	3.66	7	80.0	1.19	0.24	33.04	14	14.3	14.50	0.99
	35.48	4.05	13	80.0	1.42	0.24	34.65				
TL2	22.7	3.87	7	80.0	1.80	0.24	39.76	14	19.0	17.76	1.07
	41.38	3.99	13	80.0	1.80	0.24	39.26				
TL3	23.6	3.77	7	80.0	2.35	0.24	45.85	14	24.2	23.14	1.05
	47.1	4.05	13	80.0	2.70	0.24	49.15				
TL4	16.6	3.66	7	80.0	1.19	0.67	33.04	14	9.37	9.87	0.98
	35.48	4.05	13	80.0	1.42	0.67	34.65				
TL5	22.7	3.87	7	80.0	1.80	0.67	39.76	14	12.8	13.09	0.98
	41.38	3.99	13	80.0	1.80	0.67	39.26				
TL6	23.6	3.78	7	80.0	2.35	0.67	45.85	14	19.3	18.45	1.045
	47.1	4.05	13	80.0	2.70	0.67	49.15				

Considerable influence on depth of scour has changes of flow parameters from step to step of hydrograph. For example, in test SL4 with $Q = 16.6$ l/s, $h_f = 7$ cm, $Q/Q_b = 3.66$, $d = 0.24$ mm and $\Delta h = 1.19$ cm depth of scour was 10.1 cm in 7 hours. In test SL 19 with $Q = 35.48$ l/s, $h_f = 13$ cm, $Q/Q_b = 4.05$, $d = 0.24$ mm and $\Delta h = 1.42$ cm depth of scour was 13.6 cm in 7 hours. In test TL1 we were modeling two steps of hydrograph, where test SL4 was as first step and test SL19 as a second. The depth of scour in 14 hours TL1 was 14.3 cm, but the sum of the two separate tests SL4 and SL19 – 23.7 cm. Examples of comparison experimental data with computed depth of scour development in time by this method for steady and unsteady flow conditions are given in Figures 3.10 and 3.11.

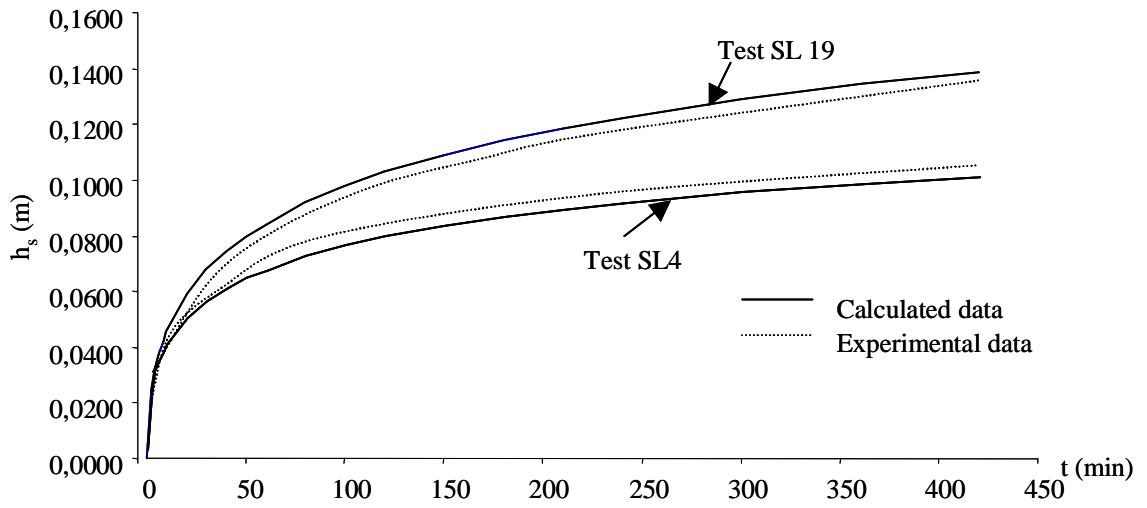


Figure 3.10. Scour development in time in steady flow conditions

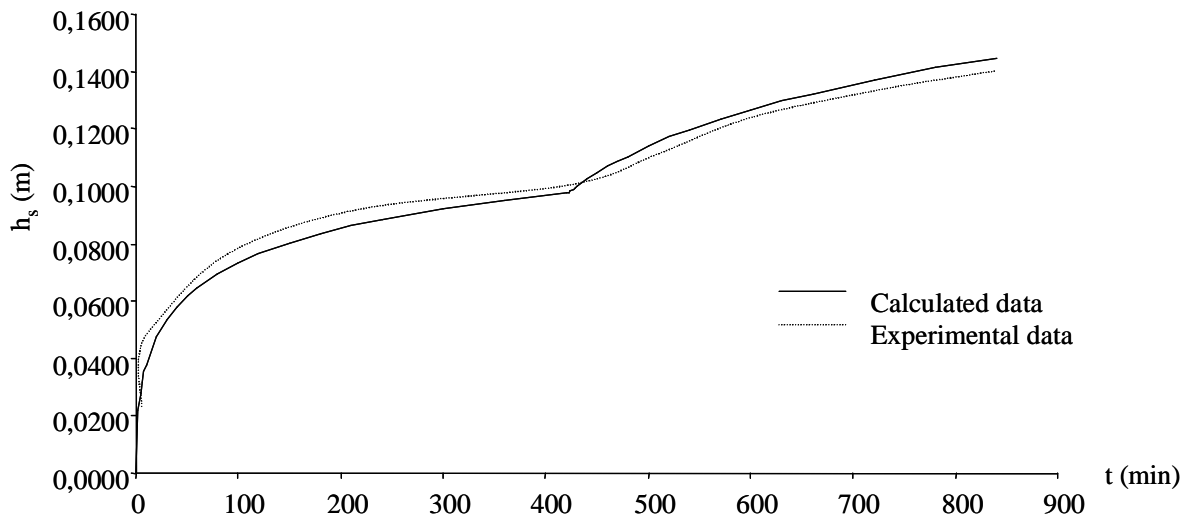


Figure 3.11. Scour development in time for unsteady flow conditions. Test TL1

3.5 Analysis of the scour depth calculation method

For analyzing the method, formulas (3.18) and (3.20) are transformed to a form that shows clearly that they contain dimensionless parameters and characteristic of the flow.

Now, formula (3.18) has the form:

$$N_i = \frac{2t_i A j^4 g^2}{p m k^4} \frac{Dh^2}{h_f^2} + N_{i-1} \quad (3.28)$$

Rotenburg and Volnov ^[53] have found that the relative maximum backwater is a function of the following parameters:

$$\frac{Dh}{h_f} = f\left(\frac{Q}{Q_b}; P_K; P_{Kb}; \frac{Fr}{i_0}; \frac{h}{h_f}\right), \quad (3.29)$$

Where Q/Q_b = flow contraction rate, $P_K = V_K^2/gh$ = kinetic parameter of flow in contraction in open-flow conditions, h = average flow depth in contracted section, $P_{Kb} = V^2/gh_f$ = kinetic parameter of the open flow in natural conditions, Fr/i_0 = ratio of the Froude number to the river slope, h/h_f = relative flow depth, and h_f = flow depth in floodplain. Calculation of kinetic parameter of the open-flow in contracted section (bridge opening) is close to calculation of Froude number, but with the different flow velocity used.

In the general form, Eq. (3.28) can be written as:

$$N_i = \frac{2Ag^2 j^4 h^2}{pm k^4 h_f^2} \frac{1}{\left(\frac{d}{h_f}\right)^{0.25}} \cdot \left\{ \frac{P_K}{2} \left[\left(\frac{Q}{Q_b}\right)^2 - 1 \right] + \frac{1}{2} P_{Kb} \sqrt{\frac{1}{Fr/i_0}} \left[\left(\frac{Q}{Q_b}\right)^2 + 1 \right] + P_{Kb} \right\}^2 \cdot t_i + N_{i-1} \quad (3.30)$$

From Eq. (3.30), relative depth of scour is a function the next parameters:

$$\frac{h_s}{h_f} = 2(x-1) = f\left(\frac{Q}{Q_b}; P_K; P_{Kb}; \frac{Fr}{i_0}; \frac{d}{h_f}; \frac{bV_0}{V_l}; \frac{h}{h_f}; t; N_{i-1}\right) \quad (3.31)$$

where d/h_f = the relative grain size of the riverbed and N_{i-1} = the scour formed during the previous time step.

Depth of scour depends also on the side-wall slope of abutment k_m (Yaroslavcev ^[68]), the shape of the abutment k_s (Richardson and Davis ^[50]), and the angle of flow crossing k_α (Richardson et al. ^[52]).

In the general form, the relative depth of scour is a function of the dimensionless parameters and time ^[19]:

$$\frac{h_s}{h_f} = 2(x-1)k_mk_sk_a = f\left(\frac{Q}{Q_b}; P_K; P_{Kb}; \frac{Fr}{i_0}; \frac{d}{h_f}; \frac{bV_0}{V_l}; \frac{h}{h_f}; t; N_{i-1}; k_m; k_s; k_a; a_{fl}; t_{fl}\right), \quad (3.32)$$

where a_{fl} = the unsteadiness of the flow and t_{fl} = the flood duration.

Further a graphical dependence of the relative scour depth on different flow and bed parameters are showed. Figure 3.12 shows the relative scour depth dependence from flow contraction rate. With increase in the contraction of the flow Q/Q_b , consequently with increase length of protruding structure, the relative scour depths increases. Tests were associated with equal Froude numbers. Laboratory data of tests SL1, SL4, SL7, SL10 for $Fr_3 = 0.075$; tests SL2, SL5, SL8, SL11 for $Fr_2 = 0.1037$; tests SL3, SL6, SL9, SL12 for $Fr_1 = 0.1237$ were used. Results argue that flow contraction rate is significant parameter influencing scour depth.

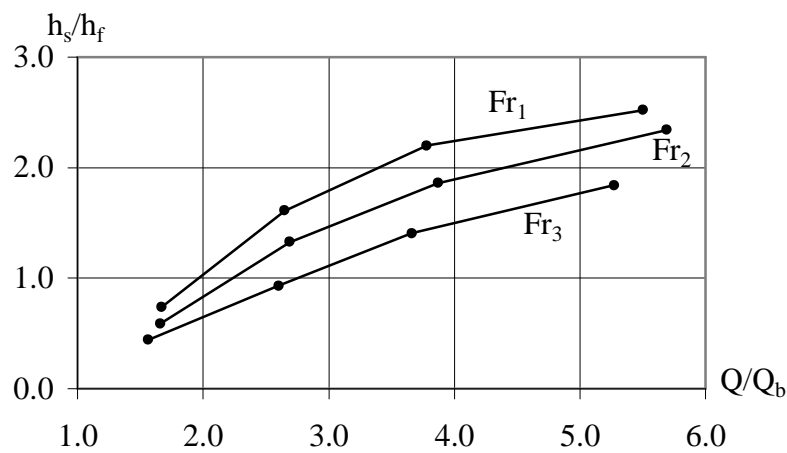


Fig. 3.12. Relative depth of scour versus the flow contraction rate

The dependence of the relative depth of scour on the relative grain size is presented in Fig. 3.13. For test SL1 with $Fr = 0.075$, $Q/Q_b = 5.27$ scour development were calculated for 7

hours changing medium grain size $d = 0.24 \dots 2.00$ mm. With increase in the relative grain size, the relative depth of scour reduces. In the case of a stratified bed, it is necessary to introduce the layer thickness H_d into the initial data, taking into account the grain size.

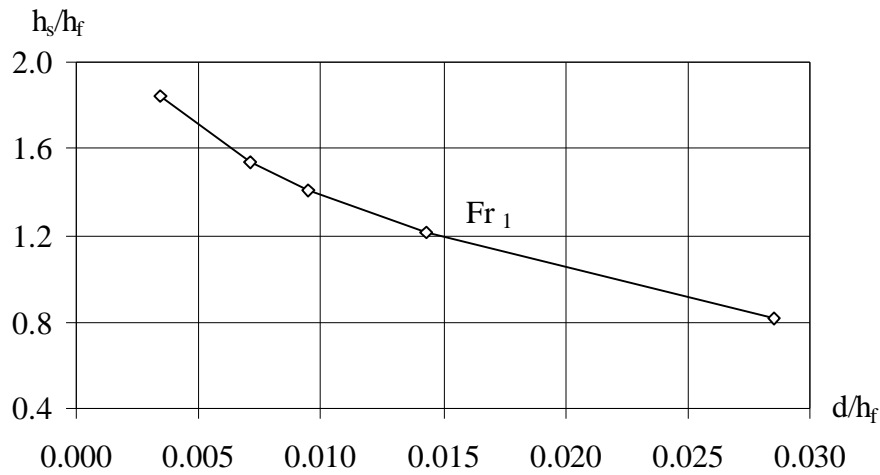


Fig. 3.13. Relative depth of scour versus the relative grain size

The influence of the open-flow parameters, such as the kinetic parameter of the flow equal to v^2/gh_f and the Froude number relative to the slope $Fr/i_0 = v^2/gL_a i_0$, is shown in Figs. 3.14 and 3.15. The quieter is the flow, the smaller is the kinetic parameter of the flow v^2/gh_f , and the smaller is the scour depth. The laboratory data were grouped according to similar flow contraction rate as: tests SL1, SL2, SL3 for $(Q/Q_b)_1$; tests SL4, SL5, SL6 for $(Q/Q_b)_2$; tests SL7, SL8, SL9 for $(Q/Q_b)_3$.

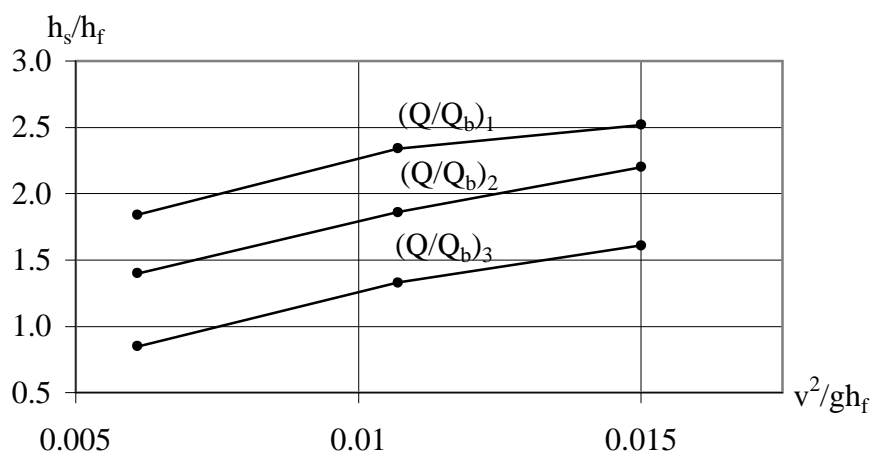


Fig. 3.14. Relative scour depth versus the kinetic parameter of the flow

As seen from the Figure 3.15, the smaller the ratio between the inertia and frictional forces, the smaller the value of $Fr/i_0 = v^2/gL_a i_0$, and the greater the relative scour depth.

Froude number was calculated for the flow obstructed by a structure length. The laboratory data were grouped according to similar Froude numbers as: tests SL1, SL4, SL7, SL10 for $Fr_1 = 0.075$; tests SL2, SL5, SL8, SL11 for $Fr_2 = 0.1037$; tests SL3, SL6, SL9, SL12 for $Fr_3 = 0.1237$.

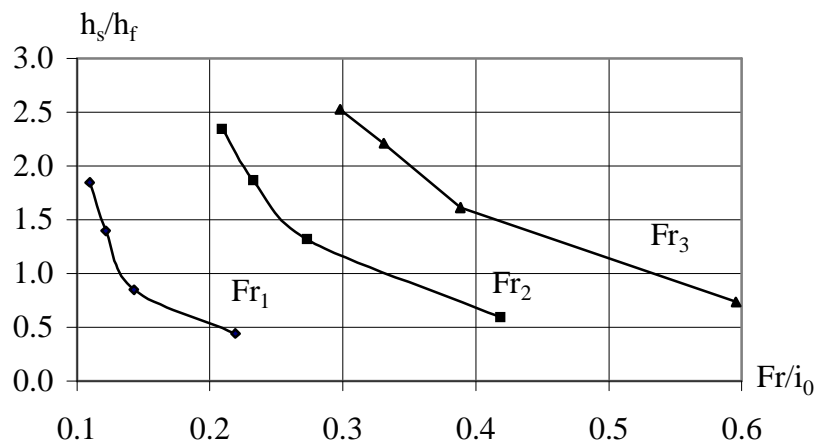


Fig. 3.15. Relative depth of scour versus the Froude number in relation to the slope

With development of the scour depth, the ratio of bV_0/V_l decreases. The greater is the scour depth, the more is the difference between the velocities V_0 and V_l (Fig. 3.16). Local flow velocity and velocity at which sediment movement starts were calculated at the beginning of scouring (with plane bed). Test data were grouped according to equal Froude number: $Fr_1 = 0.075$ (tests SL1, SL4, SL7, SL10).

The development of scour was restricted by the duration of the flood. The scour ceases on the peak of the hydrograph or just after it. Figure 3.17 shows the depth of scour as a function of the flood duration. For calculation of scour development in one steady-state time step following data were used: $Q/Q_b = 1.42$, $h_f = 2.3$ m, $Dh = 0.406$ m, $V_0 = 0.66$ m/s, $V_l = 2.29$ m/s, $d = 0.5$ mm, $g = 1.6$. Contrary to experiments in hydraulics flumes, in the real flood, the time of scour development is restricted by duration of the flood, and therefore the depth of scour does not reach the equilibrium stage.

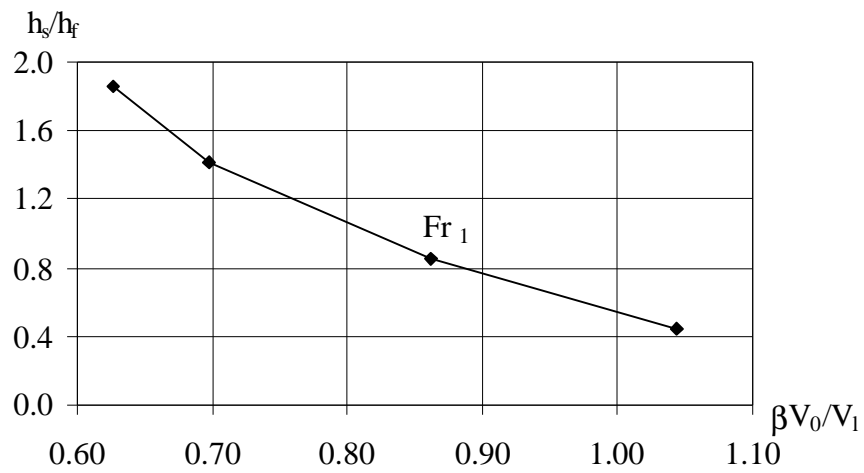


Fig. 3.16. Relative depth of scour versus velocity ratio

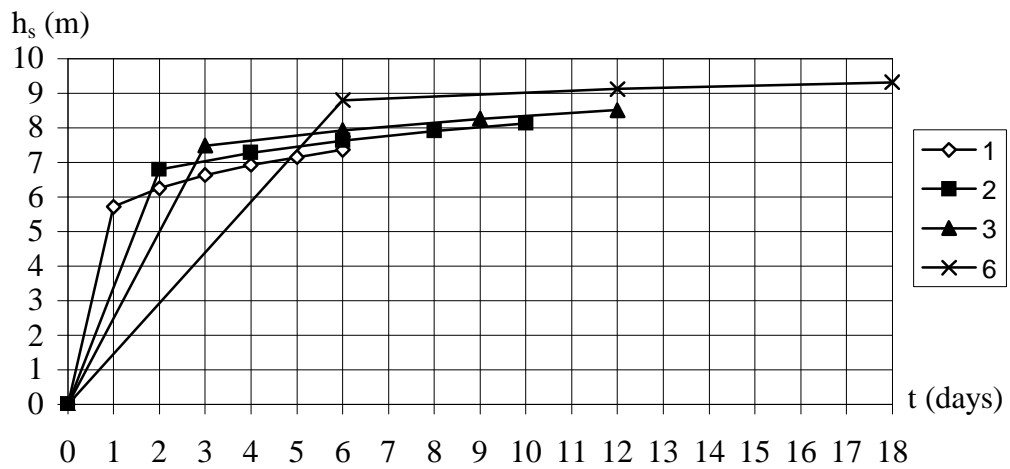


Fig. 3.17. Depth of scour development during the flood. Duration of time intervals of the hydrograph 1, 2, 3, and 6 days.

3.6 Conclusions

Differential equation of equilibrium of the bed sediment movement for clear water was developed and a new method for calculating the scour development with time at the abutments during the flood was elaborated. Method was confirmed by experimental data (Gjunsburgs and Neilands ^{[16]; [17]; [18]}).

Depth of scour can be determined by this method at any step of hydrograph or after one, two, or several floods. Equilibrium depth of scour can't be reached during one or even several floods because the time of the flood is restricted. Scour stop at the peak of the flood or later, when $V_{lt} = k\beta V_{0t}$.

Local velocity V_{lt} is decreasing in steady flow conditions because the depth of scour hole is developing and V_{lt} is increasing from step to step of hydrograph. Velocity at which starts the sediment movement V_{0t} was increasing because of the depth of scour development and because of the flood. The time of scour is less then time of flood.

The calculation of scour depth development by proposed method is mathematically complicated and long lasting; therefore program "RoBo" was developed and used (see Appendix 1) in computer modeling. "RoBo" is simple, but powerful tool with mathematical algorithm written in Microsoft[®] Excel[®] program. The following parameters must be inputted: initial flow depth in the floodplain, flow contraction rate, maximum backwater, grain size, specific weight of the bed material, and thickness of the bed layers. After calculation we have local flow velocity, sediment critical velocity, and scour depth changes at the end of each time interval and time step of hydrograph.

4 PRACTICAL APPLICATION SLOKA WWTP

The Jurmala wastewater treatment plant is situated at the western skirts of the town on the bank of the Lielupe River, in the Sloka region. The plant was built in 2007 and put into operation in 2008. The plant has conventional primary treatment without primary settling, activated sludge process for enhanced biological phosphorus and nitrogen removal and sludge treatment by mechanical thickening and dewatering. The Figure 4.1 present wastewater treatment plant activated sludge and secondary clarifier process layout.

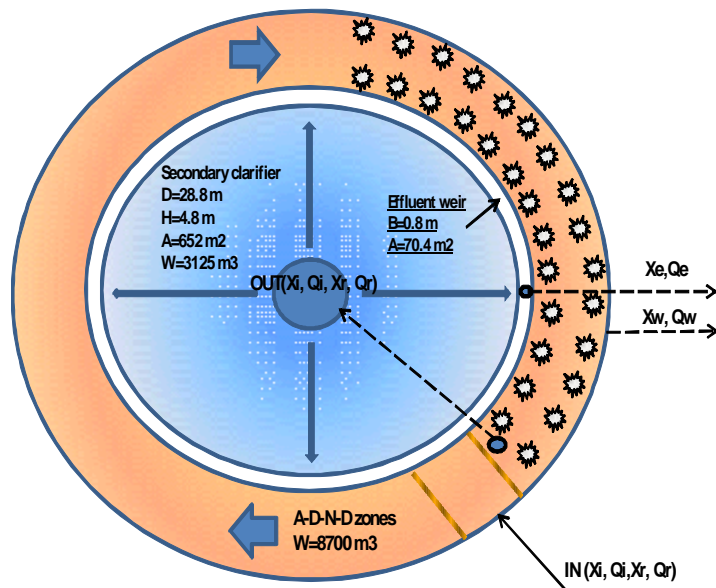


Figure 4.1. Wastewater treatment activated sludge and clarifier process layout

This study describes the hydraulic flow and mass flux evaluation of secondary clarifier at Sloka. The aim of study is to examine the individual effect of the scouring on sludge particle escaping from clarifier due to local velocities increase. The study also describes the results of a full-scale clarifier test for the flow rate 250 m³/h, 500 m³/h and simulated for emergency flow rate, 750 m³/h, when the one process line will be closed. The effluent suspended solids concentration have been measured and calculated on daily basis every hour, and presented as a daily average value, but for emergency flow calculated. The comparison between measurements and calculation is done.

To avoid in study any effect from activated sludge treatment process influence on sludge particle size and sedimentation performances, the sludge index *SVI*, ml/g was

measured, but activated sludge process was controlled by system mass balance, and process results by software AQUA (Aqua, User Manual, Version 3.4, 2008), which based on daily laboratory measurements.

To examine the effect on sludge particle escaping from clarifier the following standard clarifier design parameter such as overflow load, underflow load, sludge blanket depth, weir load, detention time, and design feature of the process on secondary effluent quality and was compared with laboratory results on suspended solids concentration in effluent.

4.1 Clarifier standard parameter evaluation

4.1.1 Flow velocity measurements

A measurement grid was established within a cross-section of the secondary clarifier. Velocity measurements at fixed location of the grid were measured in order to establish a velocity profile. The grid consisted of 30 points for measurements. Velocity measurements were taken at 1.0, 2.0, 3.0, 4.0, 5.0, and 6.0 m from the clarifier outlet baffle, at depths of 0.5, 1.0, 1.5, 2.0 and 2.5 m below the water surface. Additional measurements were taken at effluent weir wall, at depths of 0.5, 1.0, 1.5 m below the water surface.

The local flow velocities were measured for flows $250 \text{ m}^3/\text{h}$ and $500 \text{ m}^3/\text{h}$ with calibrated MarshMcBirney ultrasonic velocity device and modelled by CFD, SSIIM (2007) [57] for emergency flow $750 \text{ m}^3/\text{h}$. Since measurements were made with regard to the depth from the water level for different flow rates, the location of fixed measuring points was not changed during the test period, but water level in the effluent weir was always under the changes.

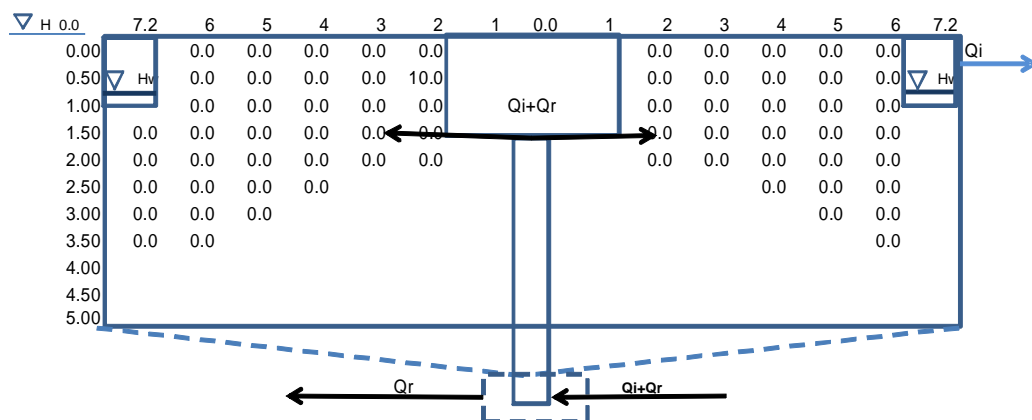


Figure 4.2. The locations of the cross sections used for velocity measurements

The velocity profiles were measured at different cross sections within the clarifier. Figure 4.2 shows the locations of the cross sections used for velocity measurements

4.1.2 Clarifier performance control

The wastewater treatment plant process control was based on system mass balance presenting by Figure 4.3 and by Eq. (4.1), Tchobanoglous and Burton^[63].

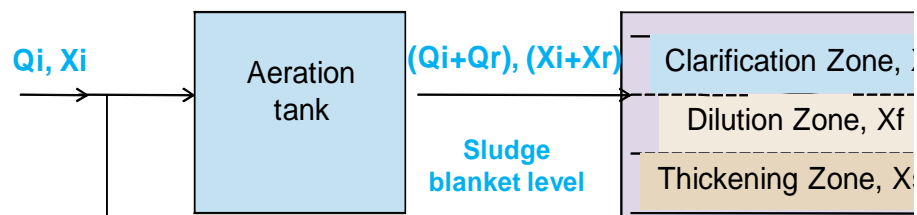


Figure 4.3. Sloka WWTP activated sludge process layout

Process mass balance:

Accumulation = Input – Output + Generation – Consumption

Generation = Consumption = Zero

Accumulation = Input – Output

$$\frac{dX}{dt} = (Q_i + Q_r) \cdot X_i - Q_r \cdot X_r - Q_e \cdot X_e - Q_w X_w; \quad (4.1)$$

where X_i , X , X_f , X_e , X_w the sludge concentration mg/l in influent, process tank, dilution zone, effluent, Q_i , Q_r , Q_e , Q_w flow rates m³/h at inflow, recycle flow, effluent and waste sludge.

The masses of suspended solids in the effluent and the wastage flows are ignored, i.e. because $Q_w \ll Q$, $Q_w \ll Q_r$, $X_e \ll X_i$ and $X_e \ll X_r$; thus, X_e and Q_w are not involved in the modeling procedure.

Recycle flow sludge concentration Eq. (4.2) by Tchobanoglous and Burton^[63] :

$$X_r = \left(\frac{Q_i + Q_r}{Q_r} \right) \cdot X_i. \quad (4.2)$$

The efficiency of secondary treatment is traditionally assessed by solids removal efficiency and compared to the over flow loading rate - *OFR*. Using the traditional approach

for assessing clarifier performance, the suspended solids removal efficiency was compared to hydraulic loading rate (Figure 4.4).

The effluent suspended solids removal efficiency E is calculated:

$$E = \frac{X_i - X_e}{X_i} \times 100\%. \quad (4.3)$$

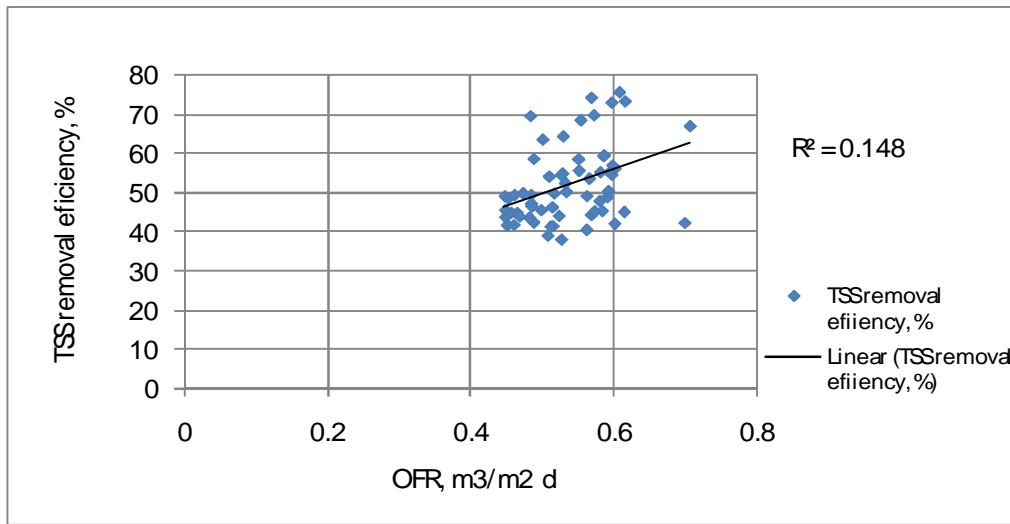


Figure 4.4. The effect of hydraulic loading rate on suspended solids removal efficiency

The scattered data reveal weak correlation between overflow rate loading and removal efficiency. Similar observations has made by other researchers (Weber and Rowe ^[67]). It was hypothesized that the absence of correlation could be explained by the fact that removal efficiency is affected by a number of factors such as the concentration of non settle able solids, sludge blanket depth, and flow velocity features of the clarifier. Thus, the cumulative effect of these factors on removal efficiency may exceed the effect of hydraulic loading; therefore in this study suspended solids concentration on effluent as a control parameter is used.

4.1.3 Sludge particle size and settling velocity

The amount of the solids and the particle size of the solids that do not settle are in some way related to how well the activated sludge is flocculated. In Sloka WWTP effluent TSS is low the sludge is considered to be well flocculated. If the effluent TSS be high and the supernatant and effluent clear with the individually visible particles pinpoint flock are being produced. If the effluent TSS is high and the supernatant and effluent are turbid deflocculating

occurs. Despite several investigations of the flocculation of activated sludge and a number of different possible theories there is still not no generally accepted explanation of why activated sludge flocculates. The performance of the activated sludge process is limited by many factors. They are concerned with the biological activity of sludge microorganisms, hydraulic disturbances within the system that affect the ability of the clarifier to separate and concentrate the activated sludge from the effluent.

The traditional sludge volume index (*SVI*) is performed in study. The test is easily performed and has a widespread use in routine process control. The test apparatus is a 1-liter sedimentation vessel. Normally the test is performed without stirring although stirring is recommended by the Standard Methods, after Hultman and Hultgren ^[22]. In the study the *SVI* index was in range from 60 till 135 ml/g, which accord to the settling velocities V_0 in the range from 4 till 8 m/h.

From the literature empirical correlation between *SVI* and sludge settling exist. The following Equation (4.4) developed by Vaccari and Christodoulatos ^[66], was used.

$$V_0 = [10.86 + (0.1854 \cdot SVI)] \cdot e^{(SVI/62.5)} \quad (4.4)$$

where V_0 = sludge particle settling velocity in m/h; *SVI* = sludge volume index.

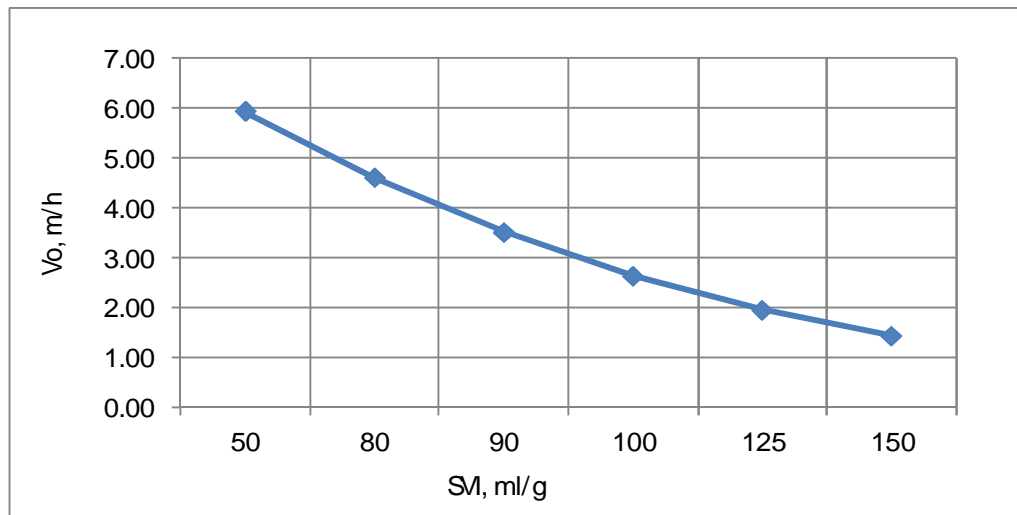


Figure 4.5. Sludge sedimentation variation vs. *SVI*

4.1.4 Relation between effluent suspended solids concentration and SVI

The Equation (4.4) currently is the best available; however, needs to be field calibrated. Particles at low solids concentrations settle as separate entities and do not move together in a visible layer. This makes it hard to measure the settling velocity at low solids concentrations.

The Figures 4.6, 4.7, and Tables 4.1, 4.2, illustrates the effluent suspended solids concentration (X_e) variations for the flow rates 250 m³/h and 500 m³/h. These figures show that high variation exists for flow rate 500 m³/h, but always was $X_f > X_e$. When the SVI is kept in highest level 135 mg/l, there have no possibility for scoring, but when the smaller range $SVI=60$ ml/g, then scouring can occur and suspended solids concentration in effluent was investigated.

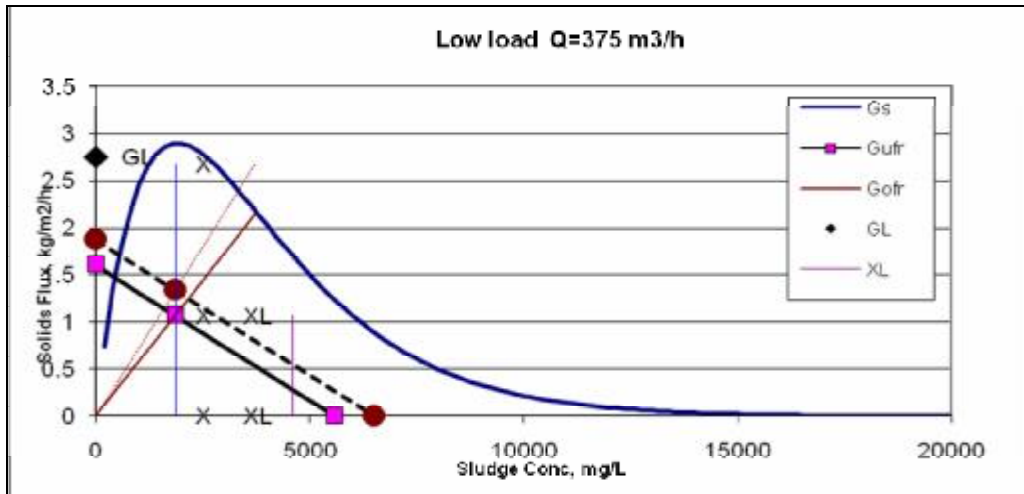


Figure 4.6. Low load flux scenario

Table 4.1

Relation between effluent TSS and SVI for low load conditions

OFR, m ³ /m ² d	SVI=135	SVI=100	SVI=60	Calculated TSS, mg/l
0.583	4.32	5.83	9.72	2.1
0.642	4.75	6.42	10.69	3.0
0.70	5.19	7.0	11.67	3.2

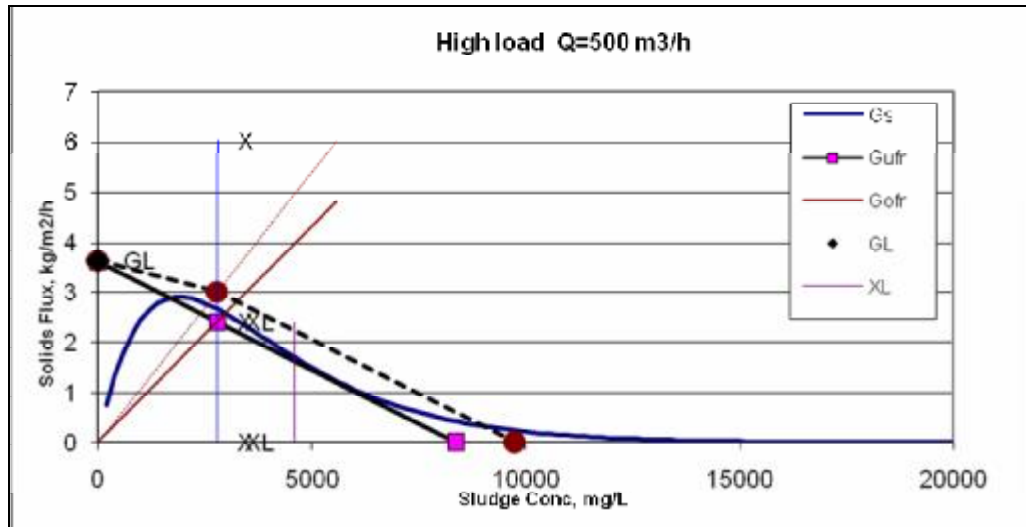


Figure 4.7. High load flux scenario

Table 4.2

Relation between effluent TSS and SVI for high load conditions

OFR, m ³ /m ² d	SVI=135	SVI=100	SVI=60	Calculated TSS, mg/l
22.08	6.8	9.19	15.31	7.5
24.24	7.49	10.1	16.84	11.0
26.40	8.17	11.02	18.37	14.2

There was no significant impact on suspended solids in effluent within the flow variations

4.1.5 Secondary clarifier working zones

Accordingly to Bretscher et al. ^[7], Figure 4.8 presents secondary clarifier working zones as follows: (1) clarification, (2) dilution, (3) thickening and (4) compression. In these zones, the following suspended solids concentrations are defined: (1) Inlet concentration, X_i , (2) effluent concentration, X_e , (3) diluted concentration, X_f , (4) sludge blanket concentration, X_{sb} , and (5) return sludge concentration, X_r . Similarly, the following flow rates are defined: (1) Inlet, Q_i , (2) outlet, Q_e , (3) return sludge, Q_r , and (4) surplus (waste) sludge, Q_w .

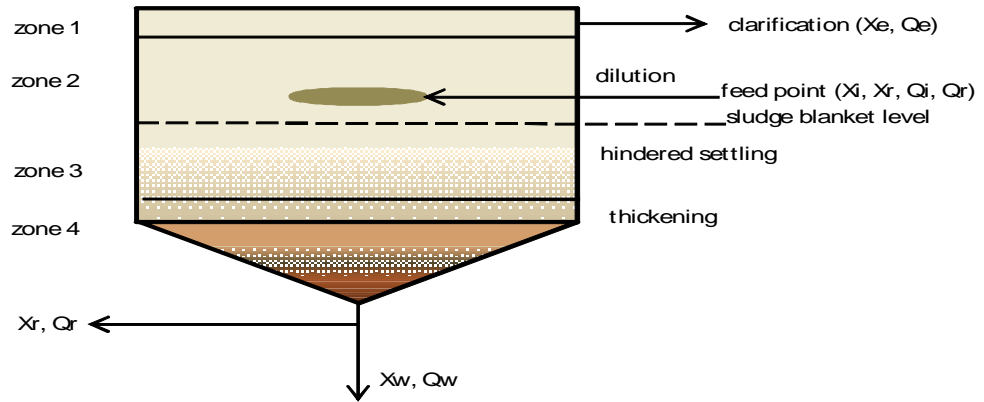


Figure 4.8. Secondary clarifier working zones

4.1.6 Flow loading rates

The flow hydraulic rates are given in the Table 4.3.

Table 4.3

Hydraulics loads in year 2009

No	Parameter	Value
1	Overflow loading rate - OFR ($\text{m}^3/\text{m}^2 \text{ d}$)	20-60
2	Mean velocity - V_0 , (m/min)	0.15-0.90
3	Water depth - H, (m)	3.8
4	Detention time (h)	6-10
5	Weir loading rate ($\text{m}^3/\text{m d}$)	100-200
6	Solid flux loading rate ($\text{kg}/\text{m}^3 \text{ d}$)	49-98

4.1.7 Detention time t

Detention time t (h):

$$t = \frac{Q}{W}, \quad (4.5)$$

where W = volume of clarifier, m^3 ; Q = flow, m^3/h .

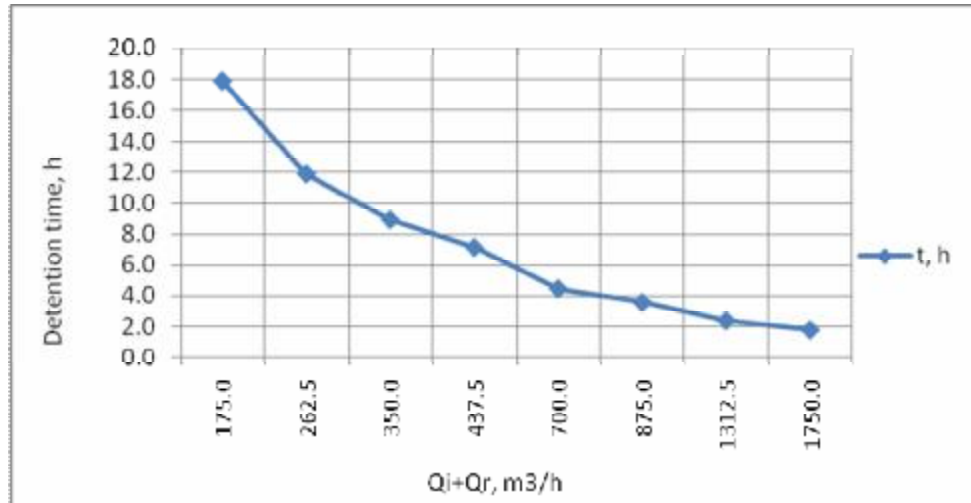


Figure 4.9. Detention time t variation for different flow rates

4.1.8 Overflow rate OFR

Overflow rate – OFR , (m^3/m^2 d):

$$OFR = \frac{Q}{A}, \quad (4.6)$$

where: A = clarifier surface area, m^2 ; $A = 651 \text{ m}^2$;

4.1.9 Effluent hydraulic

The researchers Vaccari and Christodoulatos^[66], Tekippe^[64] studying clarifiers have long proposed that the effluent suspended solids concentration is highly sensitive to the effluent hydraulics. Upon viewing the velocity profiles in the simulations, it is clear that the model predicts a greater fluid velocity in the effluent zone as the OFR increases. There is a very strong correlation between the effluent fluid velocity and the OFR . Figure 4.10 plots the fluid velocity over the effluent weirs versus the OFR . The results are a strongly linear correlation, which has a statistical R squared value of 0.98. This is expected because of the continuity condition imposed in the solution. The volume of fluid (minus the RAS flow) must equal the volume flowing over the effluent weirs.

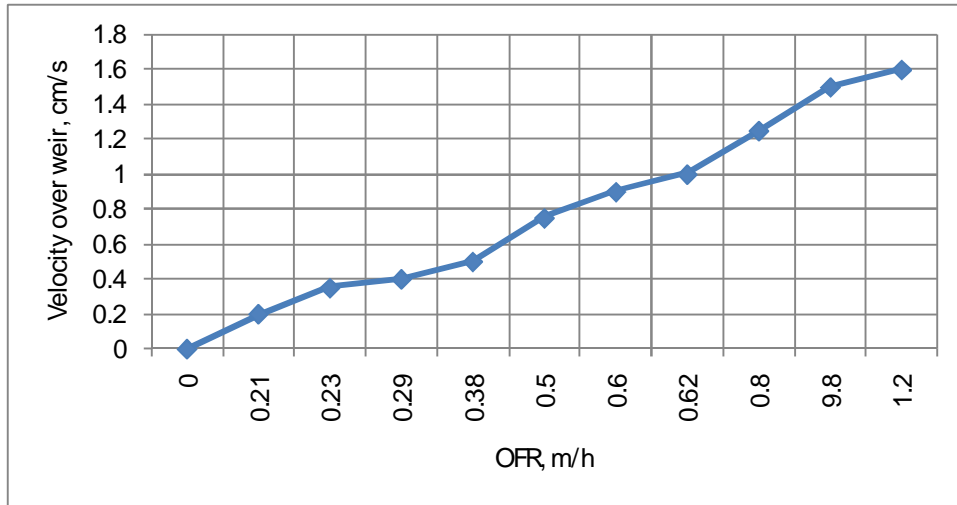
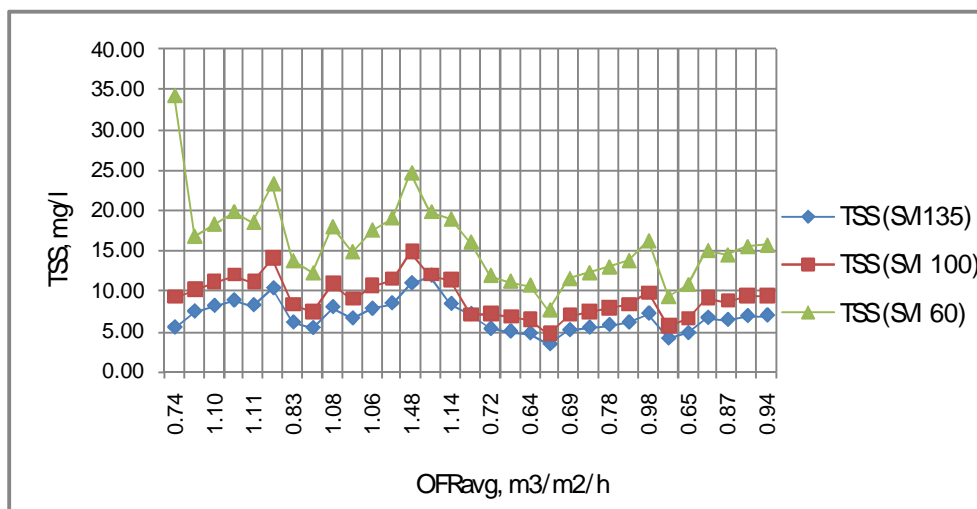


Figure 4.10. Velocity over weirs versus OFR

However, like the *OFR*, the results do not suggest a strong correlation between the effluent fluid velocity and the effluent suspended solids concentration for all the data. Some field tests in the past have suggested that suspended solids concentration is dependent on the effluent zone hydraulics, yet the data results do not provide support or disagreement with this correlation. It appears that the suspended solids concentration is more sensitive to other parameters such as the solids loading, Q_r flow rate, and the location and magnitude of recirculation zones that induce sludge blanket scouring.

As the suspended solids concentration in effluent is always controlled by measurements, but treatment process by calculation model, to avoid situations, when it depends upon process performance, therefore in studies is included studies and model, to keep good relation between, substrate utilization rate and ammonia conversions and giving the sludge particles with know settling velocity V_0 .



Figures 4.11.OFR versus effluent TSS

The Figure 4.11 shows that effluent suspended solids concentration be sensitive to the clarifier geometries at the low solids loading rate of 2.04 kg/m²/h and at the higher solids loading rates of 4.08 and 5.10 kg/m²/h.

For each surface overflow rate, there is a range of measured and simulated suspended solids concentration. Figure 4.12 shows the effluent suspended solids concentration versus the surface overflow and shows not a very strong correlation between the two. This graph suggests that increasing of the loading rate will increase the suspended solids concentration, and that the surface overflow rate is not a significant parameter within the tested range. In fact, the curves of the two different surface overflow rates lay close on top of each other. This agrees well with the results of calculation, the effluent suspended solids concentration was not affected significantly by the surface overflow rate until it was greater than 1.0 m/h. Another surface overflow rates used in calculation and measurement were 0.34 and 0.38 m/h.

The results showed almost negligible dependence of the effluent suspended solids concentration increase on the surface overflow rate within the entire range tested of 0.52 to 1.15 m/h. Also, the effluent solids concentration did not show a dependence on the solids loading rate until the high loading of 5.10 kg/m²/h was used.

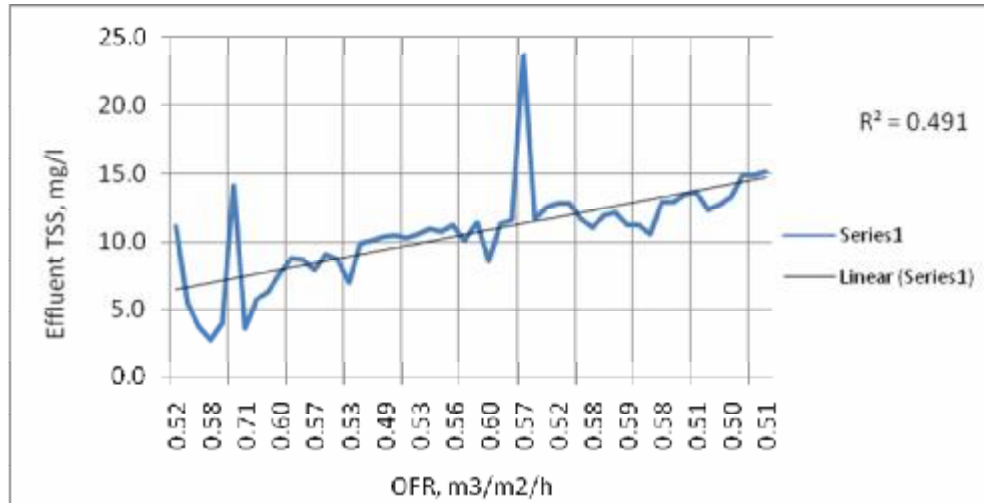


Figure 4.12. Suspended solids performances on average OFR flowrate

4.1.10 Weir loading rate

The weir-loading rate is calculated as following:

Weir loading rate = Q/A_w , where A_w = weir surface area, m².



Figure 4.13. Effluents launder with overflow weir

In the study only one circular radial flow clarifier was in use and one a single peripheries weir, is used within the normal range of values 100 - 154 m³/m d. The water then runs over the weir into a collection trough all along the whole perimeter of the tank. From there, it would run into pipe to take the water to outlet. The Figures 4.14, 4.15 shows OFR

variation versus weir load for low and high loads and figure 4.16 give the effluent suspended solids variation what accord to different flow rates.

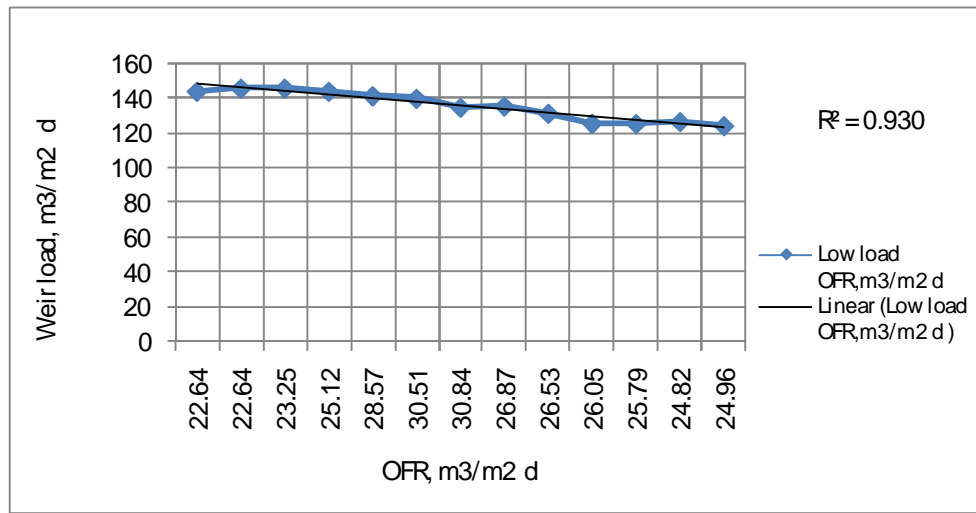


Figure 4.14. The low load OFR dependency versus weir load

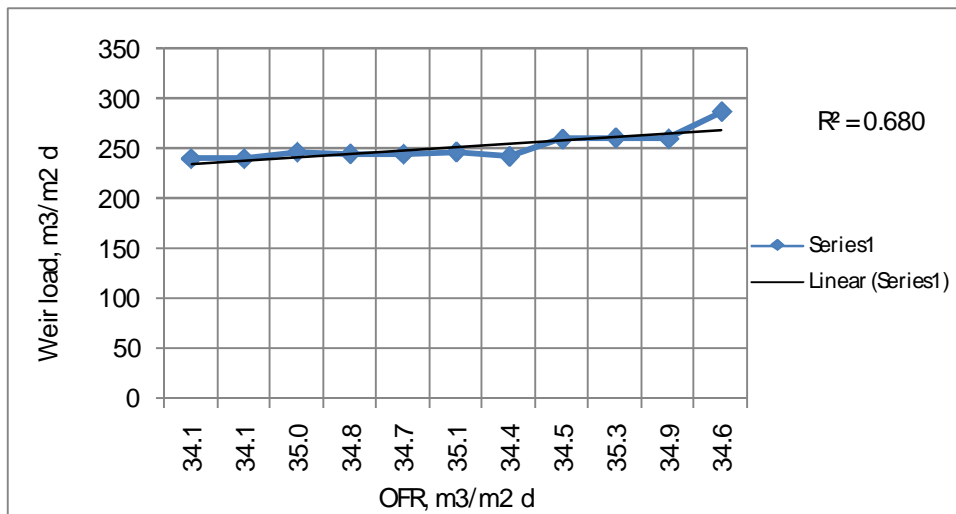


Figure 4.15. The high load OFR dependency versus weir load

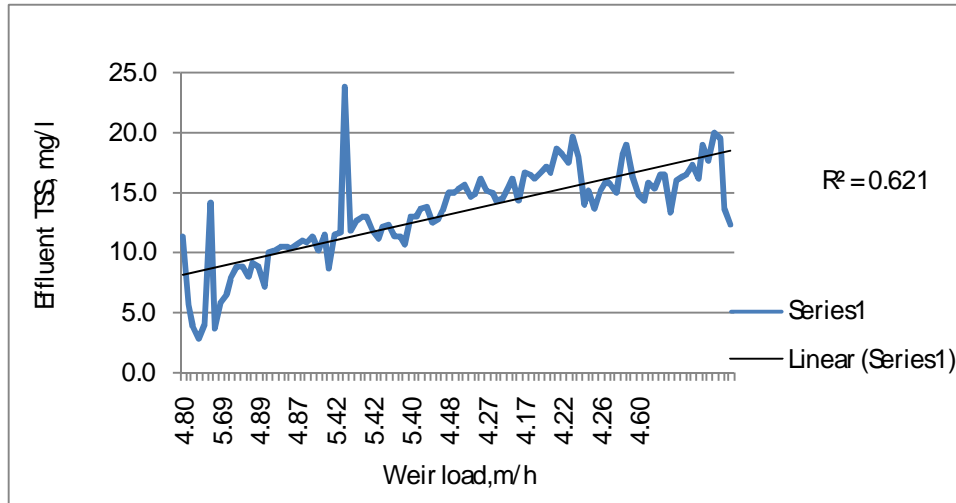


Figure 4.16. The dependency weir load versus effluent suspended solids concentration

4.1.11 Sludge blanket height H_{sb} and concentration X_{sb}

The presence of a high sludge blanket will inevitably mean failure for the clarifiers operation. As the sludge blanket moves lower, there is less of a scouring effect from the influent density waterfall since it has less energy, the greater the fall distance, the higher the influent waterfall potential energy. However, if a feed well baffle is present and the sludge blanket levels are high, the flow dispersed flocculated particles, or forced under the baffle at a higher velocity, which then further scours the sludge blanket and resuspends the solids. Also, even though the magnitude of the scouring is not as great when the influent waterfall has less distance to travel before encountering the sludge blanket, the scouring occurs at a higher elevation, and consequently closer to the effluent weir. When this happens, the resuspended solids have less of a travel distance to the effluent weirs, which affect to higher suspended solids concentrations in effluent.

For the calculation of sludge blanket concentration X_{sb} combination equations was taken from Halttunen ^[20] and Nielsen et al. ^[45] to get the following equation:

$$X_{sb} = \frac{X_r}{\sqrt{1 + \frac{H_{sb}}{H} \cdot \frac{Q}{Q_r} \cdot \frac{SVI}{X_r}}}, \quad (4.7)$$

where SVI = Sludge volume index.

The boundary condition is a function of the ratio of the downward settling flux (deposition) and the upwards-turbulent flux (resuspension). Sediment is found in two layers

on the floor of the tank: a bed load layer containing settled material with a high concentration and a suspended solids layer.

Figures 4.17 and 4.18 presented the sludge blanket measurements and calculation results for the flow rate from 250 to 500 m³/h, and SVI for both cases was 135 ml/g.

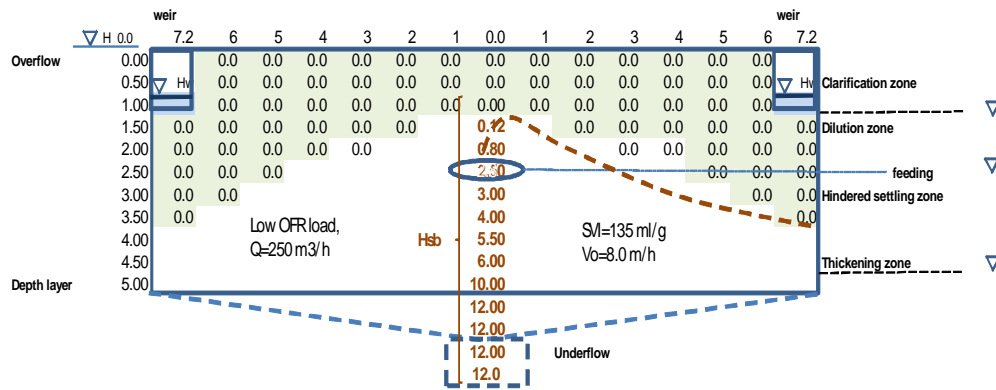


Figure 4.17. Sludge concentration profile in vertical direction distribution and blanket height for flow rate 250 m³/h

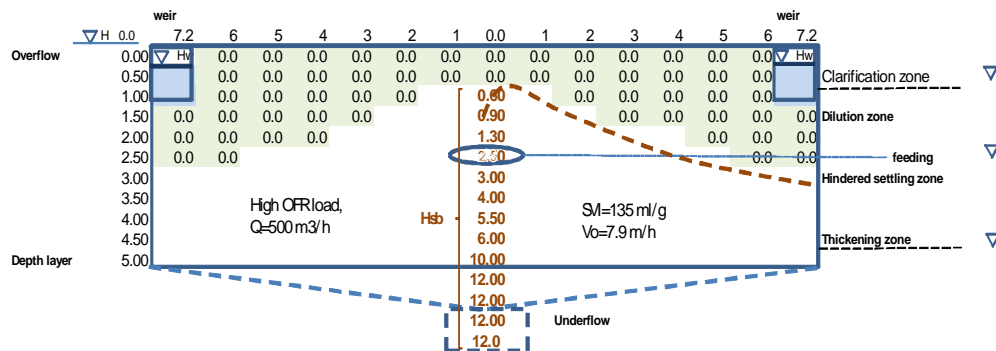


Figure 4.18. Sludge concentration profile in vertical direction distribution and blanket height for flow rate 500 m³/h

To avoid and control the scouring effect from sludge blanket on effluent suspended solids concentration, the height of sludge blanket H_{sb} where calculated and following mass balance were written by Stamou et al. [56]:

$$M_{sb} = X_{sb} \cdot V_{sb} = X_{sb} \cdot A_{sb} \cdot H_{sb} \quad (4.8)$$

where M_{sb} = mass of suspended solids in sludge blanket (kg); X_{sb} = average concentration of suspended solids in the sludge blanket (kg/m³); V_{sb} = volume of the sludge blanket (m³); and A_{sb} = surface area of the sludge stock (m²).

4.1.12 Dilution zone concentration X_f

In steady state conditions X_f can be determined using the mass balance in the inlet zone (Figure 4.19), which is written as follows Tchobanoglous and Burton ^[63]:

$$(Q_i + Q_r) \cdot X_i = (Q_r + V_S \cdot A) \cdot X_f \quad (4.9)$$

and

$$X_f = \frac{Q_i + Q_r}{Q_r + V_S \cdot A} \cdot X_i; \quad (4.10)$$

$$X_f = \frac{(1 + Q_r / Q_i) \cdot X_i}{(Q_r / Q_i + V_S / (Q_i / A))} \quad (4.11)$$

where V_S = settling velocity of the sludge particle (m/d); $OFR_{avg} = Q_i / A$ = overflow rate (m/d); and $V_S / (Q_i / A) = H_a$ = Hazen Number.

In Equations (4.10 – 4.12) the process of settling is modeled as a flow of the suspended solids in the direction of gravity with velocity V_S . In simple mathematical models, V_S is assumed to be constant. A more realistic approach is to use a Settling Velocity Curve (SVC), in which, the suspended solids are divided into classes, due to the variation of particle diameter, each having a discrete settling velocity Stamou et al. ^[55]. In practice, however, it has been found that V_0 is a function of the local suspended solids concentration (X_i) and belongs to the hindered settling, due to the agregadation of particles Takacs et al. ^[61].

In this study the small flocculated sludge particle was found in the clarification and dilution zones, which form the suspended solids concentration in effluent, launder.

To use the V_0 velocities, which strongly depends on SVI and is in range from 8 till 4 m/h for the upper layers (clarification and dilution zones), where different sedimentation process takes place was not possible. In this study only for clarifier zones 3 and 4 Vaccari and Christodoulatos ^[66] equation to calculate sludge particle sedimentation velocity V_0 , is used, and data good correspond to author results for the hindered settling and thickening zones, but the value correlation for clarification zone, there suspended solids concentration was not satisfactory. In study was found, that V_0 calculations week correspond to measured velocity values for the clarifier upper zones, where the size of particles are not the same as in the hindered settling zones. The velocity was in the range from 0.1 till 0.05 m/h, and is much smaller then V_0 , what was from 4 m/h till 9 m/h, depending on existing SVI value. To

overcome this difficulty a simpler approach was adopted and to calculate the suspended solids concentration in dilution or clarification zones per each, the system mass balance was used, but the local velocities was calculated and measured by separate layers each on site.

The following mass balance equation for dilution zone was used Stamou et al. ^[56]:

$$X_f = \frac{Q_i + Q_r}{Q_r + V_S} \cdot X_i \quad (4.12)$$

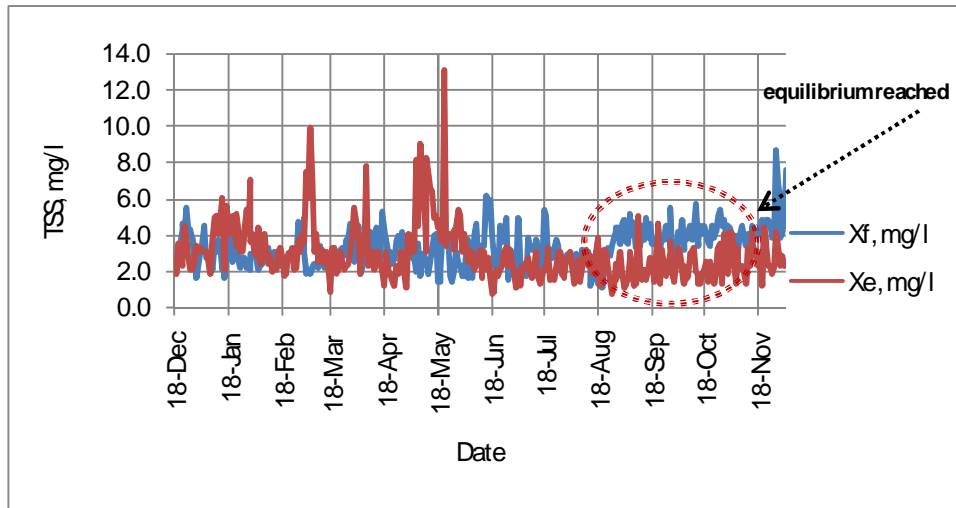


Figure 4.19. X_f variations for two different flow rates

Figure 4.19 illustrate the X_f variations at flow rates 250 m³/h to 500 m³/h. These figures show that high variation only for flow rate 500 m³/h, but always $X_f > X_e$. When the SVI is kept in highest level 135 mg/l, there have no possibility for scoring, but when the smaller range $SVI=60$ ml/g, then scouring can occur and suspended solids concentration in effluent is investigated.

4.1.13 The scouring velocity determination

The hydraulic load of the clarifier is chosen also independently provided that the velocity of the wastewater in the tank is not too high to produce scouring. If the mean velocity V_0 velocity in the tank is too high and it exceeds the scour velocity, settled solids can be scoured from the zones.

If the water velocity in the tank dilution or clarification zone is too high, i.e., it exceeds the scour velocity settled solids can be resuspended, i.e., scoured even from sludge blanket from the bottom of the tank or small particles from the dilution zone can escape into effluent launder and thus increase the effluent TSS concentration.

The settling velocity for microflocs was calculated by Dupont and Dahl, after Hultman and Hultgren ^[22], and presented model covers both the free settling zone and the hindered settling zone and therefore it has an increasing settling velocity for increasing concentrations at low SS concentrations and a decreasing settling velocity for increasing concentration at high SS concentration and following formula was used:

$$V_s = V_0 \cdot \exp \left[-0.5 \left[\frac{\ln \left(\frac{X_{ss} + X_{pp}}{n_1} \right)}{n_2} \right]^2 \right] \quad (4.13)$$

where V_s = settling velocity for microflocs, m/h; V_0 = maximum settling velocity for macroflocs, m/h; X_{ss} = macrofloc concentration in the settling tank, g/m³; X_{pp} = concentration of primary particles in the influent to the settling tank, g /m³; n_1, n_2 = sludge characterization constants.

The scour velocity taken into account Equation (4.14) and boundary conditions for the scouring zone can be calculated Takamatsu et al. ^[62] and Zhou et al. ^{[71]; [72]}:

$$V_{scour} = \sqrt{\left(8 \cdot \beta \cdot g \cdot \frac{d_p}{f} \right) \cdot \left(\frac{r_s - r_w}{r_w} \right)} \quad (4.14)$$

where β = constant (0.04 for unigranular sand, 0.06 for sticky interlocking materials); f = Darcy - Weisbach friction factor (0.02 to 0.03).

If the settling velocity of a particle is smaller than critical velocity, then it may or may not settle out depending on its starting position. This situation implies that particles with a higher initial position than this particle will all escape, and those with lower initial position will all settle out. The ratio of settling can be calculated as described earlier, by equation (4.13) and $V_{scour} < V_{lt}$.

4.1.14 CFD

In this study the SSIIM (version 1.1) ^[57] CFD software was used. All the experiments run in this thesis were done with structured grids. “SSIIM 1.1” for structured grids is meant. SSIIM is an abbreviation for Sediment-Simulation-In-Intakes with Multi-block option. The program is made for use in River/Environmental/Hydraulic/Sedimentation Engineering, SSIIM ^[57].

The Navier-Stokes Equations describe the velocity and pressure fields in a water body, i.e., in a volume element in the flow. The equations were developed for laminar flow, but using Reynolds averaging and a turbulence model; the equations also model turbulent flow.

$$\frac{\partial U_i}{\partial t} + U_j \frac{\partial U_i}{\partial x_j} = \frac{1}{r} \frac{\partial}{\partial x_j} \left[-P d_{ij} - r \overline{U_i U_j} \right] \quad (4.15)$$

Where U_i = local velocity; x_i = space dimension; d_{ij} = Kronecker Delta (if $i = j$ then 1, else 0); r = fluid density; P = pressure; $\overline{U_i}$ = averaged velocity.

The three space directions are x_1 , x_2 and x_3 . The index 1 indicates the stream wise direction, 2 the cross-stream wise direction and the 3 the vertical direction.

The modeling result of velocity distribution is presented in Figure 4.24, and verification with field measurements was done.

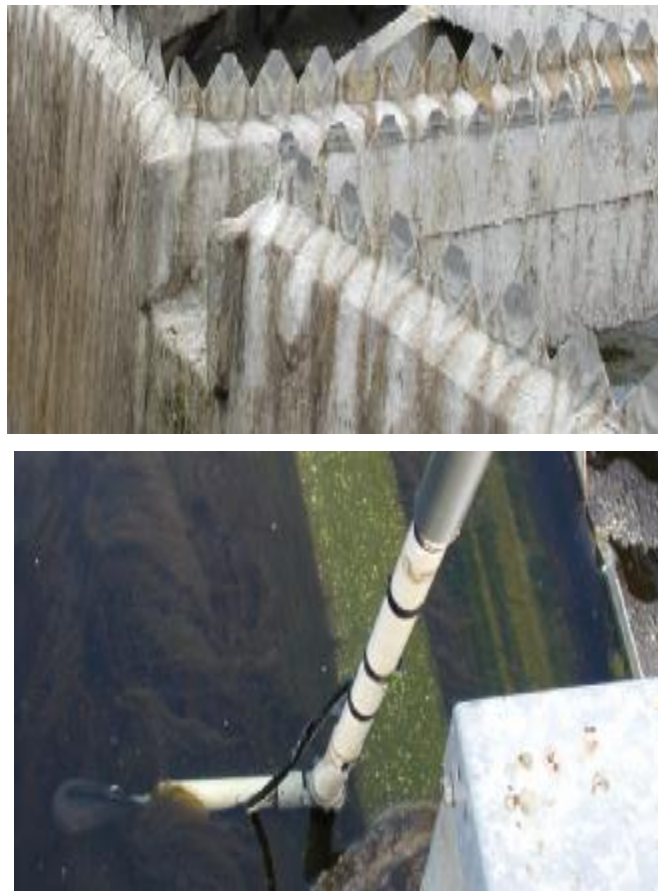


Figure 4.20. Field measurements

4.2 Application results

The aim of study was to examine the individual effect of the scouring on sludge particle escaping from clarifier due to variation of overflow loads, sludge blanket depth, weir loads and local velocity distribution. The control parameter was the effluent suspended solids concentration from secondary clarifier. The study describes the results of a full-scale clarifier test for the flow rate 250 m³/h and 500 m³/h, and the simulation results for the flow 750 m³/h, when in operation one process line.

4.2.1 Sedimentation velocities V_s and V_0

The determination the relation between V_s and V_0 impact on sludge particle sedimentation for different flow rates are showed in Figures 4.21 and 4.22.

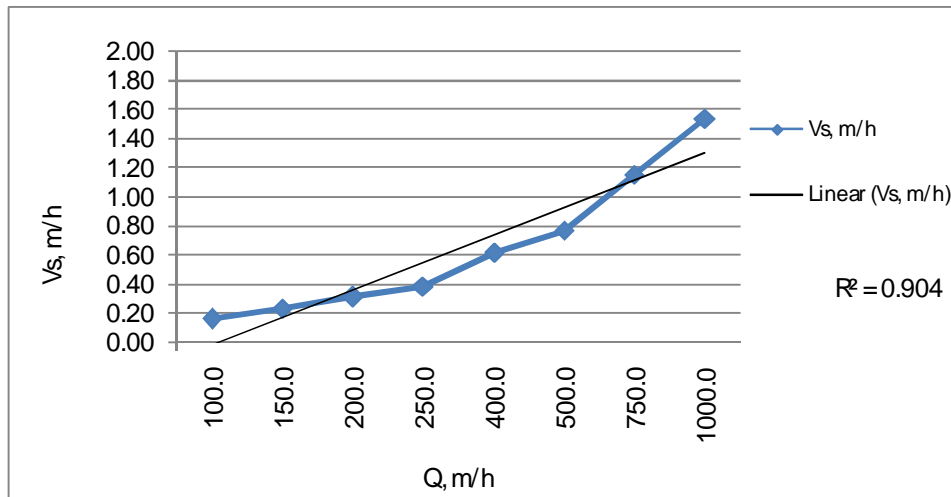


Figure 4.21. Average velocity for different flow rates

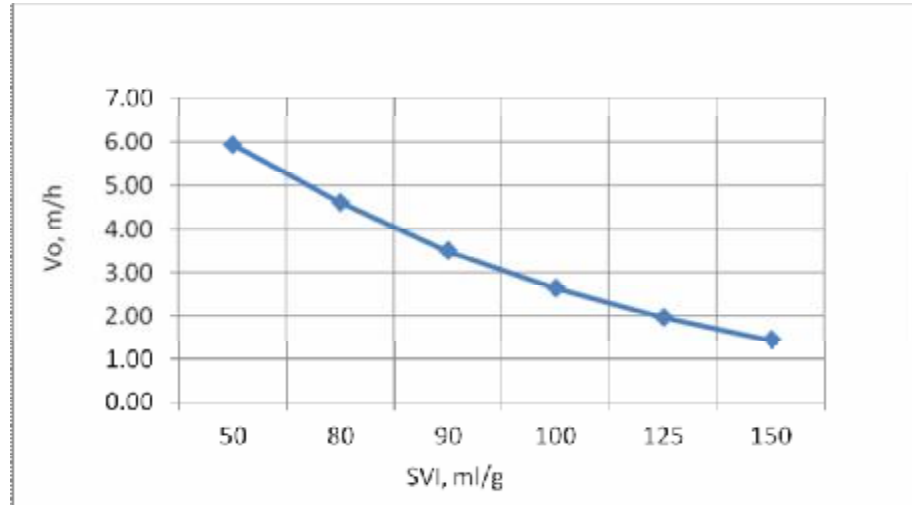


Figure 4.22. Sludge particle sedimentation velocity dependency on SVI

4.2.2 Scouring development variation for different flow rates

The influent hydraulics is largely governed by the hydraulic loading, which is the sum of the influent Q_i and the Q_r flow per unit of clarifier surface area. The clarifier geometry, such as the side water depth and the feed skirt depth also affect the influent hydraulics. All studies have high sludge blanket levels, which cause the influent flow to become moved upward, as is shown in the corresponding Figures 4.23 and 4.24. When the flow is directed upward, in some cases it creates a short-circuiting flow-path to the effluent weirs. In others, it creates additional recirculation zones that are highly unstable to develop in the settling zone. In field study two recirculation zones were found in the settling zone, which increases the amount of scour .

The suspended solids concentration distributions and velocity profiles in Figures. 4.23, 4.24 and 4.25, provide a typical illustration how the particle scouring process occurs for different investigated flow rates in the secondary clarifier. This suggests that the underflow flow rate is a one of main parameter in keeping the sludge blankets in design height, thus, preventing a clarifier from failing. The Figure 4.26 show the vertical velocity profiles for emergency load region, $Q=750 \text{ m}^3/\text{h}$.

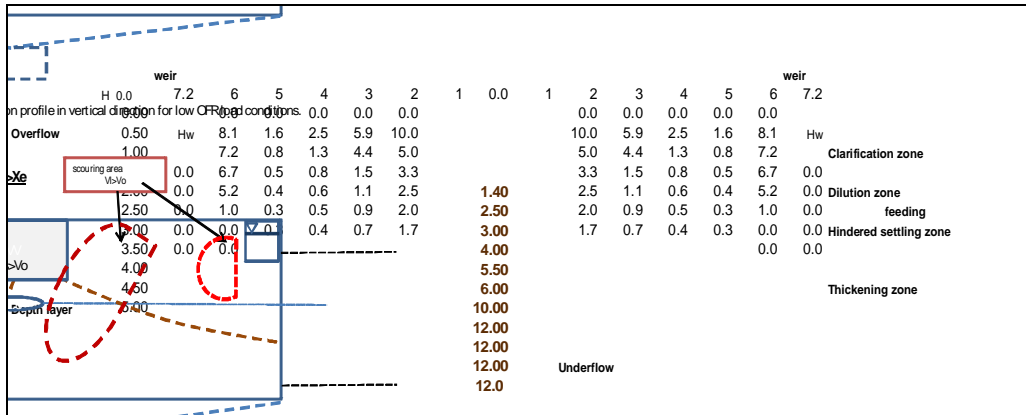


Figure 4.23. Scenario 1. Vertical velocity profiles for low load region, $Q=250 \text{ m}^3/\text{h}$

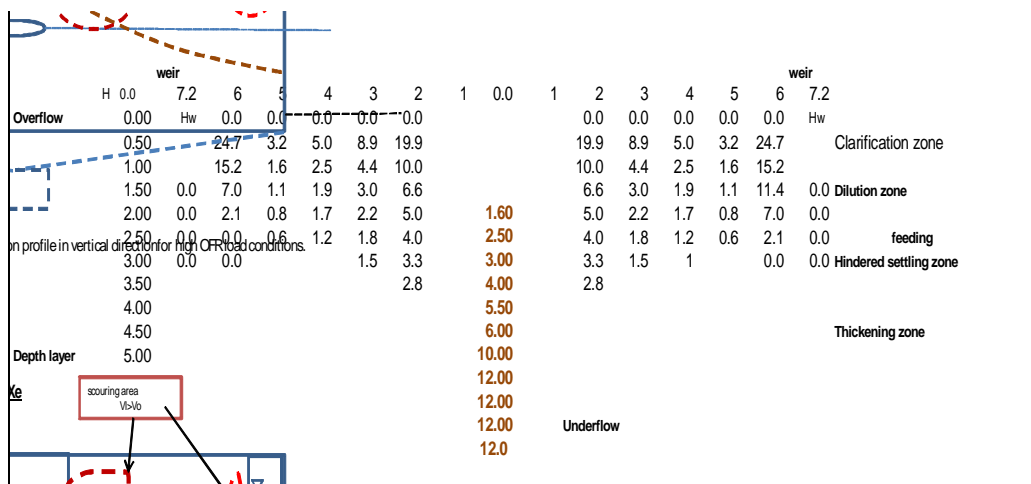


Figure 4.24. Scenario 2. Vertical velocity profiles for high load region, $Q=500 \text{ m}^3/\text{h}$

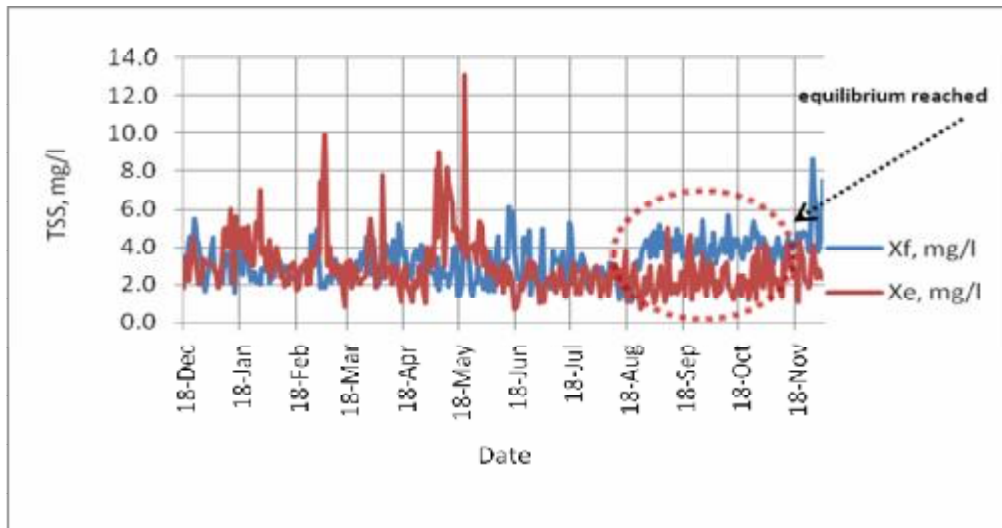


Figure 4.25. X_f variation for loads $500 \text{ m}^3/\text{h}$

Equilibrium region

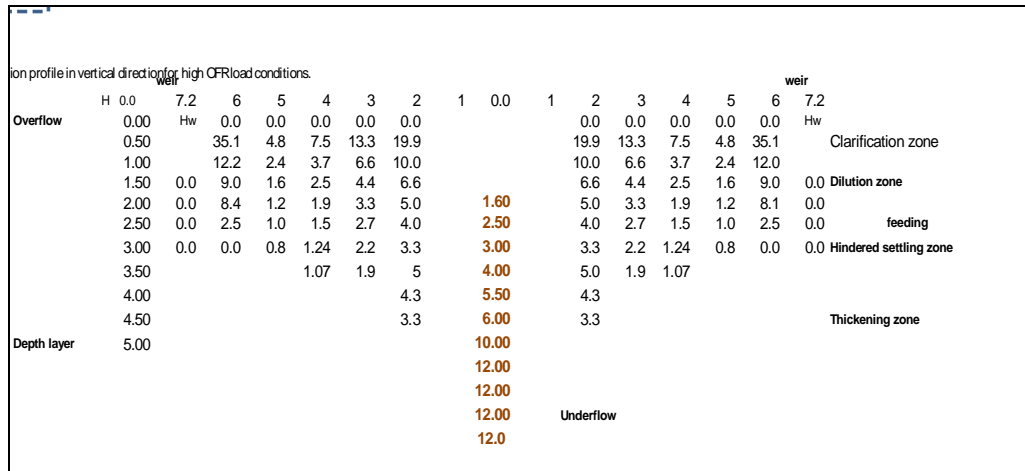


Figure 4.26. Scenario 3. Vertical velocity profiles for emergency load region, $Q=750 \text{ m}^3/\text{h}$

4.2.3 Effluent suspended solids variation

The scouring process develops within a time and the time steps were used for its calculations. The previously performed calculations, of which only for high flow rate to $500 \text{ m}^3/\text{h}$ was reached equilibrium and produced permanent effluent suspended solids concentrations, while the other two were unstable and did not reach equilibrium within the time. Each calculation was run for time steps ranging from one to several hours. For the emergency flow the effluent suspended solids increases considerably within a time as the scouring process develops.

However, it was observed that by decreasing the flow rate, the effluent suspended solids concentration would decrease more, more slowly. Nevertheless, an equilibrium result of effluent suspended solids concentration is sensitive to the time steps, as it accord to scouring calculation method. The Figure 4.27 shows the performance of effluent suspended solids increase due to scouring process development in time.

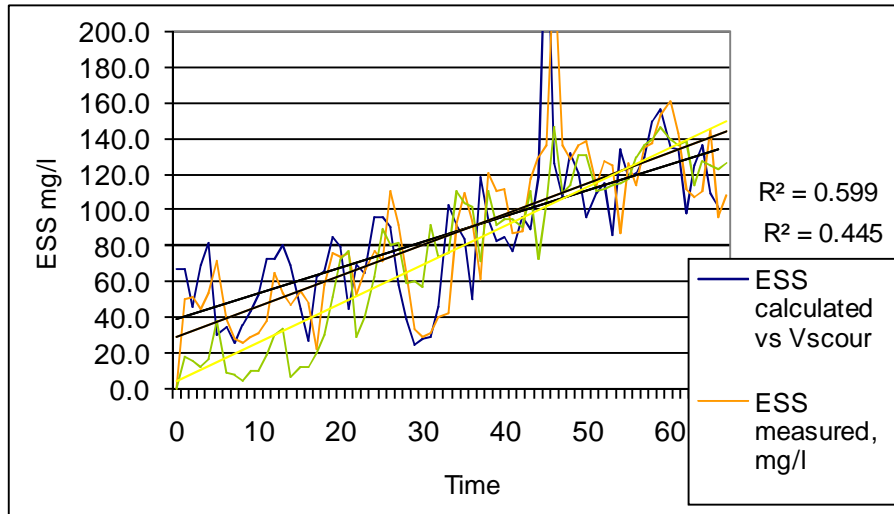


Figure 4.27. Effluent suspended solids concentration variation for emergency flow

CONCLUSIONS

1. Differential equation of the bed sediment movement for clear water was used and a new method for calculating the scour development in time at the abutments during the flood was elaborated. Method was confirmed by experimental data.
2. The theoretical analysis of the new elaborated method allowed us to estimate the influence of hydraulics and river-bed parameters on the scour at engineering structures in the flood during the time.
3. The practical application of the method was performed for Jurmala town wastewater treatment plant, to avoid the suspended solids particle escaping from process tanks, thus preventing the pollution of Lielupe River.
4. The teoretical analysis of the presented method method show dependency of relative depth of scour from flow contraction rate, relative grain size of the river bed and its distribution over the depth, Froude number in relation to the river slope, unsteadiness of the flow, ratio of the local velocity to the velocity at which the sediment movement starts, engineering structure shape, angle of flow crossing, time of scour, and duration of the flood;
5. The realtive scour depth depends on the time of scour (fig. 3.11).
6. With increase of the contraction rate the relative depth of scour increasing (fig.3.12).
7. With decrease of relative grain size the depth of scour increasing (fig. 3.13).
8. In the study was determined the effect relative scour depth changes versus the kinetic parameter changes of the flow and Froude number (fig. 3.14., 3.15).
9. With relative velocity ratio increase the relative depth of scour increases (fig.3.16).
10. In studies was determined the scour depth development at any step of hydrograph after one, two or several floods (fig.3.17).
11. The local velocity V_{lt} is decreasing in steady flow conditions because the depth of scour hole is developing and critical velocity is increasing.
12. To examine the secondary clarifier hydraulic flow pattern was found that it must be always linked with activated sludge process results, to have adequate sludge settling parameters for define wastewater and flux flow rates and that

the increase of suspended solids concentration in effluent was originated by increase of the local velocities inside the tank (fig.4.27).

REFERENCES

1. Ahmad M. Experiments on the design and behaviour of spur dikes// Proc. of International Hydraulics Convention (ASCE and IAHR). - Minneapolis, MN, U.S.A.: University of Minnesota, 1953. - pp. 145-159.
2. Ahmed F. and Rajaratnam N. Observations on flow around bridge abutment// Journal of Engineering Mechanics. – 2000. – Vol. 126(1). - pp. 51-59.
3. Ahmed F.H., Kamel A., and Abdel Jawad S. Experimental determination of the optimal location and contraction of sedimentation tank baffles// Journal of Water, Air and Soil Pollution. – 1996. – Vol. (92). – pp. 251-271.
4. Anderson N.E. Design of final settling tanks for activated sludge// Sewage Works Journal. – 1945. – Vol. 17(1). - pp. 50-65.
5. Barbhuiya A.K. and Dey S. Local scour at abutments: a review// Journal Sādhanā. – 2004. - Vol. 29(5). - pp. 449-476.
6. Baud O. and Hager W.H. Tornado vortices in settling tanks// Journal of Environmental Engineering. – 2000. – Vol. 126(2). - pp. 189-191.
7. Bretscher U., Krebs P. and Hager W.H. Improvement of flow in final settling tanks// Journal of Environmental Engineering. – 1992. – Vol. 118(3). - pp. 307-321.
8. Cardoso A.H. and Bettess R. Effect of time and channel geometry on scour at bridge abutments// Journal of Hydraulic Engineering. – 1999. – Vol. 125(4). - pp. 388-399.
9. Chang F.M. and Davis S. Maryland SHA procedure for estimating scour at bridge abutments. Part 2 – Clear water scour. ASCE Compendium: Stream Stability and Scour at Highway Bridges, Richardson and Lagasse (eds.). - Reston, VA, U.S.A.: ASCE, 1999. - pp. 412-416.
10. Chiew Y.M. Local scour at bridge piers. Report No. 355 – New Zealand: Department of civil engineering, University of Auckland, 1984.
11. Clark M.M. Critique of Camp and Stein's RMS velocity gradient// Journal of Environmental Engineering – 1985. – Vol. 111(6). - pp. 741-754.
12. Dongol D.M.S. Local scour at bridge abutments. Research Report No. 544. - Auckland, New Zealand: School of Engineering, University of Auckland, 1994. – 409 pp.
13. Froehlich D.C. Local scour at bridge abutments// Proc. of National Conference on Hydraulic Engineering. – New Orleans, LA, U.S.A.: ASCE, 1989. - pp. 922-927.
14. Garde R.J., Subramanya K., and Nambudripad K.D. Study of scour around spur dikes// Journal of the Hydraulics Division. – 1961. – Vol. 87(HY6). - pp. 23-37.
15. Gill M.A. Erosion of sand beds around spur dikes// Journal of the Hydraulics Division. – 1972. - Vol. 98(HY9), - pp. 1587 -1602.
16. Gjunzburgs B. and Neilands R. Scour development on time at the abutment of the bridge on plain rivers// Proc. of Conference on Environmental Research,

Engineering and Management, Vol. 1(15). – Vilnius: Kaunas University of Technology, 2001. - pp. 8-11.

17. Gjonsburgs B. and Neilands R. Local velocity at bridge abutments on plain rivers// Proc. of Conference on Fluvial Hydraulics: River Flow 2004. - London: Taylor & Francis Group, A.A.Balkema, 2004. - pp. 443-448.
18. Gjonsburgs B., Neilands R., and Kreslins A. Abutment scour development during floods// Proc. of 17th Canadian Hydrotechnical Conference - Hydrotechnical Engineering: Cornerstone of a Sustainable Environment. - Edmonton, Alberta: CSCE/SCGC, 2005. - pp. 593-601.
19. Gjonsburgs B., Neilands R., and Neilands R.j. Scour development at bridge abutments on plain rivers during the flood: Analysis of the method// Proc. of 2nd International conference on Scour and Erosion. - Singapore: Stallion Press, 2004. - pp. 199-206.
20. Halttunen S. Thickening in an activated sludge process clarifier// Water Science Technology. – 1996. – Vol. 33(12). – pp. 171-180.
21. Hazen A. On sedimentation - Trans.: ASCE, 1904. - pp. 45-71.
22. Hultman B. and Hultgren J. Deviations from the Kynch theory in thickening sludges from wastewater treatment plants// Trib. Cebedeau. – 1980. - Vol. 33(441-442). - pp. 375-389.
23. Julien P.J. Erosion and Sedimentation. – New York: Cambridge University Press, 1995. – 286 pp.
24. Katz W.J. and Geinopolos A. A study of the solids retention characteristics of a final clarifier in the activated sludge process// Proc. of 1st Int. Water Pollution Conference. – London, UK, 1962.
25. Kinnear D.J. Evaluating secondary clarifier performance and capacity// Proc. of Florida Water Resources Conference. - Tampa, Florida: USA, 2000.
26. Kouchakzadeh S. and Townsend R.D. Maximum scour depth at bridge abutments terminating in the floodplain zone// Canadian Journal of Civil Engineering. – 1997. – Vol. 24. – pp. 996-1006.
27. Kothyari U.C., Garde R.J., and Ranga Raju, K.G. Temporal variation of scour around circular bridge piers// Journal of Hydraulic Engineering. – 1992. – Vol. 118(8). - pp. 1091-1106.
28. Kothyari U.C. and Ranga Raju K.G. Scour around spur dikes and bridge abutments// Journal of Hydraulic Research. – 2001. – Vol. 39(4). - pp. 367-374.
29. Lacey G. Stable channels in alluvium// Proc. of the Institution of Civil Engineers. – London, UK: William Clowes and Sons Ltd., 1930. - pp. 259-292.
30. Latishenkov A.M. Questions of artificially contracted flow. Moscow: Stroiizdat, 1960. – 214 pp. (In Russian: Латышенков А.М. Вопросы гидравлики искусственно сжатых русел. - Москва: Стройиздат, 1960. – 214 с.).
31. Larsen P. On the hydraulics of rectangular settling basins. Report No.1001. – Lund, Sweden: Department of Water Resource Engineering, Lund Institute of Technology, 1977.

32. Laursen E.M. An analysis of relief bridge scour// Journal of the Hydraulics Division. – 1963. – Vol. 92(HY3). - pp. 93-118.
33. Levi I.I. Engineering hydrology. - Moscow: Vishaja Shkola, 1968. – 235 pp. (*in Russian*: Леви И.И. Инженерная гидрология. - Москва: Высшая школа, 1968. – 235 с.).
34. Lim S.V. Equilibrium clear-water scour around abutment// Journal of Hydraulic Engineering. – 1997. – Vol. 123(3). - pp. 237-243.
35. Lim S.Y. and Cheng N.S. Prediction of live-bed scour at bridge abutments// Journal of Hydraulic Engineering. – 1998. – Vol. 124(6). - pp. 635-638.
36. Liu H.K., Chang F.M., and Skinner M.M. Effect of bridge construction on scour and backwater. Report CER 60 HKL 22. - Fort Collins, CO, U.S.A.: Department of Civil Engineering, Colorado State University, 1961. – 118 pp.
37. Melville B.W. Local scour at bridge abutments// Journal of Hydraulic Engineering. – 1992. - Vol. 118(4). - pp. 615-631.
38. Melville B.W. Bridge abutment scour in compound channels// Journal of Hydraulic Engineering. – 1995. – Vol. 121(12). - pp. 863-868.
39. Melville B.W. Pier and abutment scour: integrated approach// Journal of Hydraulic Engineering. – 1997. – Vol. 123(2). - pp. 125-136.
40. Melville B.W. and Coleman S.E. Bridge scour - CO, U.S.A: Water Resources Publications, HighLands Ranch, 2000. – 550 pp.
41. Melville B.W. and Ettema R. Bridge abutment scour in compound channels// Proc. of Nat. Conf. on Hydr. – New York: ASCE, 1993. – pp. 767 – 772.
42. MSHA. Maryland State Highway Administration abutment scour program's (ABSCOUR) user manual. - Maryland, U.S.A.: MSHA, 2005. – 90 pp.
43. Neilands R., Klīve G., Gjunsburgs B., Neilands R.j. Management and protection of the trans-national rivers Lielupe and Venta in the Baltic region// Proc. of Int. Conf. River Basin Management – progress towards implementation of the European Water Framework Directive. – Budapest, Hungary: Hungarian Academy of Science, 2005.
44. Neill C.R. Guide to Bridge Hydraulics. - Toronto, Canada: Roads and Transportation Association of Canada, University of Toronto Press, 1973.
45. Nielsen M.K., Carstensen J., and Harremoës P. Combined control of sewer and treatment plant during rainstorm// Water Science Technology. – 1996. – Vol. 34(3-4). pp. 181-187.
46. Pirestani M.R., Tabatabai M.R.M., and Salehi Neyshabouri A.A. Experimental Study of scouring in the vicinity of lateral intake in u-shape channels// Proc. of 3rd Int. Conf. on Scour and Erosion. - Gouda, Netherlands: Curnet, 2006. - pp. 200 (full paper on CD, pp. 534-538).
47. Rahman M.M. and Haque M.A. Local scour estimation at bridge site: modification and application of Lacey formula// Journal of Sediment Research. – 2003. – Vol. 18(4). - pp. 333 -339.

48. Rajaratnam N. and Nwachukwu B.W. Flow near groyne-like structures// Journal of Hydraulic Engineering. – 1983. – Vol. 109(3). - pp. 463-480.
49. Richardson J.R. Discussion of “Equilibrium clear-water scour around an abutment” by S.Y. Lim// Journal of Hydraulic Engineering, ASCE, - 1998. – Vol. 124(10). - pp. 1071- 1072.
50. Richardson E.V. and Davis S.R. Evaluating scour at bridges. 3rd Ed. Hydraulic Engineering Circular No.18. Publication No. FHWA–10–90–017. - Washington, DC, U.S.A.: FHWA, USDOT, 1995. – 240 pp.
51. Richardson E.V. and Davis S.R. Evaluating scour at bridges. 4th Ed. Hydraulic Engineering Circular No.18. Publication No. FHWA NHI 01-001. - Washington, DC, U.S.A.: FHWA, USDOT, 2001. – 378 pp.
52. Richardson E.V., Simons D.B., and Julien P. Highways in the river environment (HIRE). Report No. FHWA-HI-90-016. - Washington, DC, U.S.A.: FHWA, USDOT, 1990. – 683 pp.
53. Rotenburg I.S. and Volnov V.S. Project examples of bridge crossing. – Moscow: Vishaja Shkola, 1969. – 284 pp. (*In Russian*: Ротенбург И.С., Вольнов В.С. Примеры проектирования мостовых переходов. - Москва: Высшая школа, 1969. - 284 с.).
54. Rozovskij I.L. Investigation of cross circulation at curved river flow// Meteorology and hydrology. – 1955. – Vol. 6. – 47 pp. (*In Russian*: Розовский И.Л. Исследование поперечной циркуляции на изгибе речного потока / Метеорология и гидрология. – 1955. - № 6. – 47 с.)
55. Stamou A.I., Adams E.W., and Rodi W. Numerical modeling of flow and settling in primary rectangular clarifiers// Journal of Hydraulic Research. – 1989. – Vol. 27(5). - pp. 665-682.
56. Stamou A.I., Latsa M., and Assimacopoulos D. Design of two-storey final settling tanks using mathematical models// Journal of Hydroinformatics. – 2000. – Vol. 2(4). - pp. 235-245.
57. SSIIM, Version 1.1, User Manual, SSIIM. NTKH, 2007.
58. Studenitcnikov B.I. Flow erosion capacity and riverbed calculation methods. - Moscow: Gosstroizdat, 1964. – 184 pp. (*In Russian*: Студеничников Б.И. Размывающая способность потока и методы русловых расчетов. - Москва: Госстройиздат, 1964. – 184 с.).
59. Sturm T.W. Enhanced abutment scour studies for compound channels. Final report No. FHWA-RD-99-156 - McLean, VA, U.S.A.: FHWA, USDOT, 2004. – 144 pp.
60. Sturm T.W. and Janjua N.S. Clear-water scour around abutments in floodplains// Journal of Hydraulic Engineering. – 1994. – Vol. 120(8). - pp. 956-972.
61. Takács I., Patry G.G., and Nolasco D. A dynamic model of the clarification-thickening process// Journal of Water Research. – 1991. – Vol. 25(10). - pp. 1263-1271.

62. Takamatsu T., Naito M., Shiba S., and Ueda Y. Effects of deposit resuspension on settling basin// Journal of Environmental Engineering Division. – 1974. – Vol. 100(EE4). - pp. 883-903.
63. Tchobanoglous G. and Burton F.L. Wastewater Engineering: Treatment, Disposal and Reuse. 3rd.,Ed., Metcalf & Eddy Inc: McGraw Hill, 1991. – 1334 pp.
64. Tekippe R.J. Secondary settling tank inlet design: full scale test results lead to optimization// Proc. of 75th Annual WEF Conference and Exposition on Water Quality and Wastewater Treatment. - Chicago, Illinois: USA, september 2002.
65. Van Marle C. and Kranenburg C. Effects of gravity currents in circular secondary clarifiers// Journal of Environmental Engineering – 1994. – Vol. 120(4). - pp. 943-960.
66. Vaccari D.A. and Christodoulatos C. Estimation of the Monod Model Coefficients for Dynamic Systems using Actual Activated Sludge Plant Data// Water Science Technology. – 1990. - Vol. 10. - pp. 449-454.
67. Weber S.W. and Rowe D.S. Modeling techniques for dispersed multiphase flows. In: Encyclopedia of Fluid Dynamics, Vol. 3 (Gas-liquid flows), Ed. Cheremisinoff N.P. -Houston, Texas, USA: Gulf Publishing Company, 1986.
68. Yaroslavcev I.A. Calculation of local scour at bridge piers. Bulletin No.80. – Moscow: CNIIS, 1956. – 45 pp. (*in Russian: Ярославцев И.А. Расчет местного размыва у мостовых опор. Сообщение No.80. - Москва: ЦНИИС, 1956. – 45 с.*).
69. Young G.K., Dou X., Saffarinia K., and Jones J.S. Testing abutment scour model// Proc. of Water Resources Engineering. - Memphis, TN, U.S.A.: ASCE, 1998. - pp. 180-185.
70. Young G.K., Palaviccini M., and Kilgore R.T. Scour prediction model at bridge abutments// Proc. of Hydraulics Conference, San Francisco, U.S.A: ASCE, 1993. - pp. 755-760.
71. Zhou S., McCorquodale J.A., and Vitasovic Z. Influences of density on circular clarifiers with baffles// Journal of Environmental Engineering. – 1992. – Vol. 118(6). - pp. 829-847.
72. Zhou S., McCorquodale J.A., and Zhong J. Semi-implicit skew upwind method for problems in environmental hydraulics// Int. Journal of Numerical Meth. Fluids. – 1993. – Vol. 17. - pp. 803-823.

NOTATION

The following symbols are used in this document:

A	= parameter in Levi equation;
$A_1; A_2$	= parameters;
A^*	= unobstructed flow area;
A_e	= flow area of the approach cross section obstructed by embankment;
A_s	= surface area;
a	= blocked flow area by embankment and abutment;
a_1	= opening ratio;
a_{fl}	= unsteadiness of the flow;
B	= width of scour hole;
B_{fl}	= width of floodplain;
b	= width of cylindrical pier;
b_s	= size of analogous pier;
C_D	= drag coefficient;
C_r	= best-fit coefficient in Sturm equation;
C_0	= best-fit constant in Sturm equation;
D_i	= constant parameter in steady flow time step;
$d; d_i$	= grain size;
$d_{16}; d_{84}$	= particle size for which 16%, 84%, etc. are finer by weight;
d_{50}	= median sediment size;
Fr	= Froude number;
Fr_0	= uniform flow Froude number;
Fr_1	= approach flow Froude number;
Fr_C	= Froude number of flow at critical condition of sediment motion;
Fr_d	= dens metric particle Froude number;
Fr_{fl}	= Froude number of the floodplain flow;
Fr_f	= Froude number for flume;
Fr_R	= Froude number for plain river;
FS	= factor of safety;
f	= multiplying factor, Lacey's silt factor;
g	= gravitational acceleration;
H	= bed layer height;
H_{sb}	= height of the sludge blanket
H_{inlet}	= inlet height of settler;
h	= flow depth;
h_0	= normal flow depth;
h_1	= approaching flow depth;
h_2	= total flow depth after scour (including scour depth);
h_c	= depth of flow at the abutment on the over-bank or in the main channel;
h_{contr}	= contraction scour depth;
h_{equil}	= equilibrium depth of scour;
$h_f; h_{fc}$	= average flow depth in the contraction;
h_{fl}	= flow depth in the floodplain;
h_m	= flow depth in the main channel;
h_{mid}	= medium flow depth;
h_s	= depth of scour;
h_{sc}	= total flow depth including contraction scour depth;

$h_{s,calc.}$	=	calculated depth of scour;
$h_{s,exp.}$	=	depth of scour derived from experiments;
I	=	longitudinal energy gradient;
i_0	=	river slope;
K_1	=	embankment and abutment geometric shape factor;
K_2	=	embankment alignment factor;
K	=	adjustment factor;
K_d	=	sediment size factor in Melville equation;
K_G	=	channel geometry factor in Melville equation;
K_{hL}	=	flow depth – foundation size factor in Melville equation;
K_I	=	flow intensity factor in Melville equation;
K_s	=	abutment shape factor;
K_s^*	=	adjusted shape factor in Melville equation;
K_{ST}	=	spill-through abutment shape factor in Sturm equation;
K_θ	=	abutment alignment factor in Melville equation;
K_θ^*	=	adjusted alignment factor in Melville equation;
K_σ	=	sediment gradation factor in Melville equation;
k	=	coefficient depending on flow contraction rate;
k_f	=	spiral-flow adjustment factor in Chang and Davis equation;
k_m	=	coefficient depending on the side-wall slope of abutment;
$k_s; K_1$	=	coefficient depending on the abutment shape;
k_v	=	velocity adjustment factor in Chang and Davis equation;
$k_\alpha; K_2$	=	coefficient depending on the angle of flow crossing;
k_1	=	multiplying factor in Lacey equation;
k_2	=	multiplying factor depending on flow intensity and angle of inclination in Ahmad equation;
L	=	flume/channel width; sedimentation distance;
L'	=	length of active flow obstructed by the embankment;
L_a	=	abutment length;
L_a'	=	abutment length projected normal to flow;
L_b	=	bridge opening;
M	=	geometric contraction ratio;
M_1	=	discharge contraction ratio in Sturm equation;
M_{ss}	=	mass of suspended solids in clarifier;
M_{sb}	=	mass of suspended solids in sludge blanket;
$1/m$	=	slope of the scour hole wall;
N_i	=	parameter;
N_{i-1}	=	parameter;
n	=	Manning's roughness coefficient;
n_m	=	Manning's roughness coefficient in main channel;
n_{fl}	=	Manning's roughness coefficient in floodplain;
OFR	=	overflow rate;
P_K	=	kinetic parameter of the open flow;
P_{Kb}	=	kinetic parameter of the flow under the bridge;
Q	=	flow discharge;
Q_a	=	discharge in obstructed area over a length equal to abutment length;
Q_b	=	flow discharge in the area of bridge opening;
Q_c	=	flow discharge in main channel for uniform flow in compound channel;
Q_e	=	flow obstructed by the abutment and approach embankment;

Q_f	=	discharge across the width of the scour hole with plain bed;
Q_{fl}	=	discharge in the approaching floodplain;
Q_{obst}	=	obstructed discharge in the approach section;
Q_s	=	sediment discharge out of scour hole;
Q_{sc}	=	discharge across the width of the scour hole with scour depth h_s ;
Q_w	=	flow discharge at a specific width near tip of abutment;
Q/Q_b	=	flow contraction rate;
q	=	flow rate per unit width;
q_1	=	flow rate per unit width in approach section;
q_2	=	flow rate per unit width in the contracted section;
R	=	hydraulic radius;
Re_f	=	Reynolds number for flume;
Re_R	=	Reynolds number for river;
S	=	specific gravity;
SLR	=	sludge loading rate;
SVI	=	sludge volume index;
TSS	=	total suspended solids;
t	=	time;
t_i	=	time interval;
t_{equil}	=	equilibrium time;
t_{fl}	=	flood duration;
t^*	=	dimensionless time;
u^*	=	shear velocity;
u^*_1	=	approaching section shear velocity;
u^*_C	=	critical shear velocity;
V	=	average flow velocity;
V_1	=	approach flow velocity;
V_c	=	critical flow velocity;
V_{cc}	=	critical velocity for the un-constricted approach flow in the main channel evaluated for normal flow depth h_c in the main channel;
V_e	=	flow velocity in obstructed area by embankment and abutment;
V_{flc}	=	critical velocity for the un-constricted approach flow in the floodplain evaluated for h_{fl} ;
V_K	=	average flow velocity in bridge opening in open-flow conditions;
V_R	=	resultant flow velocity adjacent to tip of the abutment;
V_{xc}	=	approaching flow critical velocity;
V_{cc}	=	critical velocity for the approaching flow in the main channel;
V_{flc}	=	critical velocity for the approaching flow in the floodplain;
V_l	=	local flow velocity;
$V_{l.calc.}$	=	calculated local flow velocity;
$V_{l.exp.}$	=	local flow velocity obtained in tests;
V_{lt}	=	local flow velocity at scour depth h_s ;
V_x	=	average contraction velocity;
V_0	=	local velocity at which sediment movement starts; maximum hindered settling;
V_{0t}	=	velocity at which sediment movement starts at scour depth h_s ;
V_d	=	discrete settling velocity;
V_{sb}	=	volume of sludge blanket;
w	=	volume of scour hole;

W_{calc}	=	calculated volume of scour hole;
W_{test}	=	volume of scour hole obtained in tests;
w_s	=	settling velocity of sediment;
x_i	=	inlet concentration of suspended solids;
x_r	=	return suspended solids concentration;
x_s	=	suspended solids concentration in sludge waste;
x_f	=	diluted Concentration of SS in the dilution zone;
x_{sb}	=	average concentration of SS in the sludge blanket;
x_e	=	effluent concentration of suspended solids;
α	=	opening ratio;
β	=	coefficient of reduction in the velocity because of vortex structures;
γ	=	specific weight;
γ_f	=	specific weight of water;
γ_s	=	specific weight of sediment;
Δh	=	maximum backwater level;
ΔZ	=	water level difference at the corner of abutment;
θ	=	angle of inclination;
ξ	=	independent dimensionless ratio in Sturm equation;
ρ_f	=	mass density of water;
ρ_s	=	mass density of sediment;
σ_g	=	standard deviation of the sediment size distribution;
τ	=	shear stress;
τ_c	=	critical shear stress;
τ^*_c	=	critical value of Shields' parameter;
τ_0	=	bed shear stress of approaching flow;
φ	=	velocity coefficient depending on the flow contraction rate;
φ_1	=	angle of repose of the bed material.

APPENDIXES

APPENDIX 1

ROBO. Calculation example

INITIAL DATA:				Grain size characteristics				Time step table				Time step table								
Nr.	hf (m)	Q/Qb	Δh (m)	I	d _i	Y _i	H _{d_i}	t ₁	t ₂	t ₃	t ₄	t ₅	t ₆	t ₇	t ₈	t ₉	t ₁₀	Total	3 days	
1	0.19	1.000	0.174	1	0.0005	1.60	10.0	t ₁₁	0.0209	t ₁₁	0.125	Nr.	V _l (m/s)	Nr-1	1	1.5148	-0.0333			
2	0.98	1.330	0.204	2	0.0010	1.80	1.0	t ₂	0.0209	t ₁₂	0.125	2	1.6270	0.2019	2	1.6270	0.2019			
3	1.72	1.490	0.365	3	0.0015	1.90	1.3	t ₃	0.0417	t ₁₃	0.125	3	2.1678	0.7465	3	2.1678	0.7465			
4	2.30	1.420	0.406	4	0.0025	2.00	99.9	t ₄	0.0417	t ₁₄	0.250	4	2.2902	2.1394	4	2.2902	2.1394			
5	1.26	1.140	0.127					t ₅	0.0417	t ₁₅	0.250	5	1.2898	64.8727	5	1.2898	64.8727			
6	0.87	1.080	0.100					t ₆	0.083	t ₁₆	0.250	6	1.1461	355.9718	6	1.1461	355.9718			
7	0.19	1.000	0.174					t ₇	0.083	t ₁₇	0.250	7	1.5148	1107276.8915	7	1.5148	1107276.8915			
8	0.98	1.330	0.204					t ₈	0.083	t ₁₈	0.250	8	1.6270	203.0720	8	1.6270	203.0720			
9	1.72	1.490	0.365					t ₉	0.083	t ₁₉	0.250	9	2.1678	17.2228	9	2.1678	17.2228			
10	2.30	1.420	0.406					t ₁₀	0.125	t ₂₀	0.500	10	2.2902	6.4616	10	2.2902	6.4616			
11	1.26	1.140	0.127									11	1.2898	119.1949	11	1.2898	119.1949			
12	0.87	1.080	0.100									12	1.1461	685.0671	12	1.1461	685.0671			

CALCULATIONS AND RESULTS:																					
Nr.	t _i (day)	d _i (m)	Y _i	V ₀ (m/s)	V ₁ (m/s)	A _i	m	D _i	t (day)	N _i	Index	i	i+1	f(i)	f(i+1)	X _{d(N_i)}	h _s (m)	B (m)	W (m ³)	V _{lt} (m/s)	V _{0t} (m/s)
0	0	0.0005	1.60	0.355	1.515	29.234	1.65	0.0137	0	-0.03	2	-0.03	-0.03	1.00	1.05	1	0.0	0.0	0.0	1.515	0.355
1	0.0209	0.0005	1.60	0.355	1.515	29.234	1.65	0.0137	0.021	10.50	24	8.59	11.80	2.20	2.30	2.259	0.4786	0.7896	0.1562	0.706	0.436
2	0.0209	0.0005	1.60	0.355	1.515	14.686	1.65	0.0273	0.042	15.78	25	11.80	15.93	2.30	2.40	2.397	0.5307	0.8757	0.2131	0.665	0.442
3	0.0417	0.0005	1.60	0.355	1.515	13.391	1.65	0.0299	0.083	25.43	27	21.16	27.72	2.50	2.60	2.565	0.5947	0.9813	0.2999	0.622	0.450
4	0.0417	0.0005	1.60	0.355	1.515	11.840	1.65	0.0339	0.125	33.96	28	27.72	35.87	2.60	2.70	2.677	0.6371	1.0512	0.3686	0.596	0.455
5	0.0417	0.0005	1.60	0.355	1.515	10.836	1.65	0.0370	0.167	41.76	29	35.87	45.89	2.70	2.80	2.759	0.6683	1.1028	0.4256	0.578	0.458
6	0.0830	0.0005	1.60	0.355	1.515	10.104	1.65	0.0397	0.250	56.25	30	45.89	58.11	2.80	2.90	2.885	0.7162	1.1817	0.5237	0.553	0.463
7	0.0830	0.0005	1.60	0.355	1.515	8.999	1.65	0.0446	0.333	69.15	31	58.11	72.90	2.90	3.00	2.975	0.7504	1.2381	0.6023	0.536	0.467
8	0.0830	0.0005	1.60	0.355	1.515	8.220	1.65	0.0488	0.416	80.94	32	72.90	201.33	3.00	3.50	3.031	0.7719	1.2736	0.6556	0.526	0.469
9	0.0830	0.0005	1.60	0.355	1.515	7.733	1.65	0.0518	0.499	92.02	32	72.90	201.33	3.00	3.50	3.074	0.7883	1.3007	0.6983	0.519	0.471
10	0.1250	0.0005	1.60	0.355	1.515	7.364	1.65	0.0544	0.624	107.92	32	72.90	201.33	3.00	3.50	3.136	0.8118	1.3395	0.7627	0.508	0.473
11	0.1250	0.0005	1.60	0.355	1.515	6.838	1.65	0.0586	0.749	122.69	32	72.90	201.33	3.00	3.50	3.194	0.8337	1.3755	0.8259	0.499	0.475
12	0.1250	0.0005	1.60	0.355	1.515	6.352	1.65	0.0631	0.874	136.40	32	72.90	201.33	3.00	3.50	3.247	0.8539	1.4090	0.8877	0.491	0.477
13	0.1250	0.0005	1.60	0.355	1.515	5.903	1.65	0.0679	0.999	149.15	32	72.90	201.33	3.00	3.50	3.297	0.8728	1.4401	0.9478	0.484	0.479
14	0.2500	0.0005	1.60	0.355	1.515	5.488	1.65	0.0731	1.249	172.85	32	72.90	201.33	3.00	3.50	3.389	0.9079	1.4980	1.0667	0.470	0.482
15	0.2500	0.0005	1.60	0.355	1.515	4.721	1.65	0.0849	1.499	193.24	32	72.90	201.33	3.00	3.50	3.468	0.9380	1.5477	1.1765	0.460	0.485
16	0.2500	0.0005	1.60	0.355	1.515	4.066	1.65	0.0986	1.749	210.80	33	201.33	477.87	3.50	4.00	3.517	0.9565	1.5782	1.2475	0.453	0.487
17	0.2500	0.0005	1.60	0.355	1.515	3.667	1.65	0.1093	1.999	226.63	33	201.33	477.87	3.50	4.00	3.546	0.9674	1.5962	1.2905	0.450	0.488
18	0.2500	0.0005	1.60	0.355	1.515	3.433	1.65	0.1168	2.249	241.46	33	201.33	477.87	3.50	4.00	3.573	0.9776	1.6130	1.3317	0.446	0.489
19	0.2500	0.0005	1.60	0.355	1.515	3.214	1.65	0.1247	2.499	255.34	33	201.33	477.87	3.50	4.00	3.598	0.9871	1.6287	1.3711	0.443	0.489
20	0.5000	0.0005	1.60	0.355	1.515	3.010	1.65	0.1332	2.999	281.33	33	201.33	477.87	3.50	4.00	3.645	1.0050	1.6582	1.4468	0.438	0.491
1	0.0209	0.0005	1.60	0.536	1.627	12.492	1.65	0.0226	3.020	0.653	13	0.522	0.699	1.55	1.60	1.587	1.1503	1.8980	2.1698	1.096	0.601
2	0.0209	0.0005	1.60	0.536	1.627	11.808	1.65	0.0240	3.041	0.879	14	0.699	0.917	1.60	1.65	1.641	1.2569	2.0739	2.8306	1.060	0.606

APPENDIX 2

Results of computer modeling, experimental and calculated SLOKA

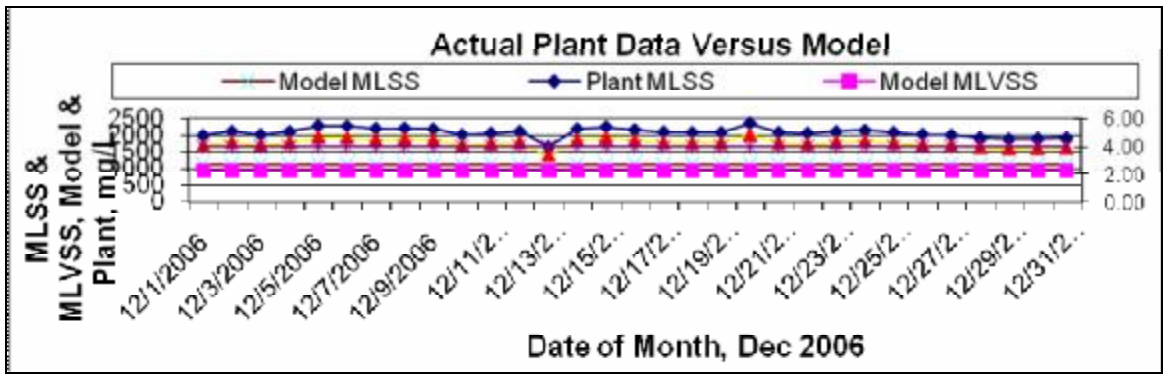
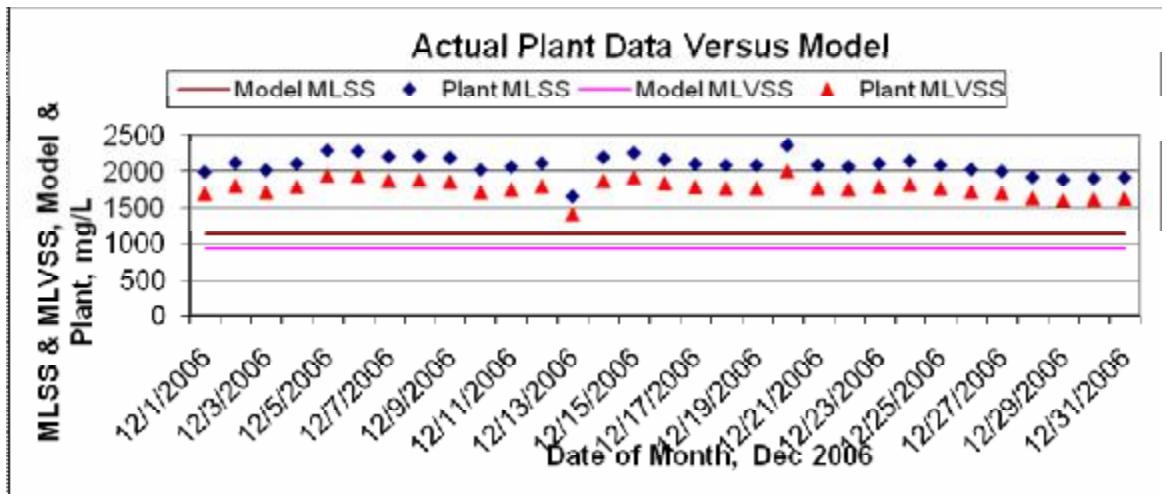
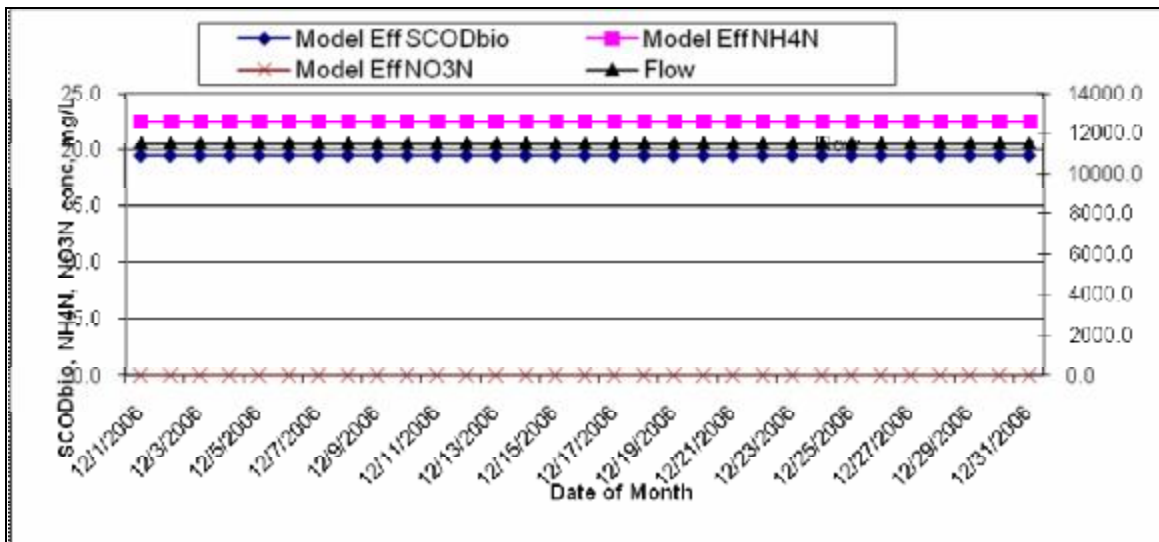
WWTP data

No	Date	Qi (m ³ /day)	Qr (m ³ /day)	(Qi+Qr)(m ³ /day)	WWTP ,X1 (mg/l)	X1 (Kg/m ³)	SLOR ,X(Kg/m ³)	Xr (Kg/m ³)
0	0	0	0	0	0	0	0	0
1	18-Dec-2008	8099	4859.4	12958.4	113.0	0.113	0.048025	0.1277465
2	19-Dec-2008	8099	4859.4	12958.4	159.0	0.159	0.067575	0.1797495
3	20-Dec-2008	8316	4989.6	13305.6	200.0	0.2	0.085	0.2261
4	21-Dec-2008	8986	5391.6	14377.6	221.0	0.221	0.093925	0.2498405
5	22-Dec-2008	10218	6130.8	16348.8	209.0	0.209	0.088825	0.2362745
6	23-Dec-2008	10913	6547.8	17460.8	175.0	0.175	0.074375	0.1978375
7	24-Dec-2008	11032	6619.2	17651.2	232.0	0.232	0.0986	0.262276
8	25-Dec-2008	9612	5767.2	15379.2	211.0	0.211	0.089675	0.2385355
9	26-Dec-2008	9489	5693.4	15182.4	209.0	0.209	0.088825	0.2362745
10	27-Dec-2008	9317	5590.2	14907.2	187.0	0.187	0.079475	0.2114035
11	28-Dec-2008	9225	5535	14760	134.0	0.134	0.05695	0.151487
12	29-Dec-2008	8877	5326.2	14203.2	112.0	0.112	0.0476	0.126616
13	30-Dec-2008	8928	5356.8	14284.8	85.0	0.085	0.036125	0.0960925
14	1-Jan-2009	8646	5187.6	13833.6	163.0	0.163	0.069275	0.1842715
15	2-Jan-2009	8261	4956.36	13216.96	200.0	0.2	0.085	0.2261
16	3-Jan-2009	8250	4949.82	13199.52	251	0.251	0.106675	0.2837555
17	4-Jan-2009	8327	4996.2	13323.2	149	0.149	0.063325	0.1684445
18	5-Jan-2009	8171	4902.6	13073.6	149.0	0.149	0.063325	0.1684445
19	6-Jan-2009	7620	4571.7	12191.2	162.0	0.162	0.06885	0.183141
20	7-Jan-2009	7818	4690.8	12508.8	151.0	0.151	0.064175	0.1707055
21	8-Jan-2009	7545	4527	12072	127.0	0.127	0.053975	0.1435735
22	9-Jan-2009	8213	4927.62	13140.32	188.0	0.188	0.0799	0.212534
23	10-Jan-2009	7958	4774.8	12732.8	175.0	0.175	0.074375	0.1978375
24	11-Jan-2009	8605	5163	13768	200.0	0.2	0.085	0.2261
25	12-Jan-2009	8828	5296.8	14124.8	173.0	0.173	0.073525	0.1955765
26	13-Jan-2009	8777	5266.2	14043.2	108.0	0.108	0.0459	0.122094
27	14-Jan-2009	8592	5155.2	13747.2	159.0	0.159	0.067575	0.1797495
28	15-Jan-2009	9391	5634.6	15025.6	78.0	0.078	0.03315	0.088179
29	16-Jan-2009	9146	5487.36	14632.96	144.0	0.144	0.0612	0.162792
30	17-Jan-2009	9072	5443.08	14514.88	150.0	0.15	0.06375	0.169575
31	18-Jan-2009	8875	5324.76	14199.36	222.0	0.222	0.09435	0.250971
32	19-Jan-2009	8309	4985.4	13294.4	140.0	0.14	0.0595	0.15827
33	20-Jan-2009	8225	4935	13160	209.0	0.209	0.088825	0.2362745
34	21-Jan-2009	8063	4837.8	12900.8	193.0	0.193	0.082025	0.2181865
35	22-Jan-2009	9248	5548.8	14796.8	200.0	0.2	0.085	0.2261
36	23-Jan-2009	9157	5494.2	14651.2	129.0	0.129	0.054825	0.1458345
37	24-Jan-2009	9059	5435.4	14494.4	112.0	0.112	0.0476	0.126616
38	25-Jan-2009	9341	5604.6	14945.6	133.0	0.133	0.056525	0.1503565
39	26-Jan-2009	9320	5592	14912	134.0	0.134	0.05695	0.151487
40	27-Jan-2009	9282	5569.2	14851.2	106.0	0.106	0.04505	0.119833
41	28-Jan-2009	9596	5757.66	15353.76	112.0	0.112	0.0476	0.126616
42	29-Jan-2009	9386	5631.6	15017.6	99.0	0.099	0.042075	0.1119195
43	30-Jan-2009	9112	5467.2	14579.2	147.0	0.147	0.062475	0.1661835
44	31-Jan-2009	8945	5367	14312	144.0	0.144	0.0612	0.162792
45	1-Feb-2009	8772	5263.2	14035.2	158	0.158	0.06715	0.178619
46	2-Feb-2009	8041	4824.6	12865.6	156.0	0.156	0.0663	0.176358
47	3-Feb-2009	7926	4755.3	12680.8	122.0	0.122	0.05185	0.137921
48	4-Feb-2009	8023	4813.62	12836.32	130.0	0.13	0.05525	0.146965
49	5-Feb-2009	7780	4668	12448	140.0	0.14	0.0595	0.15827
50	6-Feb-2009	7569	4541.4	12110.4	187.0	0.187	0.079475	0.2114035
51	7-Feb-2009	7573	4543.8	12116.8	181.0	0.181	0.076925	0.2046205
52	8-Feb-2009	7989	4793.4	12782.4	190.0	0.19	0.08075	0.214795
53	9-Feb-2009	7615	4569	12184	197.0	0.197	0.083725	0.2227085
54	10-Feb-2009	7527	4516.2	12043.2	158.0	0.158	0.06715	0.178619
55	11-Feb-2009	7558	4534.8	12092.8	160.0	0.16	0.068	0.18088
56	12-Feb-2009	7063	4237.8	11300.8	198.0	0.198	0.08415	0.223839
57	13-Feb-2009	7203	4321.8	11524.8	163.0	0.163	0.069275	0.1842715
58	14-Feb-2009	7387	4432.2	11819.2	156.0	0.156	0.0663	0.176358
59	15-Feb-2009	7255	4353	11608	142.0	0.142	0.06035	0.160531
60	16-Feb-2009	7133	4279.8	11412.8	144.0	0.144	0.0612	0.162792
61	17-Feb-2009	6991	4194.72	11185.92	162.0	0.162	0.06885	0.183141

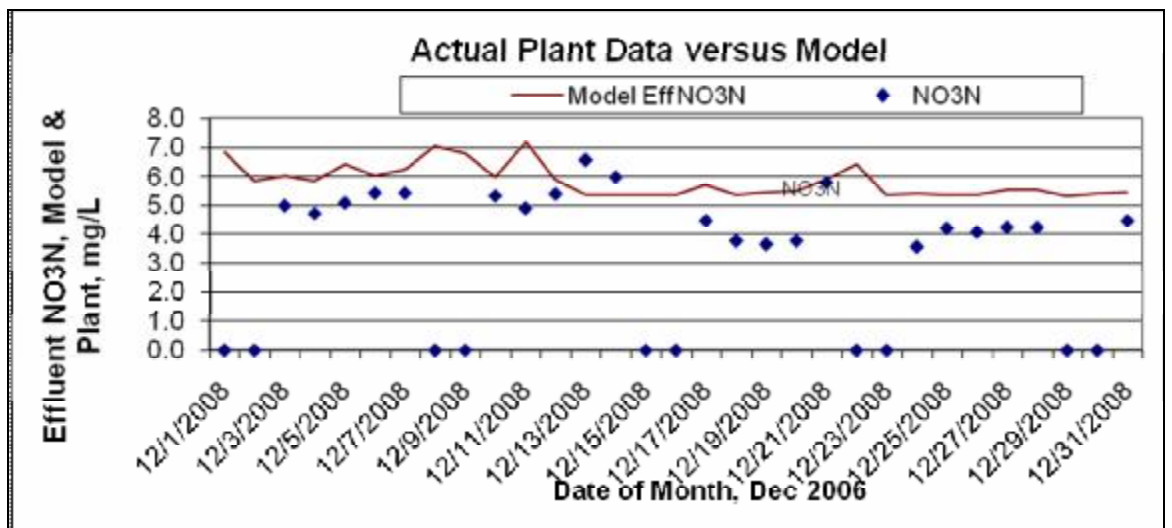
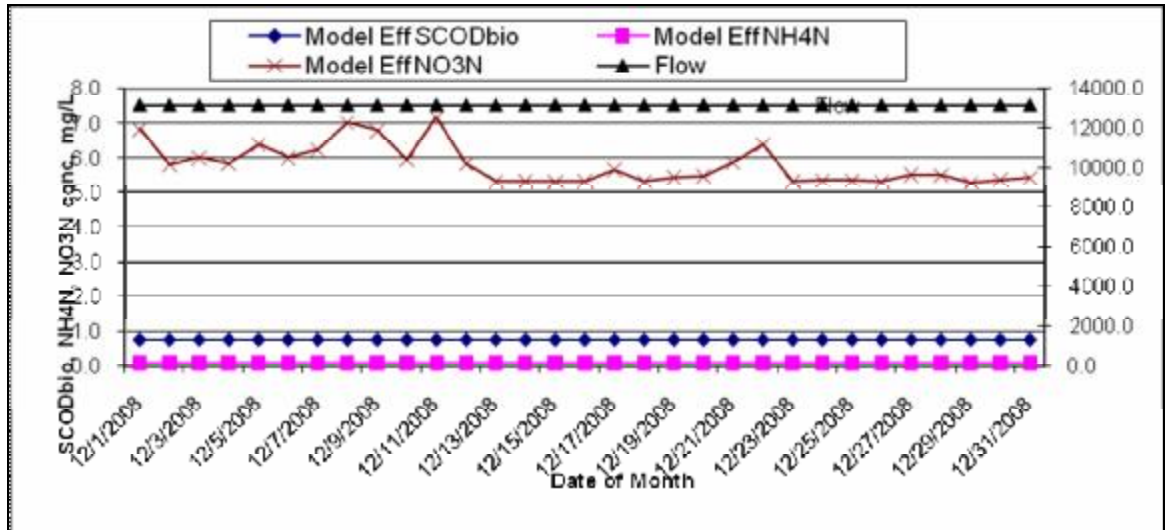
? t (day)	Xr (kg/day)	Xi,kg/day	As?Xsb?Hsb,kg	Vsb,m ³	Hsb, m	X _r ,kg/m ³	Xf,mg/l	(kg/m ³) circ	Xe,kg/m ³
0	0	0	0	0	0	0	0	0	0
1	620.7713421	622.32716	88	0.05028571	7.7231E-05	0.001975828	2.0	0.0237735	0.01113783
2	873.4747203	875.66388	90.1891597	0.02576833	3.9576E-05	0.002780148	2.8	0.0538273	0.00548377
3	1128.14856	1130.976	93.0165997	0.02657617	4.0817E-05	0.003589255	3.6	0.0740481	0.00368133
4	1347.04004	1350.4161	96.3926399	0.02754075	4.2298E-05	0.004280208	4.3	0.0841932	0.00272582
5	1448.551705	1452.1822	100.0230953	0.02857803	4.3891E-05	0.004592001	4.6	0.076397	0.00391802
6	1295.400383	1298.647	103.2697128	0.05901126	9.0632E-05	0.004101094	4.1	0.0420627	0.01410562
7	1736.057299	1740.4083	107.6207336	0.03074878	4.7225E-05	0.005494926	5.5	0.0859949	0.00355508
8	1375.681936	1379.1298	111.068558	0.03173387	4.8738E-05	0.004366019	4.4	0.0738936	0.00570769
9	1345.205238	1348.5767	114.4399997	0.03269714	5.0218E-05	0.004270293	4.3	0.0718979	0.00632839
10	1181.787846	1184.7497	117.401874	0.03354339	5.1517E-05	0.003752758	3.8	0.0604361	0.00764307
11	838.480545	840.582	119.503329	0.03414381	5.2439E-05	0.002663054	2.7	0.0367838	0.00875156
12	674.3821392	676.07232	121.1935098	0.03462672	5.3181E-05	0.002143288	2.1	0.0280569	0.00869989
13	514.748304	516.0384	122.4836058	0.03499532	5.3747E-05	0.001635789	1.6	0.0186658	0.0079617
14	955.9268334	958.32264	124.8794124	0.03567983	5.4798E-05	0.003039414	3.0	0.0480436	0.0090996
15	1120.632996	1123.4416	127.6880164	0.03648229	5.6031E-05	0.00356572	3.6	0.0641412	0.00864654
16	1404.538649	1408.0588	131.2081634	0.03748805	5.7576E-05	0.004469167	4.5	0.0881787	0.00701359
17	841.5824109	843.69164	133.3173925	0.03809068	5.8501E-05	0.002677476	2.7	0.0408383	0.00990461
18	825.8160057	827.88572	135.3871068	0.03868203	5.9409E-05	0.002628096	2.6	0.0405432	0.01007687
19	837.2657097	839.36412	137.4855171	0.03928158	6.033E-05	0.002667336	2.7	0.0455181	0.01033229
20	800.7453594	802.75224	139.4923977	0.03985497	6.1211E-05	0.002550025	2.6	0.0407684	0.0104283
21	649.9572345	651.5862	141.1213632	0.04032039	6.1926E-05	0.002070908	2.1	0.0314153	0.01024439
22	1047.286789	1049.9116	143.7461421	0.04107033	6.3077E-05	0.003332645	3.3	0.0554637	0.01055184
23	944.634495	947.002	146.1136471	0.04174676	6.4116E-05	0.003007447	3.0	0.0495485	0.01090995
24	1167.3543	1170.28	149.0393471	0.04258267	6.54E-05	0.003711947	3.7	0.0597145	0.01078678
25	1035.929605	1038.5259	151.6356619	0.0432447	6.6539E-05	0.003292646	3.3	0.0478779	0.01117725
26	642.9714228	644.58288	153.2471191	0.04378489	6.7246E-05	0.002043848	2.0	0.023765	0.01004556
27	926.6446224	928.96704	155.5695367	0.04444844	6.8266E-05	0.002946613	2.9	0.0417791	0.01142463
28	496.8533934	498.09864	156.8147833	0.04480422	6.8812E-05	0.001577532	1.6	0.0145004	0.00853601
29	893.2983091	895.53715	159.0536262	0.04544389	6.9794E-05	0.002837586	2.8	0.0357225	0.01131997
30	923.010291	925.3236	161.3669352	0.04610484	7.081E-05	0.002932379	2.9	0.0376808	0.01156842
31	1336.360342	1339.7096	164.7162092	0.04706177	7.2279E-05	0.004247173	4.2	0.0664172	0.01268564
32	789.039258	791.0168	166.6937512	0.04762679	7.3147E-05	0.002510397	2.5	0.0335089	0.01174037
33	1166.014658	1168.937	169.6160937	0.04846174	7.4429E-05	0.003710371	3.7	0.0599671	0.01257376
34	1055.54265	1058.1881	172.261564	0.04921759	7.559E-05	0.003359875	3.4	0.0529593	0.01285293
35	1254.58368	1257.728	175.405884	0.05011597	7.697E-05	0.003984443	4.0	0.0553346	0.01284047
36	801.2439099	803.25204	177.4140141	0.05068972	7.7851E-05	0.002545118	2.5	0.0288157	0.01173211
37	688.2086064	689.93344	179.1388477	0.05118253	7.8608E-05	0.002186473	2.2	0.0232628	0.01107538
38	842.6880399	844.80004	181.2508478	0.05178596	7.9535E-05	0.002675827	2.7	0.0298399	0.01200463
39	847.115304	849.2384	183.3739438	0.05239256	8.0466E-05	0.002689993	2.7	0.0300043	0.01212784
40	667.3739436	669.04656	185.0465602	0.05287045	8.12E-05	0.002119382	2.1	0.0211039	0.01091336
41	729.0118786	730.83898	186.8736577	0.05339247	8.2002E-05	0.002313744	2.3	0.0227922	0.01124704
42	630.2858562	631.86552	188.4533215	0.05384381	8.2695E-05	0.002001205	2.0	0.0188997	0.01058706
43	908.5584312	910.83552	190.7304103	0.0544944	8.3695E-05	0.002886245	2.9	0.0337673	0.01291074
44	873.704664	875.8944	192.9201463	0.05512004	8.4655E-05	0.002776405	2.8	0.0325738	0.01292492
45	940.1075208	942.46368	195.2763055	0.05579323	8.5689E-05	0.002988399	3.0	0.0371488	0.0135064
46	850.8568068	852.98928	197.4087787	0.05640251	8.6625E-05	0.002708457	2.7	0.0362666	0.01366247
47	655.8557313	657.49948	199.0525274	0.05687215	8.7346E-05	0.002088187	2.1	0.0250975	0.01233218
48	707.4336633	709.20668	200.8255441	0.05737873	8.8124E-05	0.0025199	2.3	0.0274584	0.01276979
49	738.80436	740.656	202.6771841	0.05790777	8.8937E-05	0.002352941	2.4	0.0305107	0.01331819
50	960.0678549	962.47404	205.0833692	0.05859525	8.9993E-05	0.00305885	3.1	0.046547	0.01493456
51	929.7546279	932.08484	207.4135813	0.05926102	9.1015E-05	0.002962247	3.0	0.0441212	0.0149208
52	1029.598353	1032.1788	209.9940283	0.0599829	9.2148E-05	0.00327754	3.3	0.0471198	0.01517624
53	1017.555137	1020.1054	212.5442918	0.06072694	9.3267E-05	0.003241724	3.2	0.0494192	0.01553203
54	806.6791278	808.70088	214.566044	0.06130458	9.4154E-05	0.002570347	2.6	0.0355087	0.01453546
55	820.254624	822.3104	216.62182	0.06189195	9.5056E-05	0.002613449	2.6	0.0360108	0.01468788
56	948.5849142	950.96232	218.9992258	0.06257121	9.6099E-05	0.003025183	3.0	0.0490863	0.01601925
57	796.3845687	798.38052	220.9951771	0.06314148	9.6975E-05	0.002539114	2.5	0.0366611	0.01503737
58	781.6539276	783.61296	222.9542095	0.0637012	9.7835E-05	0.002491274	2.5	0.0342087	0.0148
59	698.791443	700.5428	224.7055665	0.06420159	9.8603E-05	0.002227737	2.2	0.0296467	0.01423779
60	696.7172016	698.46336	226.4517249	0.06470049	9.9369E-05	0.002221642	2.2	0.030155	0.01441165
61	768.2252155	770.15059	228.3771013	0.0652506	0.00010021	0.002450324	2.5	0.0357595	0.01532009

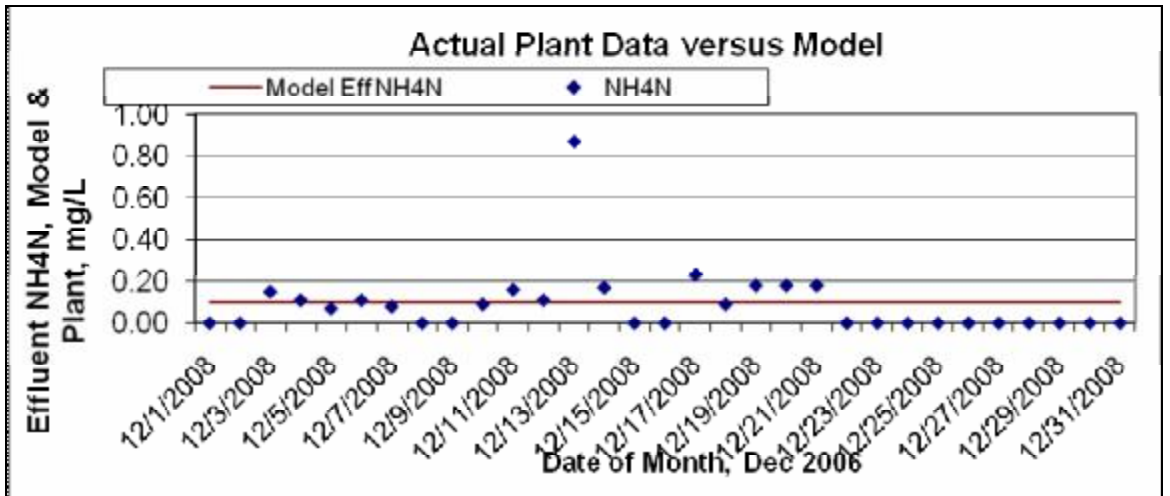
APPENDIX 3

Aqua model. Summary of calculated and experimental SLOKA WWTP performance data



Overloaded clarifier





Failed, overloaded

The scouring from sludge blanket will take place.

